

General Disclaimer

One or more of the Following Statements may affect this Document

- This document has been reproduced from the best copy furnished by the organizational source. It is being released in the interest of making available as much information as possible.
- This document may contain data, which exceeds the sheet parameters. It was furnished in this condition by the organizational source and is the best copy available.
- This document may contain tone-on-tone or color graphs, charts and/or pictures, which have been reproduced in black and white.
- This document is paginated as submitted by the original source.
- Portions of this document are not fully legible due to the historical nature of some of the material. However, it is the best reproduction available from the original submission.

MATHEMATICAL MODEL OF ONE-MAN
AIR REVITALIZATION SYSTEM

NASA CR-

147580

Prepared under Contract No. NAS 9-12526

by

University of Missouri-Columbia
Chemical Engineering Department
Columbia, Missouri

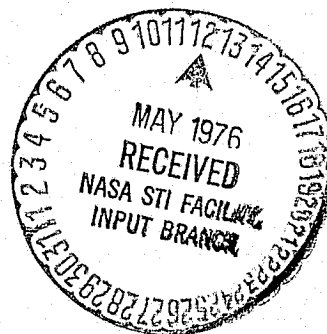
for

National Aeronautics and Space Administration

Johnson Space Center

Houston, Texas

March 1976



(NASA-CR-147580) MATHEMATICAL MODEL OF
ONE-MAN AIR REVITALIZATION SYSTEM Final
Report (Missouri Univ.) 208 P HC \$7.75
CSCI 06K

N76-22908

Unclas
G3/54 26783

TABLE OF CONTENTS

Chapter	Page
I. INTRODUCTION	1
II. LITERATURE REVIEW	6
Introduction	6
Absorption of CO ₂ in Buffer Solutions	6
Transport Phenomena in Electrolytic Solutions	9
Theory of Porous Gas-Diffusion Electrodes	12
III. PROCESS DESCRIPTION AND CELL DESIGN	16
Process Description	16
Major Requirements	17
Cell Design	18
IV. MATHEMATICAL MODELING	23
Introduction	23
Mass Transfer and Reaction Rates	24
Mathematical Model	32
Numerical Method of Solution	36
V. EXPERIMENTAL DATA	38
Introduction	38
Performance Data	38
Special Tests	40
IV. MODEL PARAMETERS	45
Introduction	45

Chapter	Page
Activity Coefficients	45
Equilibrium and Reaction Rate Constants	50
Henry's Law Constants	52
Gas-Phase Mass and Heat Transfer Coefficients	53
Transport Properties in the Electrolyte	56
Matrix Factor	59
Gas-Electrolyte Interface Area	61
VII. MODEL PREDICTIONS.	72
Introduction	72
Effect of P_{CO_2}	72
Effect of Current Density	75
Effect of Air Velocity	78
Effect of Matrix Thickness and Compression	78
Effect of Air Relative Humidity and Temperature	82
Effect of H_2 Flow Rate and Anode Active Area	86
VIII. CONCLUSIONS AND RECOMMENDATIONS	88
NOMENCLATURE	92
BIBLIOGRAPHY	97
APPENDICES	101
A. DETAILED CALCULATIONS	101
Activity Coefficients	101
Characteristic Parameters	110

Chapter	Page
Equilibrium and Henry's Law Constants	110
Diffusion Coefficients and Mobilities	111
Cathode and Anode Active Areas	113
B. COMPUTER PROGRAM	116

LIST OF TABLES

Table	Page
1. Activity Coefficients of Tetramethylammonium Halides at 25°C	101
2. Terms in Equation [6-3] for the NMe_4 -Halides.	103
3. Important Parameters of the Ions	104
4. Osmotic and Activity Coefficients of $(\text{NMe}_4)_2\text{CO}_3$, NMe_4HCO_3 , and NMe_4OH at 25°C	107
5. The Term $\log \gamma_{st}$ for the Hydroxides at 25°C	108
6. Activity Coefficients of Na_2CO_3 at 25°C	109
7. Characteristic Parameters	110
8. Average Concentrations and Equilibrium Constants	110
9. Equivalent Conductances and Diffusion Coefficients at Infinite Dilution and 25°C	111
10. Diffusion Coefficients at 25°C	112
11. Equivalent Conductances at 25°C	112
12. Coefficients of the Polynomials Used in Calculating the Ionic Diffusion Coefficients and Mobilities	114

LIST OF FIGURES

Figure	Page
1. Illustration of Partially Wetted Electrode	14
2. Cross Section in Cell Pair	19
3. Schematic of a Subcell	25
4. Activity Coefficients of $(\text{NMe}_4)_2\text{CO}_3$, NMe_4HCO_3 , and NMe_4OH at 25°C	51
5. The Limiting Slope Method for Calculating the Mass Transfer Coefficient in the Air Side	54
6. Relative Viscosities of $(\text{NMe}_4)_2\text{CO}_3$, NMe_4HCO_3 , and NMe_4OH at 25°C	57
7. Diffusion Coefficients of $(\text{NMe}_4)_2\text{CO}_3$, NMe_4HCO_3 , and NMe_4OH at 25°C	58
8. Equivalent Conductances of $(\text{NMe}_4)_2\text{CO}_3$, NMe_4HCO_3 , and NMe_4OH at 25°C	60
9. Test Data Compared with Simulation Results if the CO_2 Flux is Proportional to $\sqrt{[\text{OH}]}$ and the Air-Catholyte Area is Constant, Analytical Cell, Air Inlet Temp = 70°F, Air Dew Point = 50°F	63
10. Air-Catholyte Area Dependence on Current Density . .	64
11. Test Data Compared with Simulation Results if the CO_2 Flux is Proportional to $[\text{OH}]$ and the Air-Catholyte Area is dependent on Current Density, Analytical Cell, Air Inlet Temp. = 70°F, Air Dew Point = 50°F	65

Figure	Page
12. Electrodes of the Analytical and Full-Scale Cells	69
13. Effect of P_{CO_2} at the Air Inlet on the CO_2 Removal Rate in the Analytical Cell (the Solid Lines Represent Simulation Results)	73
14. Effect of P_{CO_2} in the Inlet Air on the CO_2 Removal Rate in the Full-Scale Cell (the Solid Lines Represent Simulation Results)	74
15. Effect of P_{CO_2} on the Hydroxyl Ion Concentration in the Catholyte of the Analytical Cell.	76
16. CO_2 Removal Efficiency in the Full Scale Cell . . .	77
17. Effect of Current Density on the Hydroxyl Ion Concentration in the Catholyte of the Analytical Cell	79
18. Effect of Air Velocity on the CO_2 Removal Efficiency in the Analytical Cell	80
19. Effect of Air Velocity on the Hydroxyl Ion Concentration in the Catholyte of the Analytical Cell.	81
20. Effect of Matrix Thickness on the CO_2 Removal Rate in the Analytical Cell.	83
21. Effect of Matrix Compression on the CO_2 Removal Rate in the Analytical Cell	84

22. The Concentration Distribution of the CO_3^{2-} , HCO_3^- and NMe_4^+ in the Analytical Cell at the Following Conditions: $P_{\text{CO}_2} = 4$ MM Hg, Current Density = 18 A/ft^2 , Air Velocity = 10 ft/sec , Air Temp. = 70°F , Air Dew Point = 60°F 87
23. The $-\log \gamma_{\text{st}}$ Term in equation [6-3] for Tetramethylammonium Electrolytes at 25°C 105

CHAPTER I

INTRODUCTION

Recycling of most of the consumables in manned spacecraft becomes essential in extended missions. The most urgent task is to supply a continuous stream of breathable oxygen to the cabin to balance the consumption. This can be derived from the metabolically produced carbon dioxide. In recent years several systems have been developed for that purpose. They consist essentially of some device to remove the CO_2 so as to keep its concentration in the cabin atmosphere below a prescribed level, followed by a reactor to decompose the CO_2 eventually into O_2 which is recycled to the cabin.

One particular method has been adopted by NASA as the most practical and reliable method for missions lasting six months or more. The recovery of O_2 from CO_2 is achieved in three steps. First, CO_2 is concentrated and mixed with H_2 in an electrochemical cell (sometimes called a hydrogen depolarized cell or HDC); the mixture is then transferred to a catalytic reactor where it is converted into water and CH_4 , the methane is then dumped into space; and finally the water vapor is electrolysed in a special electrolysis cell (called water vapor electrolysis cell or WVE) to O_2 which is recycled to the cabin and H_2 which is transferred to the concentrator.

Electrochemical CO_2 concentration provides several advantages. The process is continuous and the equivalent weight of the system

needed to maintain the atmospheric level of CO_2 concentration (0.25 mm Hg) is considerably lower than the adsorption systems which do the same duty. CO_2 compressors which are frequently needed in other systems, e.g., in the vacuum desorption from molecular sieves, are totally eliminated. In addition, the concentration of CO_2 protects the catalyst in the Sabatier reactor from contamination by the cabin air and supplies the CO_2/H_2 mixture in proper ratio to the reactor.

The development of the device was undertaken in the past five years by two private contractors, Life Systems, Inc., and Hamilton Standard Division of United Technologies. The designs agree in principle but differ in detailed mechanical design and operating conditions. One of the major problems encountered in designing the CO_2 concentrator is the need to use a concentrated carbonate solution as a cell electrolyte. The air temperature and humidity determine the electrolyte concentration at steady-state. At a high air relative humidity the electrolyte becomes more dilute and increases in volume. This may lead to electrolyte run-off in the gas cavities and is avoided in the Hamilton Standard design by providing a reservoir to absorb the excess electrolyte at humid conditions. At a low air relative humidity the concentration of the electrolyte increases and may exceed the solubility limit. In that case precipitation would commence which may lead to the crossover of the H_2 to the air stream causing a hazardous condition. This should be avoided by proper selection of the carbonate electrolyte and air humidity. K_2CO_3 was first used but was re-

placed by Cs_2CO_3 which has a higher solubility. Still, this did not allow for cell operation at air relative humidities below about 60%. Below this limit the cell performance decreased because of the loss of electrolyte and precipitation of CsHCO_3 at the anode. It was necessary to use extensive humidity controllers at the air inlet which added to the total system weight and power requirements. Through its efforts to overcome this problem, Hamilton Standard introduced aqueous solutions of a new electrolyte, TMAC or tetramethylammonium carbonate, which have such low water vapor pressures that they can be used safely for air relative humidities as low as 35% without significant change in performance.

Very recently, Hamilton Standard completed the design and fabrication of a full-scale device for use in one-man air revitalization systems and finished a 90-day test program to demonstrate the maintainability and durability of the device with a predicted life of two years (Huddleston and Aylward, 1975 a,b,c). The HDC and WVE cells are connected electrically in series so that the energy produced by the fuel cell reactions in the HDC cell is utilized in the water vapor electrolysis.

The cost of air revitalization in a spacecraft is measured in millions of dollars and the final design and operation of the system should lead to the minimum cost for a certain duty. The economy of the system is based on two factors: minimum system equivalent weight and minimum power requirements. The weight appears in cost of pro-

pellant needed to accelerate the spacecraft and it includes the weight of the HDC cells, WVE cells, Sabatier reactor and other auxiliary equipment. The power requirements are functions of the current densities used and the electrical efficiency of the cells. The total system cost depends greatly on the performance of the HDC cell. For example, a low CO_2 transfer efficiency would result in additional cost of the power needed to make H_2 and O_2 from the H_2O produced in the HDC cell. A poor H_2/CO_2 flow to the Sabatier reactor would lead to a low conversion efficiency which requires additional amounts of the expensive catalyst and would add to the weight of the system. The decrease in cell performance if precipitation occurs would require extra cells adding to the system weight. It is clear that an optimum design of the system is unattainable without a mathematical model that describes the performance of the HDC cell under all possible conditions.

Lin and Winnick (1974) developed a fundamental model of the early versions of the device which used Cs_2CO_3 electrolyte. The model was based on the steady-state transport equations and kinetics of the reactions which take place in the cell. Since then, several changes have taken place in the Hamilton Standard design; new electrodes and matrix materials were used and a new electrolyte was employed. It was necessary to develop a new model for the units which use TMAC electrolyte. The model should be able to simulate the new test data and predict the cell performance under all practical conditions. In that way a clear basis for design evaluation can be obtained and

optimization studies can be started.

This work describes the development of this mathematical model. The starting point will be to review all information pertaining to the electrochemical CO_2 concentration. This is followed by a brief description of the cell design, test data and their accuracy, and all useful information concerning the new electrolyte and modifications of the cell design. Chapter IV summarizes the equations which form the basis of the steady-state mathematical model. The important model parameters are then evaluated and used to predict the cell performance over a wide range of operating conditions. Conclusions and recommendations of areas of possible improvements are finally presented.

CHAPTER II

LITERATURE REVIEW

Introduction

In this chapter several topics are discussed which are intimately related to the electrochemical concentration of CO_2 . These include the chemical absorption of CO_2 in buffer solutions, transport phenomena in electrolytic solutions, and theory of gas electrodes. This will be useful in the development of the mathematical model in a later chapter.

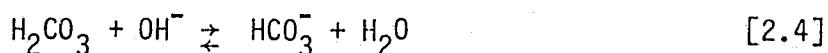
Absorption of CO_2 in Buffer Solutions

The absorption of CO_2 in aqueous solutions can take place by two mechanisms depending on the pH of the solution. At a pH greater than 10 the basic mechanism predominates



The first step is slow and rate-determining while the second step is instantaneous (Kern, 1960). At a pH less than 8 the acidic mechanism predominates





Here the second step is instantaneous while the first step is rate-determining. At pH in the 8-10 range, both mechanisms are important.

The rate equation for the first mechanism is

$$-\frac{d[\text{CO}_2]}{dt} = k_i [\text{CO}_2] [\text{OH}^-] \quad [2.5]$$

The rate constant k_i was measured by Pinsent et al. (1956) over the range 0 to 40°C. The dependence of k_i on the ionic strength of the solution, μ , could be represented by an equation of the form

$$\log k_i = g + \ell \mu \quad [2.6]$$

where g is a constant dependent on the temperature and ℓ is another constant dependent on the temperature and the ionic species in the solution.

The rate equation for the second mechanism is

$$-\frac{d[\text{CO}_2]}{dt} = k_{iii} [\text{CO}_2] \quad [2.7]$$

The measurements of k_{iii} taken by several workers were summarized by Edsall (1968). The ionization constants of carbonic acid as obtained from cell measurements were reported also by Harned and Owen (1958).

The problem of simultaneous diffusion and chemical reaction was treated rather extensively by Astarita (1967). He classified processes of chemical absorption into different regimes according to the

relative magnitudes of the characteristic diffusion and reaction times. For gas absorption with a first-order chemical reaction, the process is considered in the fast reaction regime if

$$D_L/h_L^2 \gg 1/k \quad [2.8]$$

where D_L is the molecular diffusivity of the absorbing gas in the liquid phase, h_L is its mass transfer coefficient in the liquid phase, and k is the reaction rate constant. Under this condition the absorption rate per unit area of the interface, N , can be calculated by the following equation derived from penetration theory:

$$N = \sqrt{D_L k} (C^+ - C^-) \quad [2.9]$$

where C^+ and C^- are the concentrations of the reactant at the gas-liquid interface (the gas solubility as ordinarily defined) and the equilibrium concentration, respectively.

The physical solubility of a gas in a liquid containing electrolytes which react with the gas cannot be determined from equilibrium measurements used for other gases. Only kinetic measurements can give an estimate of the solubility in that case (Nysing and Kramers, 1957). However, the solubility can be obtained approximately by the equation (Van Krevelen and Hoftijzer, 1948)

$$\log (C^+/C^{+\circ}) = - c \mu \quad [2.10]$$

where C^+ and $C^{+\circ}$ are the solubilities in the electrolytic solution

and in water, respectively, and c is a coefficient which can be considered as the sum of elements characteristic of the cations and anions present in the solution and of the dissolved gas

$$c = c_+ + c_- + c_G \quad [2.11]$$

Transport Phenomena in Electrolytic Solutions

Mass transfer in electrolytic solutions can be expressed by the Nernst-Planck equation (Newman, 1973) which, in one dimension, has the form

$$N_j = -\left(D_j \frac{dC_j}{dx} + z_j F u_j C_j \frac{d\phi}{dx}\right) + C_j v \quad [2.12]$$

where N_j is the flux of the species j in the x direction, D_j is the ionic diffusion coefficient, C_j is the ionic concentration, z_j is the ionic charge, F is the Faraday's constant, u_j is the ionic mobility, ϕ is the electrical potential, and v is the bulk velocity of the solution.

Ionic mobilities at infinite dilution can be calculated from the limiting values of ionic equivalent conductance, λ_j° , by the equation

$$u_j^\circ = \lambda_j^\circ / |z_j| F^2 \quad [2.13]$$

The ionic diffusion coefficients at infinite dilution can also be calculated from the values of λ_j° by the Nernst-Einstein equation

$$D_j^\circ = RT \lambda_j^\circ / |z_j| F^2 \quad [2.14]$$

where R is the gas constant and T is the absolute temperature. This equation leads to the following equation for the diffusion coefficient of a binary electrolyte at infinite dilution, D° :

$$D^\circ = D_+^\circ D_-^\circ (z_+ - z_-)/(z_+ D_+^\circ - z_- D_-^\circ) \quad [2.15]$$

Several experimental methods have been described for the measurement of the conductances and diffusion coefficients of electrolytes in concentrated solutions (Robinson and Stokes, 1959). These can be combined with the transference numbers, which can be obtained by cell measurements, to estimate the ionic mobilities and diffusion coefficients. In the absence of direct experimental data the diffusion coefficients can be calculated from the mean activity coefficients of the electrolyte, γ_{\pm} , by the following equation

$$D = D^\circ \eta^\circ \left(1 + \frac{d \ln \gamma_{\pm}}{d \ln m} \right) / \eta \quad [2.16]$$

where m is the molality and η and η° are the viscosities of the solution and the solvent respectively. This equation is a simplified form of equations [11-67] of Robinson and Stokes (1959). For more accurate calculations additional terms are required to account for the electrophoretic and hydration effects. These terms change the values by a few percent and certainly are insignificant in the present calculations since the diffusion coefficients are reduced drastically because of the presence of the matrix.

The relation between the conductance and viscosity in concentrated solutions of strong electrolytes is described by the equation (Wishaw and Stokes, 1954)

$$\Lambda = (\Lambda^{\circ} - \frac{p\sqrt{C}}{1+q}) (1 + \frac{\Delta X}{X}) \eta^{\circ} / \eta \quad [2.17]$$

where Λ is the equivalent conductance, X is the electric field, and p and q are arbitrary constants.

In the absence of transference numbers the individual mobilities and diffusion coefficients in concentrated solutions can be calculated in a simple way (Lin and Winnick, 1974). The ionic diffusion coefficients can be calculated with the assumption that the relation between D^{+} , D^{-} , and D is the same as at infinite dilution

$$D = D_{+}D_{-}(z_{+} - z_{-})/(z_{+}D_{+} - z_{-}D_{-}) \quad [2.18]$$

and

$$D_{+} = D_{+}^{\circ} D_{-}/D_{-}^{\circ} \quad [2.19]$$

In the same way the ionic mobilities can be calculated from the equivalent conductance. The ionic mobilities and diffusion coefficients can then be calculated in a multicomponent solution utilizing their dependence on the viscosity of the solution. The values of u_i and D_i in multicomponent solutions are calculated by the relations

$$D_m = D\eta/\eta_m \quad [2.20]$$

and

$$u_m = u \eta / \eta_m \quad [2.21]$$

where the subscript m refers to the multicomponent mixture.

To calculate the effective mobilities and diffusion coefficients in a porous matrix it is necessary to multiply their values in matrix-free solutions by a matrix labyrinth factor, α . The most widely used equations for calculating α in a porous medium are the following equations by Wheeler (1951) and Mackie and Meares (1955), respectively:

$$\alpha = \epsilon / 2 \quad [2.22]$$

and

$$\alpha = \epsilon^2 / (2 - \epsilon) \quad [2.23]$$

where ϵ is the porosity.

Electroneutrality is preserved in the solution except in the double layer near the electrodes which has a thickness of less than 100 Å. Because there are several anions (CO_3^{2-} , HCO_3^- , and OH^-) in the solution and only one cation in appreciable concentrations the concentration of the cation varies across the matrix to preserve solution electroneutrality. This gives rise to concentration overpotential in the solution which adds to the power losses of the cell.

Theory of Porous Gas-Diffusion Electrodes

Electrode reactions involving one or more gaseous components require an intimate contact between the gas and electrolyte in the vicinity of the solid electrode. Because of the capillary forces, this

can best be realized in a porous electrode. The performance of gas-diffusion electrodes depends largely on the penetration of the gas and electrolyte into the electrode pores.

Several models have been described which simulate the microstructure of the electrode pores and the contact between the gas and electrolyte phases (Bockris and Srinivasan, 1969), but their success depends on the manner of preparation of the electrode. For instance, teflon added to the catalyst particles in the electrode matrix, such as those used in the HDC cells, decreases the wetting power of the electrode. The situation in this case is probably similar to that shown in Fig. 1 (Austin, 1968). The gas-electrolyte area decreases as the electrolyte penetrates into the electrode pores towards the gas side. For a certain gas pressure there is a limit for the electrolyte penetration. The capillary equilibrium in the electrode pores depends on the surface tension of the electrolyte and the pore radius (Markin et al., 1966).

The surface tension of the electrolyte depends on the concentrations and specific nature of the ions (Randles, 1963). Highly hydrated ions and tetraalkylammonium ions are classified as surface-active ions because they tend to increase the surface tension with concentration at a higher rate than other ions. Electroosmotic forces also influence the solvent transport in porous media under the applied electrical field (Lakshminarayanaiah, 1969), and result in the dependence of the electrolyte circulation on the current density distribution in the electrode structure (Huddleston and Aylward, 1973).

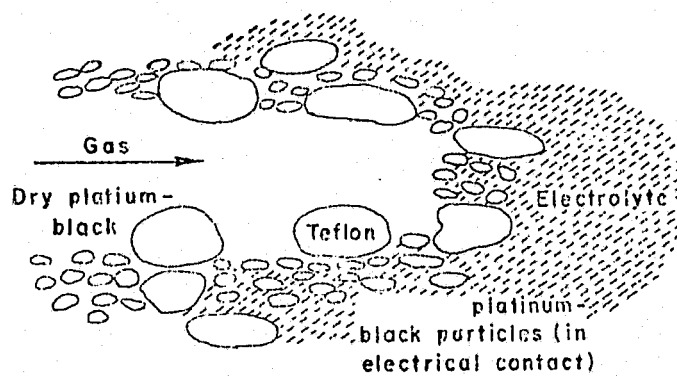


Fig. 1 Illustration of Partially Wetted Electrode

Mass transport processes play an important role in the performance of gas-diffusion electrodes. Convection and diffusion bring the reactants from the bulk gas phase to the electrode surface. Inside the electrode pores two mechanisms are possible for the transport in the gas phase; gas diffusion under a concentration gradient and gas permeation under a total pressure gradient.

Four types of gas diffusion mechanisms are also possible depending on the relative magnitudes of the mean free path of the gas molecules and the pore diameter (Austin, 1968). In the electrolyte phase filling of the electrode pores; diffusion, ionic migration, and convection may all restrict. Convective currents result from temperature and surface tension gradients in the electrode pores and random fluctuations of the gas pressure. This results in a relatively uniform concentration in the electrolyte throughout the electrode.

Electrode processes are usually studied in relation to the overpotential-current density dependence. Electrode overpotential consists of three components; activation, concentration, and ohmic. The equations derived for the overpotential-current density dependence on the basis of simple mathematical models (Bockris and Srinivasan, 1969) do not predict the correct values because of the geometric complexity of the practical pore systems. However, they can give insight to the desirable properties of the electrodes to obtain the maximum power output from a fuel cell.

CHAPTER III

PROCESS DESCRIPTION AND CELL DESIGN

Process Description

Carbon dioxide is continuously removed from the cabin air as it passes over the cathode of the HDC cell. Oxygen in the air diffuses first into the liquid film within the cathode pores and reacts to form hydroxyl ions



CO₂ diffuses simultaneously and reacts with the OH⁻ ions to form carbonate ions



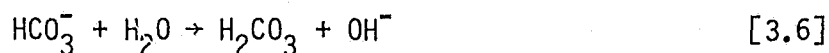
Pure hydrogen is fed into the anode side. After diffusing into the liquid film at the anode, it forms hydronium ions



The lowered pH of the anolyte favors a higher bicarbonate concentration according to the equilibrium [2.2]. These HCO₃⁻ ions dissociate to CO₂ which is removed by the H₂ stream



Because of the low pH at the anode, the HCO_3^- ions react to form carbonic acid which also dissociates to CO_2



These reactions combined result in H_2O production, pumping the CO_2 from a low partial pressure at the cathode side to a high partial pressure at the anode side, and the generation of electrical energy. The water vapor is carried by the air stream to the WVE cell and the CO_3/H_2 mixture is fed to the Sabatier reactor. The generated electrical energy is used in the WVE cell. The concentrator cell is cooled solely by the flowing air stream.

Major Requirements

The main function of the concentrator is to maintain the CO_2 partial pressure in the cabin atmosphere at about 3mm Hg. However, it should be flexible enough to accommodate normal atmospheric concentrations of CO_2 (0.25 mm Hg). For one-man requirements, a CO_2 removal of 2.20 lb/day is needed. With the present design, it is possible to obtain a removal rate of 2.40 lb/day at 3mm Hg (Huddleston and Aylward, 1975c). The concentrator consisted of four identical cells.

Energy requirements are also important in long-space missions. The design should allow no more than 50 $\mu\text{V/hr}$ of long term voltage decay rate. The voltage decay rate for the combined WVE and HDC cells in the present design does not exceed 42 $\mu\text{V/hr}$. In addition, the con-

centrator should show stable performance in the air relative humidity range of 35 to 90%.

Cell Design

Cell configuration

The concentrator is shown schematically in Fig. 2. It is based on the "cell pair" concept in which back to back hydrogen electrodes facilitate the maintainability of the system. The electrodes are 1 ft^2 each and this relatively large size is chosen to minimize the total cell weight by reducing the percentage of the wasteful peripheral material. The cathode chamber is made of titanium and it has 96 rectangular air ducts $0.2 \text{ " } \times 0.19 \text{ "}$ each. The length of the air path is 6 inches.

Hydrogen flows in a serpentine path in a cross flow manner with respect to the air stream. The center housing is designed in such a way as to minimize the pressure drop in the H_2 stream (Huddleston and Aylward, 1973). Hydrogen flows at a rate of $600 \text{ cm}^3/\text{min}$ with a back pressure of 1 psig. The use of pre-bent housing employing spacers of rigid material guarantees a uniform matrix thickness at the specified H_2 pressure (Russell, 1973).

The cell is provided with a reservoir of porous 'Tissuquartz' which absorbs the excess electrolyte during cell flooding at humid conditions and returns it to the matrix during drying conditions.

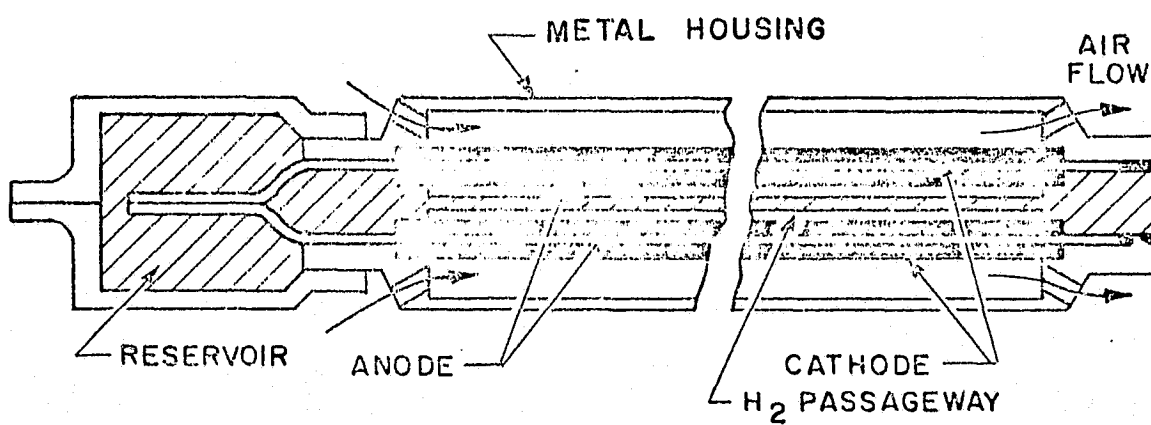


Fig. 2 Cross Section in Cell Pair

Cell electrodes

The design of the electrodes is of major importance for cell performance. Both the electrodes in the present design are made of platinum precipitated on a metallic screen with teflon binder. The teflon binder, being hydrophobic, minimizes flooding problems. The amount of catalyst loading and the manufacturing procedure determines the electrodes performance. The thickness of the electrodes is of the order of 3 to 7 mils.

Cell matrix

The matrix material and compression are selected to obtain minimum internal cell resistance, chemical stability under the operating conditions, and maximum CO_2 removal efficiency. In the present design, the matrix consists of one layer of Tissuquartz (18 mils) sandwiched between two layers of fuel cell asbestos (20 mils each) and the whole compressed to 25 mils. This matrix set was tested while saturated with Cs_2CO_3 solution and a six-month endurance test showed that the matrix maintains sufficient compression resistance (60 psig) to provide good interface contact between the matrix, electrodes, and housings (Huddleston and Aylward, 1973).

Humidity control

Previous versions of the device used Cs_2CO_3 electrolyte (Winnick et al., 1974). Cell drying occurred when the air relative humidity dropped below 60%. At these conditions, CsHCO_3 starts to precipi-

tate at the anode because of its low solubility. This required extensive humidity control and cell cooling which was acceptable in the six-man subsystem.

For a one-man subsystem it is desirable to use an electrolyte solution which has lower vapor pressures and thus has higher stability in low humidity environments. Investigation led to tetramethylammonium carbonate (TMAC) which enabled the operation at air relative humidities in the range of 35-90% (Huddleston and Aylward, 1972). The solubility of NMe_4HCO_3 is about 88 wt% at the cell temperature while the solubility of $(\text{NMe}_4)_2\text{CO}_3$ is 52 wt%. Therefore, NMe_4HCO_3 precipitation is not a problem as it is with CsHCO_3 .

The NMe_4^+ ions are somewhat unstable, forming trimethylamine and methyl ion (Huddleston and Aylward, 1972). The latter reacts with OH^- ions to form methyl alcohol. In the HDC cell, however, proper design and operation can prevent this decomposition. At the cathode, platinum black is a poor decomposition catalyst in the oxygen atmosphere. At the anode, the pH is normally low and does not promote decomposition (Huddleston and Aylward, 1972).

CO_2 removal efficiency

According to the overall cell reaction, as described above, two moles of CO_2 can be transferred for one mole of O_2 and two moles of H_2 consumed. Since the current produced is proportional to the amounts of H_2 and O_2 reacting this corresponds to 100% current efficiency, i.e., when one mole of CO_2 is transferred for each two Faradays of electricity. Sometimes this efficiency is expressed as the "Transfer Index" which is

the equivalent weight ratio of CO_2 removed for each pound of O_2 consumed. A current efficiency of 100% is equivalent to a transfer index of 2.75.

At very high partial pressures of CO_2 in the air stream the concentration of OH^- ions in the catholyte drops significantly and the HCO_3^- ions concentration increases. This may lead to the transport of CO_2 as HCO_3^- instead of CO_3^{2-} and this corresponds to 200% current efficiency since now one mole of CO_2 is transferred for each one Faraday of electricity. In the range of operation expected of the HDC cell the concentration of CO_2 in the air stream will not exceed 15 mm Hg. The CO_2 is removed through CO_3^{2-} ion transport which yields less than 100% current efficiency. However, it is possible to obtain current efficiencies slightly higher than 100% if the CO_2 concentration exceeds normal levels.

CHAPTER IV

MATHEMATICAL MODELING

Introduction

Two approaches have been used to predict the performance of the concentrator under various conditions. In the first approach, test data at selected conditions are used to obtain empirical equations relating the performance data, e.g., the CO_2 removal rate to the important parameters (Marshall et al., 1974). The second approach is based on a fundamental model of the reactions and transport mechanisms which take place in the cell (Lin and Winnick, 1974). This approach is more useful since the data can be extrapolated with more confidence to off-design conditions and can predict the effect of unstudied parameters. Furthermore, some performance characteristics can be predicted which are either difficult or impossible to measure. One example is the variation of the concentration of the different species across the matrix; which can be used to predict the incidence of precipitation or, in other words, the limits of cell operation. These concentrations can also be useful in qualitatively predicting some of the important performance parameters, e.g., the anode overvoltage.

In this chapter the various reaction mechanisms and prevailing equations for the steady-state case are described. These equations are

then combined to yield the differential equations which are used in design. The numerical methods used in solving these equations are also discussed.

Mass Transfer and Reaction Rates

The concentrator is considered to be divided into subcells in the direction of the air flow and each subcell to be subdivided into five zones as shown in Fig. 3. In each zone different reactions and mass transfer processes take place. These are examined separately for each zone. For convenience, the different species will be represented by numbers; 1 for HCO_3^- , 2 for OH^- , 3 for CO_3^{2-} , 4 for NMe_4^+ , 5 for CO_2 , and 6 for H_2O .

1. Air zone

In this zone CO_2 is transferred from the gas phase to the electrode surface and then through the cathode pores to the liquid film inside. The flux of CO_2 in this zone, N_5 , is given by

$$N_5 = h_{5c} (P_{5c} - P_{5c}^+) / RT \quad [4.1]$$

where h_{5c} is the overall mass transfer coefficient, P_{5c} and P_{5c}^+ are the partial pressures of CO_2 in the bulk gas phase and at the gas-liquid interface, respectively, R is the gas constant, and T is the temperature. The subscript c refers to the cathode region.

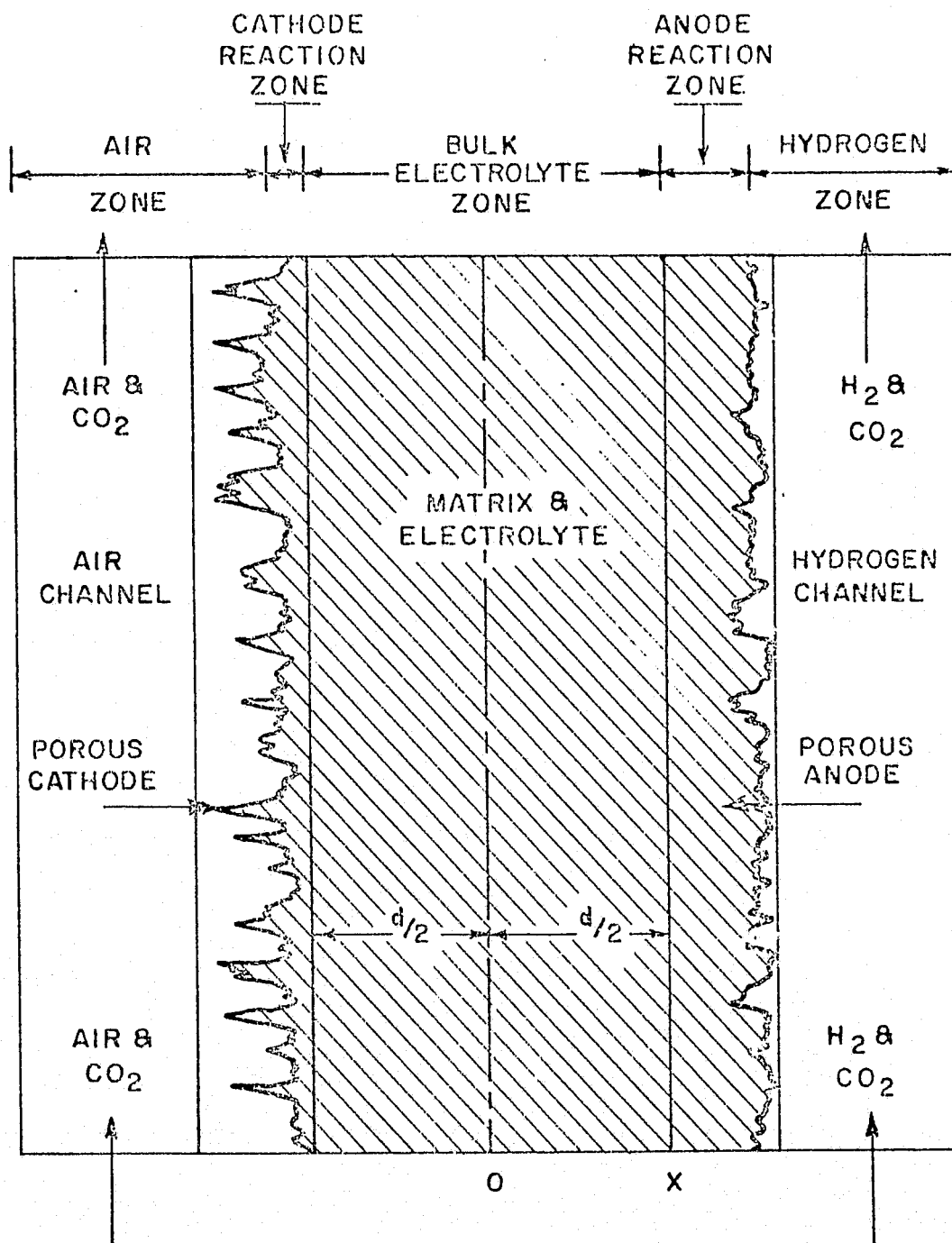


Fig. 3 Schematic of a Subcell

The relation between P_{5c}^{\dagger} and the concentration of C_{5c}^{\dagger} in the liquid film is

$$P_{5c}^{\dagger} = H C_{5c}^{\dagger} \quad [4.2]$$

where H is the Henry's law constant which is a function of the temperature and the ionic strength of the solution. The average mass transfer driving force can be taken for any subcell as the logarithmic mean of the inlet and outlet values

$$(P_c - P_c^{\dagger})_{l.m.} = (\Delta_I - \Delta_0) / \ln(\Delta_I / \Delta_0) \quad [4.3]$$

where Δ is $(P_c - P_c^{\dagger})$ and the subscripts I and 0 refer to the inlet and outlet of the subcell.

The mass balance in the air zone is given by

$$(P_{5c})_I - (P_{5c})_0 = N_5 ART / V_c \quad [4.4]$$

where V_c is the volumetric air flow rate and A is the geometric electrode area in the subcell. These equations can be combined together to give a single expression for C_{5c}^{\dagger}

$$C_{5c}^{\dagger} = [(P_{5c})_I - N_5 ART / \{V_c (1 - \exp\{-h_{5c} A / V_c\})\}] / H \quad [4.5]$$

In the same way, the water vapor pressure of the electrolyte is given by

$$P_{6c}^{\dagger} = (P_{6c})_I - N_6 ART / \{V_c [1 - \exp\{-h_{6c} A / V_c\}]\} \quad [4.6]$$

2. Cathode reaction zone

Because of the high pH at the cathode, CO_2 absorption proceeds via the basic mechanism described by equation [2.1] and [2.2]. The combination between CO_2 and OH^- ions is the rate-determining step. The local rate of reaction, r_c , is given by the equation

$$r_c = k_i (C_2 C_5^+ - C_1 / K_i) \quad [4.7]$$

where k_i is the rate constant of reaction [2.1] and K_i is its equilibrium constant. The second step is instantaneous and the corresponding equilibrium is established. The equilibrium relation is

$$C_3 / (C_1 C_2) = K_{ii} \quad [4.8]$$

The pH at the cathode is usually in the range of 13 to 14 (Huddleston and Aylward, 1973). The rate constant is in the range of $8500 \text{ sec}^{-1} (\text{mole/l})^{-1}$ (Kern, 1960). The characteristic reaction time is thus in the range from 1.2×10^{-4} to 1.2×10^{-3} sec. The characteristic diffusion time is dependent on the electrolyte hydrodynamics which cannot be measured within the pores. However, in packed towers the diffusion time is usually in the range from 5×10^{-3} to 4×10^{-2} sec (Astarita, 1967). Thus, the condition [2.8] is satisfied and the reaction can be considered in the fast-reaction regime. Mathematically, this is expressed by the equation

$$N_5 = S_c (k_i D_5 C_2)^{1/2} [C_5^+ - C_1 / (K_i C_2)] \quad [4.9]$$

where S is the total gas-electrolyte interface area per unit of electrode geometric area and D_5 is the diffusivity of CO_2 in the electrolyte. In these equations the equilibrium constants are calculated from values at infinite dilution by multiplication by the appropriate activity coefficients evaluated at average concentrations.

3. Bulk electrolyte zone

The transport of CO_3^{2-} , HCO_3^- , and OH^- ions in this zone can be expressed by equation [2.12]. It is conceivable that all the water produced by the fuel cell reaction is removed by the air stream because of the high air flow rate compared with the hydrogen flow rate. This was actually proved by measuring the dew point of the leaving air stream (Lin et al., 1974). Accordingly, the water flux in the cell is given by

$$N_6 = - I/2 F \quad [4.10]$$

where I is the cell current density. The average molar bulk velocity of the solution is given by

$$v = \frac{1}{C_T} \sum Z_j N_j \quad [4.11]$$

where Z_j is the mole fraction of the species j in solution, C_T is the total number of moles per unit volume, and the summation extends over water and all the species in solution. Since the individual fluxes are unknown beforehand, an iteration procedure is required.

However, water represents about 90% of the total number of moles in solution. For simplicity, it is assumed that the other species do not contribute to the net bulk velocity of the solution. In that case the net bulk velocity is given by

$$v = - I/2 F C_T \quad [4.12]$$

In fact, it is found that the assumption of zero bulk velocity gives the same results as obtained with the above assumption which means that the inclusion of the other species in calculating the net bulk velocity is totally unnecessary.

The individual flux of each component varies with the distance x , but the following sums are independent of x at steady state:

$$N_1 + N_3 + N_5 = N_{5T} \quad [4.13]$$

$$N_1 + N_2 + 2N_3 = I/F \quad [4.14]$$

Here N_{5T} represents the total CO_2 flux. Since the cation does not participate in the cell reaction, its flux vanishes at every point

$$N_4 = 0 \quad [4.15]$$

Substituting for the flux of each component from equation [2.12], equations [4.13] to [3.12] give the following differential equations:

$$\begin{aligned} D_1 \frac{dC_1}{dx} - F u_1 C_1 \frac{d\phi}{dx} + D_3 \frac{dC_3}{dx} - 2F u_3 C_3 \frac{d\phi}{dx} \\ + D_5 \frac{dC_5}{dx} = -N + I(C_1 + C_3 + C_5)/(2F C_T) \end{aligned} \quad [4.16]$$

$$D_1 \frac{dC_1}{dx} - Fu_1 C_1 \frac{d\phi}{dx} + D_2 \frac{dC_2}{dx} - Fu_2 C_2 \frac{d\phi}{dx} + 2 D_3 \frac{dC_3}{dx} - 4Fu_3 C_3 \frac{d\phi}{dx} = - I/F + I(C_1 + C_2 + 2C_3)/(2FC_T) \quad [4.17]$$

$$D_4 \frac{dC_4}{dx} + Fu_4 C_4 \frac{d\phi}{dx} + IC_4/(2FC_T) = 0 \quad [4.18]$$

In this zone reactions [2.1] and [2.2] are assumed to be in equilibrium. The concentrations C_2 and C_5 are given by the following equations:

$$C_2 = C_3/(C_1 K_{ii}) \quad [4.19]$$

$$C_5 = C_1/(C_2 K_i) \quad [4.20]$$

Electrical neutrality also results in the following equation:

$$C_4 = C_1 + C_2 + 2C_3 \quad [4.21]$$

4. Anode reaction zone

In this zone CO_2 is released by the decomposition of the HCO_3^- ions and H_2CO_3 by the reverse of reactions [2.1] and [2.3], respectively. The combined reaction rate constant can be obtained as follows:

$$r_a = k_i' C_1 - k_i C_5 C_2 + k_{iii}' [H_2CO_3] - k_{iii} C_5 a_6 \quad [4.22]$$

where a_6 is the water activity, k_i and k_i' are the forward and backward rate constants of reaction [2.1], and k_{iii} and k_{iii}' are the

forward and backward rate constants of reaction [2.3]. The relations between these rate constants are

$$k'_i = k_i/K_i \quad [4.23]$$

$$k'_{iii} = k_{iii}/K_{iii} \quad [4.24]$$

Since the reaction [2.4] is in equilibrium, $[H_2CO_3]$ is given by

$$[H_2CO_3] = C_1 a_6 / C_2 K_{iv} \quad [4.25]$$

where a_6 is the activity of water and K_{iv} is the equilibrium constant of reaction [2.4]. From equations [4.24] and [4.25] we obtain

$$k'_{iii}[H_2CO_3] = k_{iii} C_1 a_6 / (C_2 K_{iii} K_{iv}) \quad [4.26]$$

The equilibrium constants K_{iii} and K_{iv} are related to K_i by the relation

$$K_{iii} K_{iv} = K_i \quad [4.27]$$

By substitution of equations [4.23], [4.26], and [4.27] into equation [4.22] we obtain the following equation for the local rate of CO_2 production:

$$r_a = (k_i + k_{iii} a_6 / C_2) (C_1 / K_i - C_2 C_5^+) \quad [4.28]$$

Assuming the reaction to take place in the fast-reaction regime

$$N_5 = S_a [D_5 (k_i C_2 + k_{iii} a_6)]^{1/2} (C_1 / K_i C_2 - C_{5a}^+) \quad [4.29]$$

5. Hydrogen zone

The released CO_2 is removed by the hydrogen stream. The rate of removal is given by

$$N_5 = h_{5a}(P_{5a}^+ - P_{5a})/RT \quad [4.30]$$

where h_{5a} is an overall mass transfer coefficient in the anode zone. The equilibrium relation at the gas-liquid interface is

$$P_{5a}^+ = H C_{5a}^+ \quad [4.31]$$

The mass balance gives the following equation:

$$C_{5a}^+ = [(P_{5a})_I - N_5 RT / [V_a (1 - \exp\{-h_{5a} A / V_a\})]] / H \quad [4.32]$$

where V_a is the hydrogen volumetric flow rate in the anode zone.

Mathematical Model

The model describing the performance of the cell can be constructed from the above-mentioned equations. For simplicity, the following dimensionless variables are introduced:

$$\tilde{N}_j = N_j d / (C^* D^*) \quad j=1,2,\dots,5 \quad [4.33]$$

$$\tilde{D}_j = D_j / D^* \quad j=1,2,\dots,5$$

$$\tilde{C}_j = C_j / C^* \quad j=1,2,\dots,5$$

$$\tilde{u}_j = u_j RT / D^* \quad j=1,2,3,4$$

$$\tilde{I} = I d / (F C^* D^*)$$

$$(\tilde{P}_5)_I = (P_5)_I / (HC^*)$$

$$\tilde{K} = KC^*$$

$$\tilde{k}_c = k_i S_c^2 d^2 C^* / D^*$$

$$\tilde{k}_a = k_i S_a^2 d^2 C^* / D^*$$

$$\tilde{G} = a_6 k_{iii} / (k_i C^*)$$

$$\tilde{x} = x/d$$

$$\tilde{\Phi} = \Phi F / RT$$

$$\tilde{h}_{5c} = h_{5c} Hd / (RTD^*)$$

$$\tilde{h}_{5a} = h_{5a} Hd / (RTD^*)$$

$$\tilde{V}_c = V_c Hd / (ARTD^*)$$

$$\tilde{V}_a = V_a Hd / (ARTD^*)$$

where C^* and D^* are characteristic constant values of concentration and diffusivity and d is the thickness of the cell matrix.

By substitution and rearrangement in equations [4.7] to [4.32], the following two nonlinear differential equations are obtained:

$$\begin{aligned} f_1(\tilde{C}_1, \tilde{C}_3) \frac{d\tilde{C}_1}{dx} + f_2(\tilde{C}_1, \tilde{C}_3) \frac{d\tilde{C}_3}{dx} = - \tilde{N}_{5T} \\ + \tilde{I}(\tilde{C}_1 + \tilde{C}_3 + \tilde{C}_5 - \tilde{C}_1 \tilde{u}_1 / \tilde{u}_4 - 2\tilde{C}_3 \tilde{u}_3 / \tilde{u}_4) / (2\tilde{C}_T) \end{aligned} \quad [4.34]$$

$$f_3(\tilde{C}_1, \tilde{C}_3) \frac{d\tilde{C}_1}{dx} + f_4(\tilde{C}_1, \tilde{C}_3) \frac{d\tilde{C}_3}{dx} = -\tilde{I} \quad [4.35]$$

$$+ \tilde{I}(\tilde{C}_1 + \tilde{C}_2 + 2\tilde{C}_3 - \tilde{C}_1\tilde{u}_1/\tilde{u}_4 - \tilde{C}_2\tilde{u}_2/\tilde{u}_4 - 4\tilde{C}_3\tilde{u}_3/\tilde{u}_4)/(2\tilde{C}_T)$$

where

$$f_1 = \tilde{D}_1 + \tilde{D}_4(\tilde{C}_1^2 - \tilde{C}_3/\tilde{K}_{ii})(\tilde{u}_1 + 2\tilde{u}_3\tilde{C}_3/\tilde{C}_1)/(\tilde{u}_4\tilde{\psi})$$

$$+ 2\tilde{D}_5\tilde{K}_{ii}\tilde{C}_1/(\tilde{K}_{ii}\tilde{C}_2) \quad [4.36]$$

$$f_2 = \tilde{D}_4(2\tilde{C}_1 + 1/\tilde{K}_{ii})(\tilde{u}_1\tilde{C}_1 + 2\tilde{u}_3\tilde{C}_3)/(\tilde{u}_4\tilde{\psi})$$

$$+ \tilde{D}_3 - \tilde{D}_5\tilde{K}_{ii}\tilde{C}_1^2/(\tilde{K}_{ii}\tilde{C}_3^2) \quad [4.37]$$

$$f_3 = \tilde{D}_1 + \tilde{D}_4(\tilde{C}_1^2 - \tilde{C}_3/\tilde{K}_{ii})[\tilde{u}_1 + \tilde{u}_2\tilde{C}_3/(\tilde{K}_{ii}\tilde{C}_1^2) + 4\tilde{u}_3\tilde{C}_3\tilde{C}_1]/(\tilde{u}_4\tilde{\psi})$$

$$- \tilde{D}_2\tilde{C}_3/(\tilde{K}_{ii}\tilde{C}_1^2) \quad [4.38]$$

$$f_4 = \tilde{D}_4(2\tilde{C}_1 + 1/\tilde{K}_{ii})(\tilde{u}_1\tilde{C}_1 + \tilde{u}_2\tilde{C}_3/(\tilde{K}_{ii}\tilde{C}_1) + 4\tilde{u}_3\tilde{C}_3)/(\tilde{u}_4\tilde{\psi})$$

$$+ 2\tilde{D}_3 + \tilde{D}_2/(\tilde{K}_{ii}\tilde{C}_1) \quad [4.39]$$

and $\tilde{\psi}$ is given by

$$\tilde{\psi} = \tilde{C}_1^2 + 2\tilde{C}_1\tilde{C}_3 + \tilde{C}_3/\tilde{K}_{ii} \quad [4.40]$$

The boundary conditions are

$$\begin{aligned} \tilde{N}_{5T} = & (\tilde{k}_c \tilde{C}_2 \tilde{D}_5)^{1/2} \{ (\tilde{P}_{5c})_I - \tilde{N}_{5T} / [\tilde{V}_c (1 - \exp\{-\tilde{h}_{5c}/\tilde{V}_c\})] \\ & - \tilde{C}_1 / \tilde{C}_2 \tilde{K}_i \} \quad \text{at } \tilde{x} = -\frac{1}{2} \end{aligned} \quad [4.41]$$

$$\begin{aligned} \tilde{N}_{5T} = & [\tilde{k}_a \tilde{D}_5 (\tilde{C}_2 + \tilde{G})]^{1/2} \{ \tilde{C}_1 / \tilde{K}_i \tilde{C}_2 - (\tilde{P}_{5a})_I \\ & - \tilde{N}_{5T} / [\tilde{V}_a (1 - \exp\{-\tilde{h}_{5a}/\tilde{V}_a\})] \} \quad \text{at } \tilde{x} = \frac{1}{2} \end{aligned} \quad [4.42]$$

As it has been assumed, all the water produced by the cell reaction goes to the air stream. In dimensionless form, equation [4.6] becomes

$$\tilde{P}_{6c}^+ = (\tilde{P}_{6c})_I + \tilde{I} / \{ 2\tilde{V}_c [1 - \exp(-\tilde{h}_{6c}/\tilde{V}_c)] \} \quad [4.43]$$

Since the catholyte consists mainly of $(\text{NMe}_4)_2\text{CO}_3$, its vapor pressure data can be used to obtain the catholyte concentration

$$\tilde{C}_4 = F(\tilde{P}_{6c}^+, T) \quad [4.44]_m$$

The catholyte temperature for the Hamilton Standard design varies linearly along the length of the air path and can be calculated from the rate of heat generation and the cell dimensions (Lin et al., 1974). The rate of heat generation, Q , is calculated by the equation

$$Q = (\Delta H_R N_6 - EI/J)A \quad [4.45]$$

where ΔH_R is the heat of formation of water vapor, E is the cell voltage, and J is the heat/energy conversion factor. The last three equations provide the additional boundary condition

$$\tilde{C}_1 + \tilde{C}_3/(\tilde{C}_1 \tilde{K}_2) + 2\tilde{C}_3 = \tilde{C}_4 \quad \text{at } \tilde{x} = -\frac{1}{2} \quad [4.46]$$

Numerical Method of Solution

The nonlinear differential equations [4.34] and [4.35] describe the variation of \tilde{C}_1 and \tilde{C}_3 across the cell matrix. The concentrations of other components, \tilde{C}_2, \tilde{C}_4 , and \tilde{C}_5 are implicitly included in these equations and can be calculated from the equilibrium relations [4.19] and [4.20] and the electroneutrality relation [4.21]. The complexity of these equations, apart from the high non-linearity of the coefficients, lies in the fact that these equations include the unknown parameter, \tilde{N}_{5T} , which in turn is a function of the boundary conditions. These boundary conditions consist of two relations between \tilde{C}_1 and \tilde{C}_3 , [4.41] and [4.42], which implicitly include the parameter \tilde{N}_{5T} . An independent boundary condition, [4.44], is obtained from the water and energy balance on the cell and it relates \tilde{C}_1 and \tilde{C}_3 at $\tilde{x} = -\frac{1}{2}$.

Shooting methods (Roberts and Shipman, 1971) are suitable for this kind of two-point boundary value problems. The procedure is to assume a value for \tilde{N}_{5T} , to calculate \tilde{C}_1 and \tilde{C}_3 at $\tilde{x} = -\frac{1}{2}$ for this value of \tilde{N}_{5T} , and then to integrate the differential equation from $\tilde{x} = -\frac{1}{2}$ to $\tilde{x} = \frac{1}{2}$. The boundary condition at $\tilde{x} = \frac{1}{2}$ can then be calculated and compared with the guessed value. Some of the shooting

methods use the difference between the calculated and predicted values to make corrections for a new guess. However, this cannot be used here because of the dependence of the differential equation and boundary conditions on the same parameter, \tilde{N}_{5T} . Instead, the new guess is chosen higher or lower according to whether the calculated value at $\tilde{x} = \frac{1}{2}$ is higher or lower than the guessed value at $\tilde{x} = -\frac{1}{2}$.

Successful application of shooting methods greatly depends on the stability of the numerical integration technique used. Predictor-corrector methods are of interest because of their relative economy in terms of the number of derivative evaluations required for a given order algorithm. The method used here is based on a predictor-corrector algorithm developed by Crane and Klopfenstein (1965). The algorithm is fourth-order and has higher absolute and relative stabilities than other predictor-corrector methods. During integration, the step size is increased or decreased in accordance with the estimated error. This guarantees a minimum number of calculations for a certain degree of accuracy which is determined by the accuracy of the computer.

Theories of convergence and inherent stability of the differential equations (Keller, 1968) cannot be examined for this problem. However, numerical experimentation shows that the solution converges as though these theories apply.

CHAPTER V

EXPERIMENTAL DATA

Introduction

This chapter summarizes all the test data and experimental information obtained with TMAC electrolyte. These data will be required for several reasons. First, they will be used to evaluate the parameters which cannot be estimated independently such as the mass transfer coefficients and gas-electrolyte interface area. Second, they will be compared with the values predicted by the model after the required coefficients have been calculated. This will indicate how close the model simulates the actual processes taking place in the cell. Fundamental property tests were also made on the electrolyte, electrodes, and matrix separately. These will help in justifying some of the assumptions made here and to explain some of the obtained results.

Performance Data

Two sets of performance data have been obtained; analytical cell data and full-scale cell data. The first series of tests were run to obtain detailed information on cell operation with TMAC and to compare these results to those obtained with Cs_2CO_3 electrolyte. The second series was run to test the long-duration performance under

design conditions. The design and measurements in each case are described in the following:

1) Analytical cell test

The analytical cell was constructed from fuel-cell pair hardware to give an electrode area of $1/24 \text{ ft}^2$ with an airflow path length of 6 inches. The matrix consisted of one layer of Tissuquartz (18 mils) sandwiched between two layers of fuel cell asbestos (20 mils each) and the whole compressed to 25 mils. The electrodes were PPF anode and DS 16-0 cathode (coded names). Air temperature was 70°F . The main test results included CO_2 removal efficiency, open-cell voltage, cathode and anode overvoltages, anolyte and catholyte pH's and IR drop across the matrix. The parameters studied were current density ($12\text{-}30 \text{ A/ft}^2$), P_{CO_2} ($0.25\text{-}4 \text{ mm Hg}$), air velocity ($5\text{-}15 \text{ ft/sec}$) and air relative humidity ($33.6 - 77.2\%$). Each test condition was run for approximately two days with at least three data readings taken each day. These data were reported by Huddleston and Aylward (1973).

2) Full-scale cell tests

Several tests have been made on the full cell by Hamilton Standard. The most recent lasted for 90 days and involved taking data for operating currents and inlet air P_{CO_2} levels over a limited range ($5\text{-}18 \text{ A/ft}^2$ and $1\text{-}3 \text{ mm Hg}$). The air flow rate was fixed at $10 \text{ ft}^3/\text{min}$ per cell which corresponds to an air velocity of 6.6 ft/sec . No other variation

of test conditions was made except for the decrease of the inlet air dew point from 60°F to 40°F in the last stage of the program. CO_2 removal efficiency and cell voltage were the measured output data. The data were recorded twice every day and were reported by Huddleston and Aylward (1975 a,b). The variation of the steady-state removal efficiency with current density and P_{CO_2} was summarized in a final report (Huddleston and Aylward, 1975 c) to NASA.

Special Tests

1) Electrolyte tests

The first investigation of the TMAC electrolyte (Huddleston and Aylward, 1972) was to determine the approximate solubility and maximum dew point depression for the carbonate, bicarbonate, and hydroxide. The solubility of these compounds at room temperature are 52 wt %, 88 wt %, and 36 wt %, respectively. The depression of the dew point of these saturated solutions are 32°F, 55°F, and 28°F, respectively. The electrochemical stability of these compounds decreases in the order: $\text{NMe}_4\text{HCO}_3 > (\text{NMe}_4)_2\text{CO}_3 > \text{NMe}_4\text{OH}$.

The important properties of the three electrolytes were reported by Aylward (1974). The density measurements were accurate to four significant figures; viscosity measurements were accurate to three significant figures; specific conductivity were accurate to three significant figures; and electrolyte-water vapor pressures were accurate to $\pm 0.5\%$.

The absorption of CO_2 in TMAC in the presence of a catalyst was tested. It was demonstrated qualitatively (Huddleston and Aylward, 1973) that small amounts of the enzyme carbonic anhydrase at very low levels are effective in accelerating the absorption reaction in TMAC. However, addition of this catalyst to the electrolyte in the analytical cell tests showed no significant improvement in the removal efficiency. This indicates that the CO_2 , OH^- reaction is not rate controlling under normal operating conditions.

An error analysis study (Russell, 1973) showed that the measured CO_2 removal-efficiencies are accurate to $\pm 4\%$.

2) Electrode tests

The selection of DS 16-0 cathode for the TMAC cells came after a series of tests on different cathode designs for cells with Cs_2CO_3 electrolyte (Huddleston and Aylward, 1973). The significant improvement of CO_2 removal efficiency with increasing electrode porosity was explained by the increase of the total available gas-catholyte interface area and the increase of the intra-cathode CO_2 gas mass transport rate. This was also explained by the increase of the electrode electronic resistance with porosity which results in a significant drop-off in the current density remote from the current collector screen. This results in a decrease of the electroosmotic pumping of the electrolyte towards the air side while the capillary force, which is independent of position from the current collector screen, returns the electrolyte towards the matrix (Huddleston and Aylward, 1973). Floating-electrode

tests showed that the cathode overvoltage increases with porosity as expected.

The anodes are of the PPF type containing 15 mg of catalyst (platinum) per cm^2 . Floating electrode tests showed that they have the lowest overvoltage among tested anodes. In the analytic cell tests the anode overvoltage obtained is typically one to two hundred millivolts greater than that obtained with the floating electrode tests. This was explained by the decrease of anolyte concentration which was shown to increase the anode overvoltage. The anode polarization consists mainly of concentration and ohmic components; the activation component is very small at the operating current densities. Characteristic X-ray examination of the anode showed that over long periods teflon migrates to the matrix side while platinum migrates to the H_2 side. This results in a decrease in the wicking rate of the anode since teflon is hydrophobic. This is responsible for the long-term power decay rate and may be remedied by current interruption and N_2 purge (Huddleston and Aylward, 1973). The problem of short-term power decay is attributed to the formation of a reduced CO_2 complex layer because of the low pH of the anolyte; the anode is reactivated by 10 sec. N_2 purge at one hour intervals (Aylward, 1975).

3) Matrix tests

The effect of matrix thickness was tested for Cs_2CO_3 electrolyte on the analytical cell (Huddleston and Aylward, 1973). One, two, and

four layers of asbestos were tested at the same compression with thicknesses of 12.5, 25, and 50 mils, respectively. The removal efficiencies (based on CO_3^{2-} transport) at 18 A/ft^2 were 66%, 98%, and 106%, respectively. Increasing the matrix thickness lowers the anolyte pH which was found to increase the chemical attack of the asbestos at the interface between the matrix and the anode causing the matrix to adhere to the anode. With TMAC electrolyte the anolyte pH does not show as strong a dependence on matrix thickness as with Cs_2CO_3 . This reduces the problem of matrix sticking, as observed experimentally (Huddleston and Aylward, 1973).

For the matrix materials used in the present cell several tests were made to determine the optimum compression, which results in a minimum internal cell resistance. The electrical resistance of the electrolyte matrix combination was measured using a special micrometer cell (Huddleston and Aylward, 1973). The matrix factor, which represents the ratio of the conductance of the matrix-electrolyte combination to that of the free electrolyte, was found to fit the following empirical equation

$$\alpha = \frac{d}{df \tau + \beta} \quad [5.1]$$

where d is the matrix thickness, f is a compression factor equal to $\frac{d}{(d-d^0)}$ where d^0 is the maximum compressed thickness defined as the original uncompressed thickness multiplied by $(1-\epsilon)$, where ϵ is the porosity, τ is the matrix tortuosity factor, and β is an empirical

constant dependent on the matrix material and electrolyte. No equation could fit data obtained for composite matrix material.

CHAPTER VI

MODEL PARAMETERS

Introduction

In this chapter the various parameters required by the model are estimated from electrolyte properties, theoretical and empirical equations and performance test data. The detailed calculations and tables are given in Appendix A. Unless otherwise specified, the values used here are at 25°C (77°F).

Activity Coefficients

Activity coefficients of electrolytes can be obtained from the vapor pressures of their solutions by (Robinson and Stokes, 1959);

$$\ln \gamma_{\pm} = (\phi - 1) + \int_0^m (\phi - 1) d \ln m \quad [6-1]$$

where the osmotic coefficient ϕ at molality m is given by

$$\phi = (-1000/\nu m M) \ln(P/P^\circ) \quad [6-2]$$

Here ν is the number of ions in solution per one molecule of electrolyte, M is the molecular weight of the solvent, and P and P° are the vapor pressures of the solution and solvent, respectively.

Evaluation of the integrand in equation [6-1] requires measurement of the vapor pressures of dilute solutions. Since accurate

measurement at low concentrations is difficult, activity coefficients have been tabulated for only a limited number of electrolytes (Robinson and Stokes, 1959). Several methods have been described for the calculation of activity coefficients where data are available only for concentrated solutions. Meissner and Tester (1972) constructed generalized charts for the calculation of the activity coefficients for certain classes of strong electrolytes. Earlier, Lietzke and Stoughton (1962) computed activity coefficients from osmotic coefficient data using a four-parameter equation containing the Debye-Huckel term for the electrostatic contribution and additional terms in ionic strength. They later presented a three-parameter equation in which the non-ideality of electrolytic solutions is attributed to both the Debye-Huckel interactions and randomized fused-salt behavior (Lietzke et al., 1968).

Tetraalkylammonium salts show significant deviation from the Debye-Huckel limiting law in dilute solutions (Pethybridge and Prue, 1968; Wen, 1972). Thus, the above-mentioned methods become unsuitable. In addition to the electrostatic and simple hydration interactions, mutual salting-out and structural hydration interactions must be considered. The mutual salting-out effects result from the fact that other ions distributed about a given ion occupy a volume in the polar solvent medium but with less polarization than an equal volume of solvent. In the case of large univalent ions such as NR_4^+ , these effects are quite significant and can be calculated from the

partial molal volumes of the cations and anions (Desnoyers and Conway, 1964). On the other hand, the structural interactions, which result from the compatibility or incompatibility of the hydration of the ions (Desnoyers et al., 1969) has been described only qualitatively. These interactions are estimated here by comparison with other properties of the solution.

Consider the model of Desnoyers and Conway (1964), wherein the activity coefficients are presumed separable into several component terms as follows:

$$\log \gamma = \log \gamma_{el} + \log \gamma_h + \log \gamma_{so} + \log \gamma_{st} \quad [6-3]$$

where the subscripts el, h, so, and st refer to the electrostatic, hydration, mutual salting-out, and structural interactions respectively. Equation [6-3] contains one more term, $\log \gamma_{st}$, than the Desnoyers-Conway equation. Equation [6-3] is assumed to apply from infinite dilution up to the lowest concentration for which osmotic coefficient data are available. Each term can then be estimated using appropriate equations, as described below.

The Debye-Huckel equation was used to calculate the electrostatic term, γ_{el} . To account for ion-pair formation, experienced even in strong electrolytes, Neff (1970) used the following form of the Debye-Huckel equation replacing the ionic concentrations with the activities:

$$\log \gamma_{el} = \frac{-0.5089 |z_+ z_-| \sqrt{\frac{1}{2} (\sum a_i z_i^2)}}{1 + 0.3291 L \sqrt{\frac{1}{2} (\sum a_i z_i^2)}} \quad [6-4]$$

This equation was tested for NaCl solutions where it was found that the distance of closest approach, L , was close to the sum of the crystallographic radii of Na^+ and Cl^- . This equation is here assumed applicable for the tetramethylammonium electrolytes with the parameter L calculated from the crystallographic radii.

The hydration term, γ_h , can be calculated either by the equation developed by Stokes and Robinson (1948) or by the following equation developed by Glueckauf (1955)

$$\log \gamma_h = (\xi - \nu) \log(1 + 0.018 \chi m) / \nu - (\xi / \nu) \log(1 - 0.018 \xi m) + 0.018 \chi (\chi + \xi - \nu) m / [2.303 \nu (1 + 0.018 \chi m)] \quad [6-5]$$

where ξ is the hydration number and χ is the ratio between the apparent molar volume of the electrolyte and the molar volume of water. This equation is preferable to the Robinson-Stokes equation since it does not contain the unknown term $\ln a_w$.

The mutual salting-out term, γ_{so} , can be calculated for an electrolyte "MA" from the following equations (Desnoyers and Conway, 1962):

for 1:1 electrolyte

$$\log \gamma_{so} = (7.156 C / 4605) [\bar{V}_- / (3L_+) + \bar{V}_+ / L_+ + \bar{V}_+ / (3L_-) + \bar{V}_- / L_-] \quad [6-6]$$

for 1:2 electrolyte

$$\log \gamma_{s0} = (7.156 \text{ C}/4605)[4\bar{V}_-/(5L_+) + 2\bar{V}_+/L_+ + \bar{V}_+/L_- + 4\bar{V}_-/L_-] \quad [6-7]$$

where \bar{V}_j and L_j are the partial molar volume and ionic radius for the ion j . To account for ion-pair formation, the same procedure used in deriving equation [6-4] was also used in modifying equations [6-6] and [6-7], i.e. the concentration was replaced by the activity and the ionic radius was taken as the crystallographic radius.

The final term, γ_{st} , can be calculated by difference for electrolytes where activity coefficients are known. According to the structural interaction model (Desnoyers et al., 1969) this term results from four types of interactions which depend on the structural properties of the ions. This term is calculated here for the tetramethylammonium halides from their tabulated activity coefficients (Lindenbaum and Boyd, 1964; Wen et al., 1966; Levien, 1965) and use these values to estimate similar terms for $(\text{NMe}_4)\text{CO}_3$, NMe_4HCO_3 , and NMe_4OH . The strong relation between the activity coefficients of electrolytes on the one hand and the viscosity B-coefficients and entropy of hydration on the other hand have been indicated by Gurney (1962). Desnoyers and Perron (1972) showed that the term $(B_j - 0.0025 \bar{V}_j^\circ)$ indicates whether the ion is 'structure-maker' or 'structure-breaker' depending upon whether this term is positive or negative, respectively. Here B_j is the ionic viscosity coefficient in the Jones-Dole equation

$$(\eta - \eta^\circ / \eta^\circ) = 1 + (z_+ B_+ + z_- B_-)C \quad [6-8]$$

This parameter ($B_j - 0.0025 \bar{V}_j^\circ$) was used as a basis of comparison. In the case of NMe_4HCO_3 , a value of B was interpolated on the basis of the entropy of hydration, s . The detailed calculations and tables are shown in Appendix A.

The calculated mean activity coefficients of the three electrolytes are shown in Fig. 4. The activity coefficients in multicomponent mixtures can be calculated using the method of Meissner and Kusik (1972):

$$\log \Gamma_{4j_m} = 1/2(\log \Gamma_{4j} + Y_{41} \log \Gamma_{41} + Y_{42} \log \Gamma_{42} + Y_{43} \log \Gamma_{43}) \quad [6-9]$$

where Y_{41} , Y_{42} , and Y_{43} are the ionic strength fractions of the corresponding electrolytes, m refers to multicomponent mixtures, and Γ_{4j} is the reduced activity coefficient defined by the equation

$$\Gamma_{4j} = (\gamma_{4j})^{1/z_4 z_j} \quad [6-10]$$

Equilibrium and Reaction Rate Constants

The equilibrium constants at infinite dilution for reactions [2-1] and [2-2] are given by the following equations (Harned and Owen, 1958):

$$\log K_i^\circ = -\log K_w - (3404.71/T) + 14.8435 - 0.032786 T \quad [6-11]$$

$$\log K_{ii}^\circ = -\log K_w - (2902.39/T) + 6.490 - 0.02379 T \quad [6-12]$$

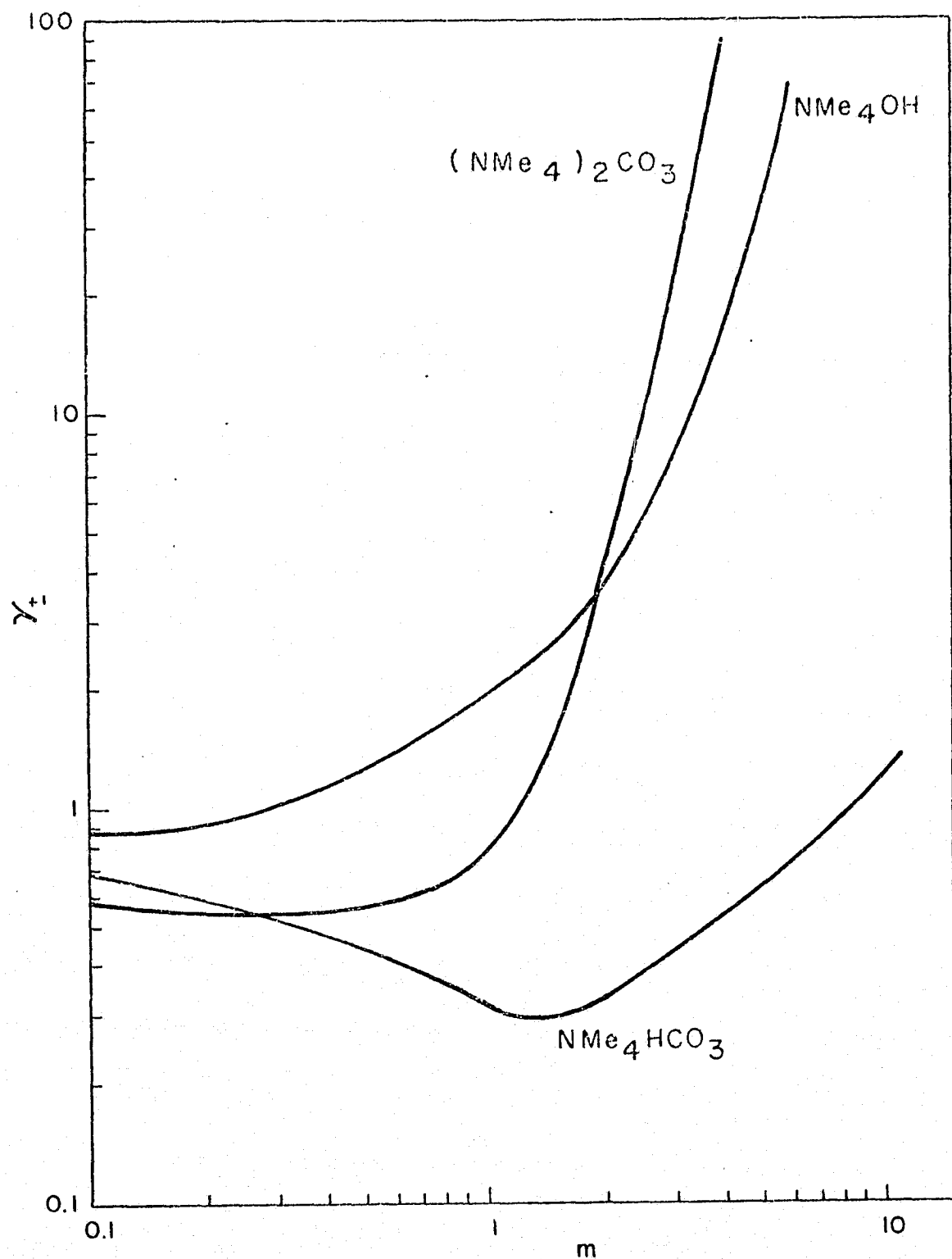


Fig. 4 Activity Coefficients of $(\text{NMe}_4)_2\text{CO}_3$, NMe_4HCO_3 , and NMe_4OH at 25°C

where K_w is the ionization constant of water, which has been reported by Robinson and Stokes (1959). The values of K_w can be approximated by the following equation:

$$- \log K_w = 4471.33/T - 6.0846 + 0.017053 T \quad [6-13]$$

The equilibrium constants used in the mathematical model were calculated from their values of infinite dilution multiplied by the appropriate activity coefficient ratio. This ratio was calculated using equations [6-9] with average concentrations estimated for the three regions; catholyte, anolyte, and bulk electrolyte. These values do not significantly affect the calculated CO_2 flux or the calculated HCO_3^- concentration at the anode. This eliminates the need for an iteration procedure to calculate the exact concentrations. The details of the calculations are shown in Appendix A.

The rate constants for reactions [2-1] and [2-3] at infinite dilution are given by the equations (Pinsent et al., 1956):

$$\log k_i = 13.635 - (2895/T) \quad [6-14]$$

$$\log k_{iii} = 329.850 - 110.541 \log T - (17265.4/T) \quad [6-15]$$

Henry's Law Constants

Henry's law constants were estimated from their values in water (Perry et al., 1963) multiplied by a factor dependent on the ionic strength of the electrolyte (Van Krevelen and Hoftijzer, 1948). At infinite dilution the Henry's law constants are approximated by the

equation

$$H^{\circ} = 10^4(13.32257 - 0.132516T + 3.198135 \times 10^{-4} T^2) \quad [6-16]$$

where H is in (mm Hg) ℓ /gmole. Equations [2-10] and [2-11] were used to calculate the values of H for the catholyte and anolyte, taking $i_+ = 0.030$, $i_- = 0.021$, and $i_G = -0.01$ (Van Krevelen and Hoftijzer, 1948). The value of i_+ used here is that value reported by these authors for NH_4^+ ion since there was no value reported for NMe_4^+ .

Gas-Phase Mass and Heat Transfer Coefficients

The mass transfer coefficients in the air zone were calculated from the limiting slope of N_{5T} against $(P_{5c})_I$ at $(P_{5c})_I = 0$ (Fig. 5). In that case C_{5c} vanishes and equation [4-5] reduces to

$$h_{5c} = - (V_c/A) \ln \left[1 - (ART/V_c) \left(\frac{dN_{5T}}{dP_{5c}} \right)_{P_{5c} = 0} \right] \quad [6-17]$$

From this equation h_{5c} can be calculated for each air velocity. Test data are available for the analytical cell at air velocity of 10 ft/sec and $(P_{5c})_I$ of 0.25, 1, and 4 mm Hg. The calculated mass transfer coefficient in that case is 233 ft/hr. At air velocity of 5 and 15 ft/sec data are available only at $(P_{5c})_I = 0.25$ mm Hg. These are insufficient to calculate the mass transfer coefficient by the limiting-slope method.

For air velocities in the range encountered in the cell, the flow is laminar. Two equations are available for mass and heat

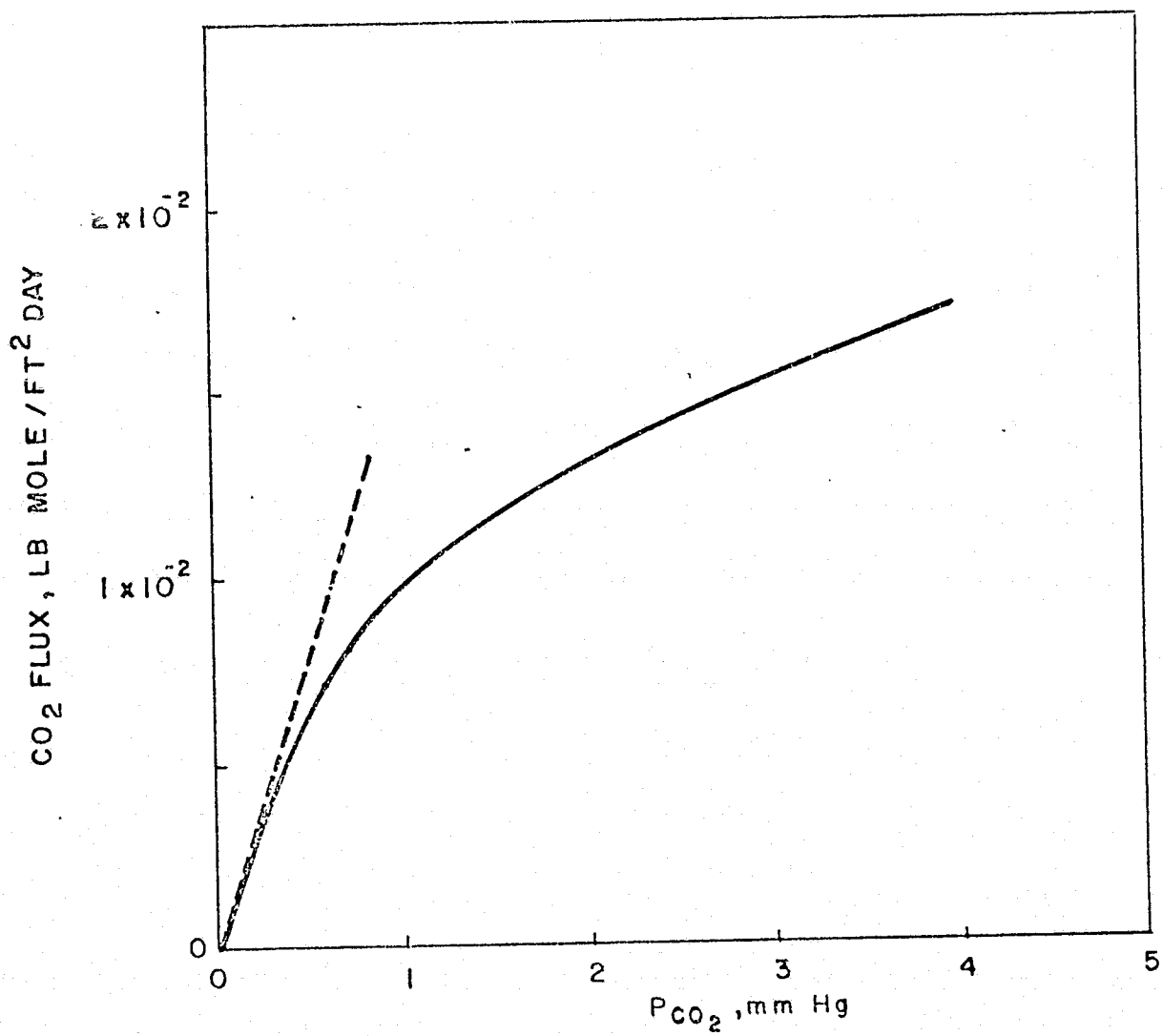


Fig. 5 The Limiting Slope Method for Calculating the Mass Transfer Coefficient in the Air Side

transfer coefficients in rectangular ducts (Knudsen and Katz, 1958). For uniform wall temperature the heat transfer coefficients are calculated by;

$$Nu = Nu_{\infty} [1 + (0.003 + 0.039 \delta_1 / \delta_2) Re Pr d_e / \delta_3] \quad [6-18]$$

For uniform heat flux the equation changes slightly to

$$Nu = Nu_{\infty} [1 + (0.003 + 0.019 \delta_1 / \delta_2) Re Pr d_e / \delta_3] \quad [6-19]$$

where Nu is Nusselt number, Nu_{∞} is its asymptotic value, δ_1 and δ_2 are the dimensions of the rectangular section, δ_3 is the length of the air duct, d_e is the equivalent diameter of the air duct and Pr is the Prandtl number. In the case of mass transfer Nu is replaced by Sh and Pr by Sc where Sh is the Sherwood number and Sc is the Schmidt number.

In our case the mass transfer coefficient in the bulk gas phase can be calculated by equation [6-18]. The value of h_{5c} at an air velocity of 10 ft/sec is 246 ft/hr calculated at an average cell temperature. Comparing these values with the value obtained previously from the limiting-slope method (233 ft/hr), it appears that the mass transfer resistance in the gas phase within the electrode pores is negligibly small. Thus, the overall mass transfer coefficient, h_{5c} , is about 94% of the value calculated by equation [6-18]. Assuming that the overall mass transfer coefficient is 94% of the theoretic-

cal value, equation [6-18] can be used to calculate h_{5c} . For the present design this reduces to the following equation for h_{5c} calculated at an average cell temperature:

$$h_{5c} = 0.94 (112 + 8.84 V_c) \quad [6-20]$$

where h_{5c} is in ft/hr and V_c is in ft^3/min .

This equation applies for both the analytical and full-scale cells since the dimensions of the air ducts are the same for both designs. Other mass transfer coefficients are calculated from equation [6-18] while the heat transfer coefficients used in the energy balance calculations (Lin et al., 1974) are calculated from equation [6-19].

Transport Properties in the Electrolyte

The diffusion coefficients of $(\text{NMe}_4)_2\text{CO}_3$, NMe_4HCO_3 , and NMe_4OH were calculated from the activity coefficients and viscosity data (Fig. 6). The detailed calculations are given in Appendix A. The values of the diffusion coefficients are shown in Fig. 7. For each electrolyte the diffusion coefficients exhibit a minimum and then a shallow maximum as the concentration increases. This complex concentration dependence is typical of diffusion in electrolytic solutions (Bhatia et al., 1957). From these values the individual ionic coefficients were calculated by the method described in Chapter II. The ionic mobilities were also calculated from the equivalent conductance

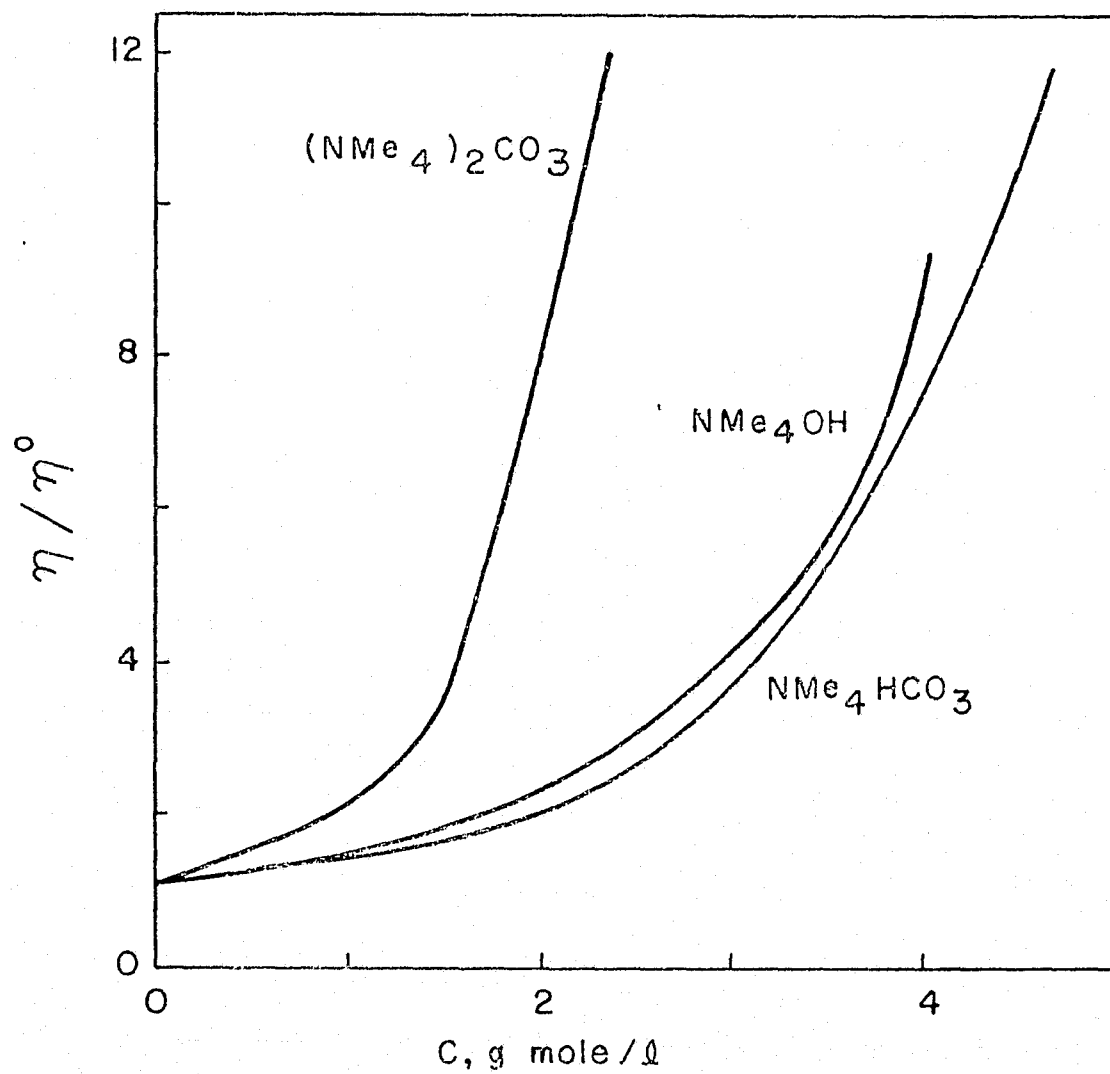


Fig. 6 Relative Viscosities of $(NMe_4)_2CO_3$, NMe_4HCO_3 , and NMe_4OH at 25°C

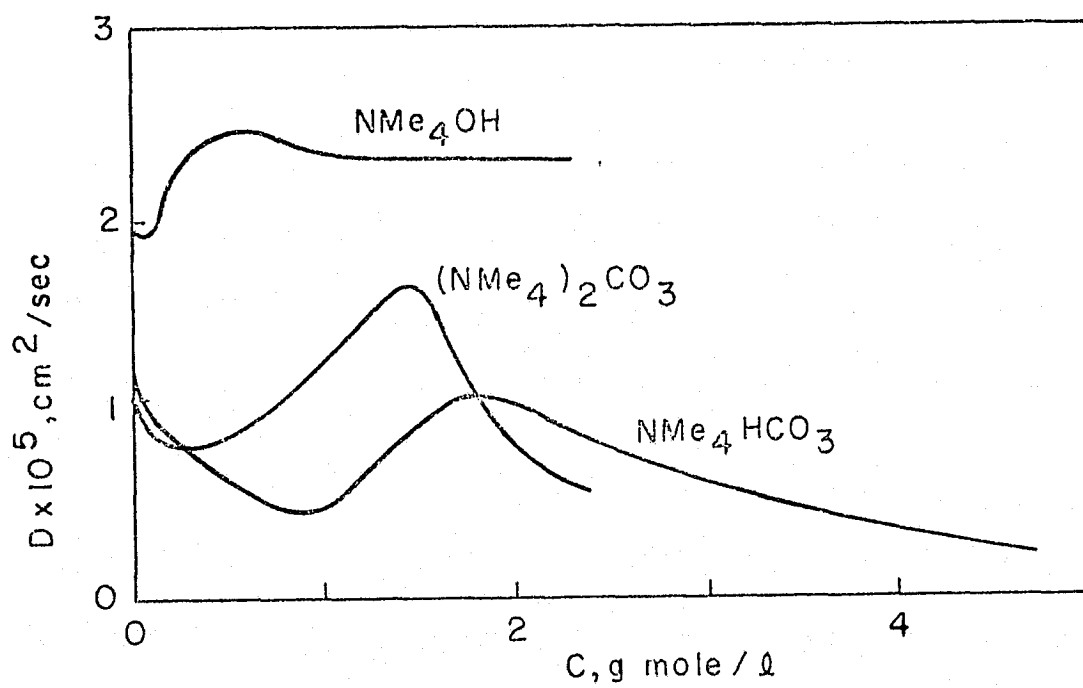


Fig. 7 Diffusion Coefficients of $(\text{NMe}_4)_2\text{CO}_3$, NMe_4HCO_3 , and NMe_4OH at 25°C

data (Fig. 8) by the method also described in Chapter II. To accommodate computer calculations, the viscosities, ionic diffusion coefficients, and ionic mobilities were fit to polynomials. These equations are given in Appendix A. Although these equations are empirical and have no real theoretical significance, they are suitable for calculations because the model is rather insensitive to moderate variations in the values of these parameters.

The diffusivities of CO_2 in the electrolyte were estimated from their values in water (Perry et al., 1963) using the following empirical equation which was obtained for the diffusion of CO_2 in liquids (McManamey and Woollen, 1973):

$$D = D^\circ (\eta^\circ / \eta)^{0.47} \quad [6-21]$$

Matrix Factor

The matrix, as mentioned earlier, consists of two sheets of fuel-cell asbestos with an uncompressed thickness of 40 mils and one sheet of Tissuquartz between with an uncompressed thickness of 18 mils. The matrix is compressed to a final thickness of 25 mils. From Fig. 39 of Huddleston and Aylward (1973), the corresponding loading is 128 psig. At this loading the same two sheets of fuel cell asbestos can be compressed only to 23 mils. This indicates that the Tissuquartz layer is compressed to approximately 2 mils. The matrix labyrinth factors for the asbestos and the Tissuquartz layers at this compression are 0.342

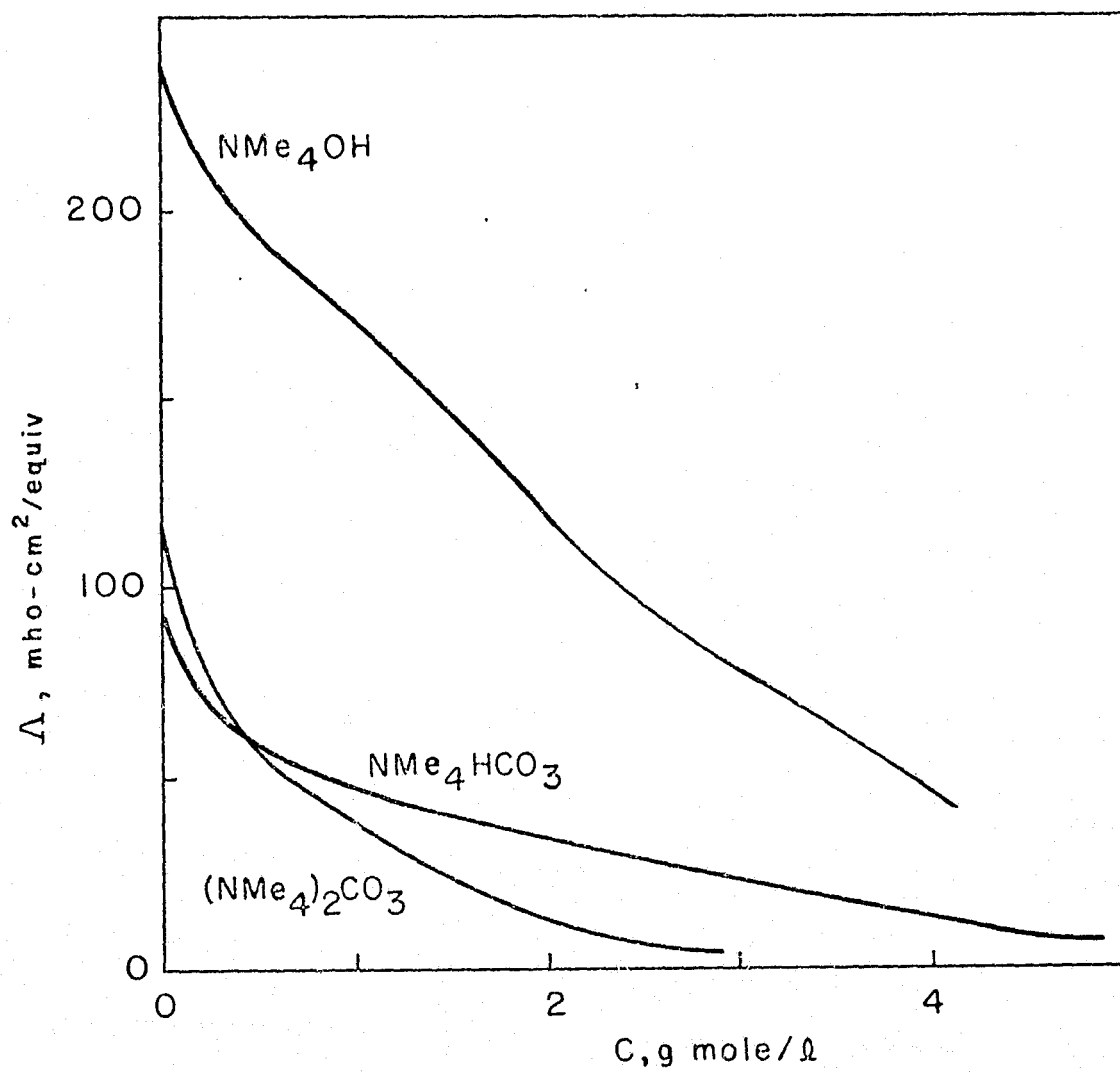


Fig. 8 Equivalent Conductances of $(\text{NMe}_4)_2\text{CO}_3$, NMe_4HCO_3 , and NMe_4OH at 25°C

and 0.314, respectively, estimated from the conductivity measurements (Huddleston and Aylward, 1973). The average matrix factor is then about 0.340. The mobilities and diffusion coefficients are multiplied by this factor to obtain the effective values in the matrix zone.

Gas-Electrolyte Interface Area

Two parameters must be obtained from test data: the air-catholyte interface area and the hydrogen-anolyte interface area. Experimental methods based on adsorption measurements measure the total internal solid surface area (Srinivasan and Gileadi, 1968). On the other hand, dilatometry measurements can provide an estimate of the electrolyte film area extending inside hydrophilic electrodes which provides the active surface for electrode reactions (Moren, 1975). Neither of these methods can give an estimate of the true gas-electrolyte interface area in partially wetted electrodes as those used in the HDC cells.

The gas-electrolyte interface area is determined by several forces acting on the electrolyte surface; gas pressure, electroosmotic forces and capillary forces. The presence of the asbestos matrix in the vicinity of the electrode matrix adds another complication because of the difference in their porosities and their affinity to the electrolyte. Thus, the true gas-electrolyte interface area can only be obtained empirically from test data.

The calculated N_{5T} is independent of the chosen value of S_a but does depend on the chosen value of S_c . The latter parameter determines the concentration of OH^- ions in the catholyte which determines, in turn, the rate of CO_2 absorption reaction and the fraction of the current carried by the CO_3^{2-} and HCO_3^- ions in the matrix zone. The value of S_c can be chosen so that the calculated CO_2 flux matches the experimental values for both the analytical and full-scale cells.

In equation [4-9] the term $C_1/(K_1 C_2)$ is in the range 10^{-13} - 10^{-11} gmole/l while C_{5C}^+ is in the range 10^{-9} - 10^{-6} gmole/l. The equation can thus be simplified to the following form:

$$N_{5T} = S_c (k_i D_5 C_2)^{1/2} C_{5C}^+ \quad [6-22]$$

This equation suggests that, with C_{5C}^+ calculated by equation [4-5], the value of N_{5T} is proportional to $(C_2)^{1/2}$ for constant values of S_c , k_i , and D_5 . At a given total ionic strength, the last three parameters are constant. Figure 9 shows some experimental data obtained with the analytical cell for a constant air relative humidity, or in other words, at the same catholyte ionic strength. These values are compared with those calculated using the same value of the parameter $(S_c k_i D_5)$. The agreement as shown in Fig. 9 is unsatisfactory since this parameter is presumably independent of $(P_{5C})_I$. Better fitting can be obtained if N_{5T} is assumed to be proportional to C_2 rather than $(C_2)^{1/2}$ and the active area changing with the current density as shown in Fig. 10. In that case the calculated CO_2 flux fit the experimental data within experimental error as shown in Fig. 11.

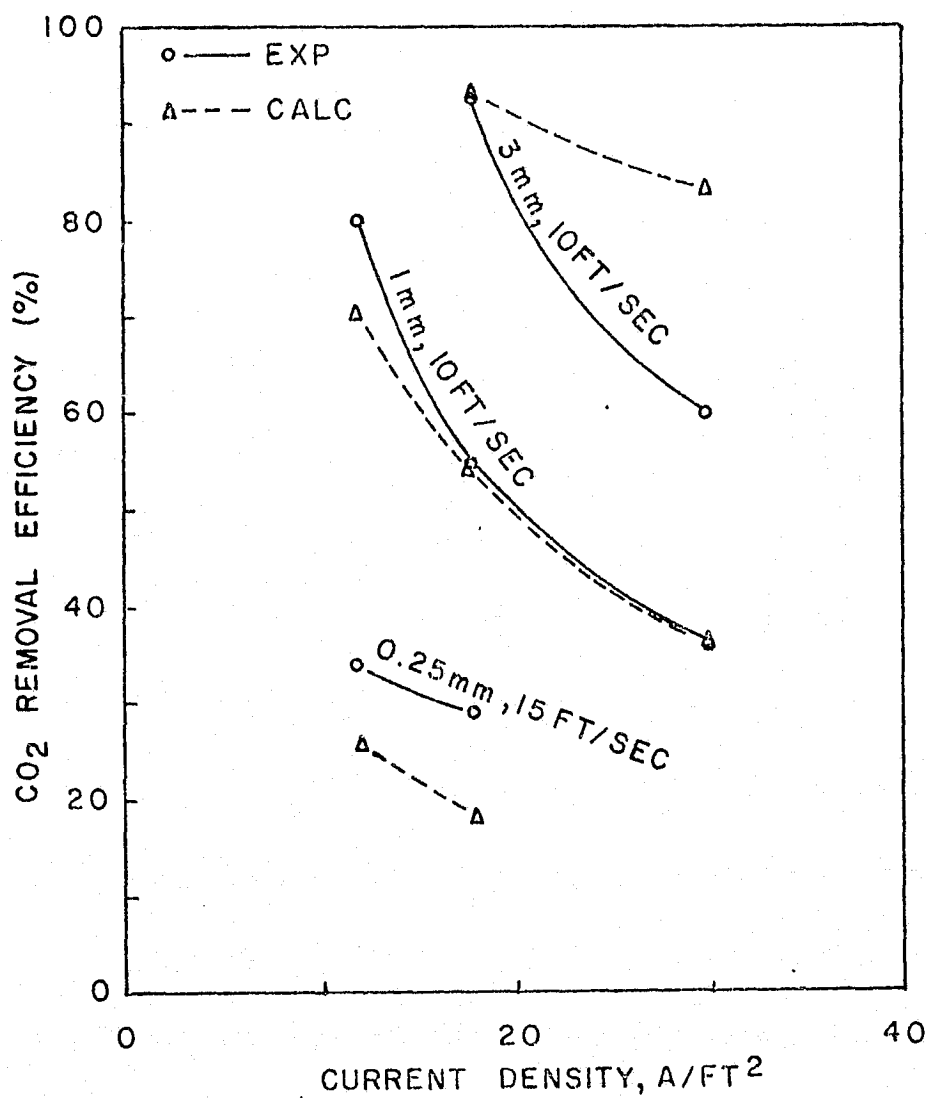


Fig. 9 Test Data Compared with Simulation Results if the CO_2 Flux is Proportional to $\sqrt{[\text{OH}]}$ and the Air-Catholyte Area is Constant, Analytical Cell, Air Inlet Temp. = 70°F, Air Dew Point = 50°F

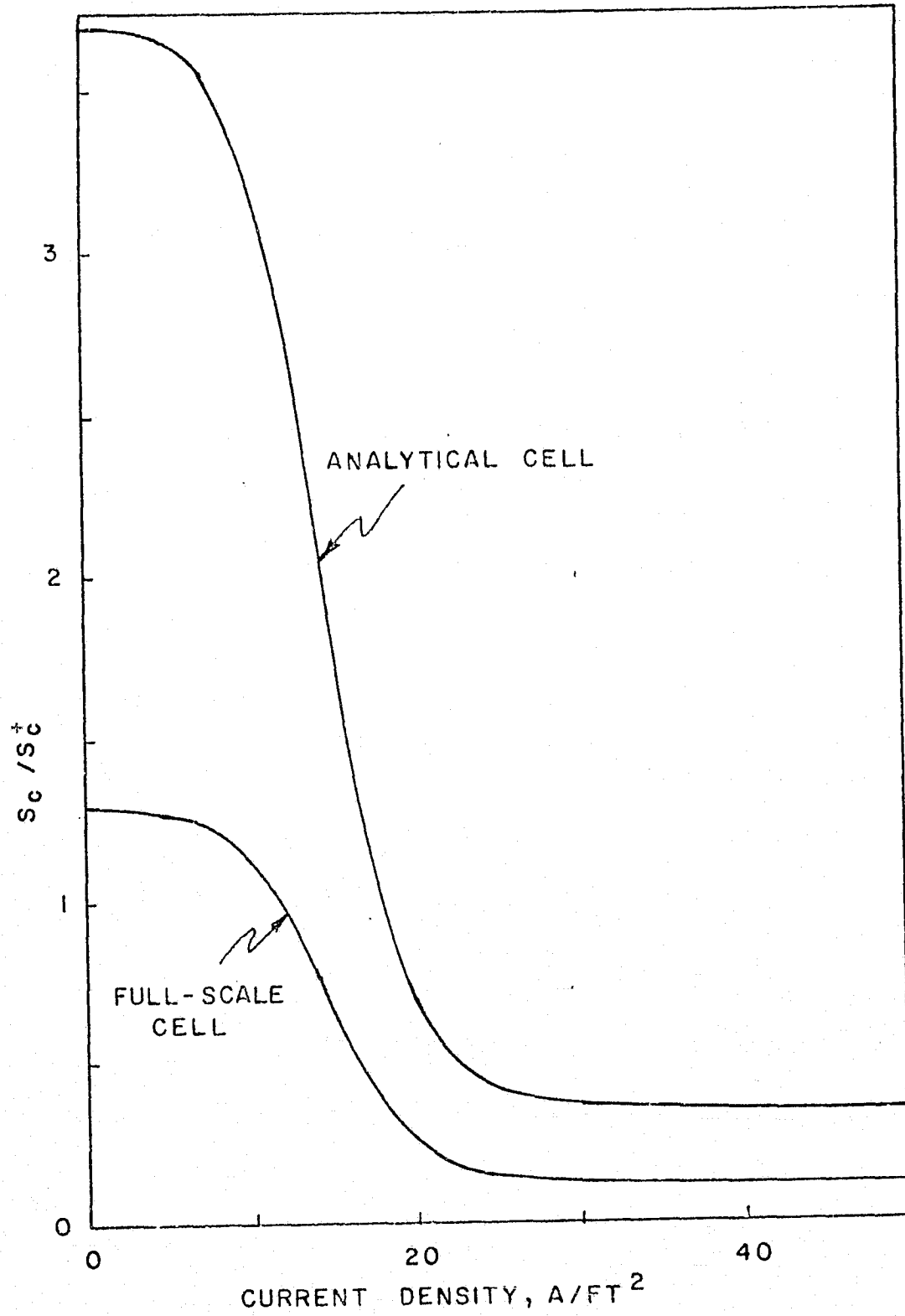


Fig. 10 Air-Catholyte Area Dependence on Current Density

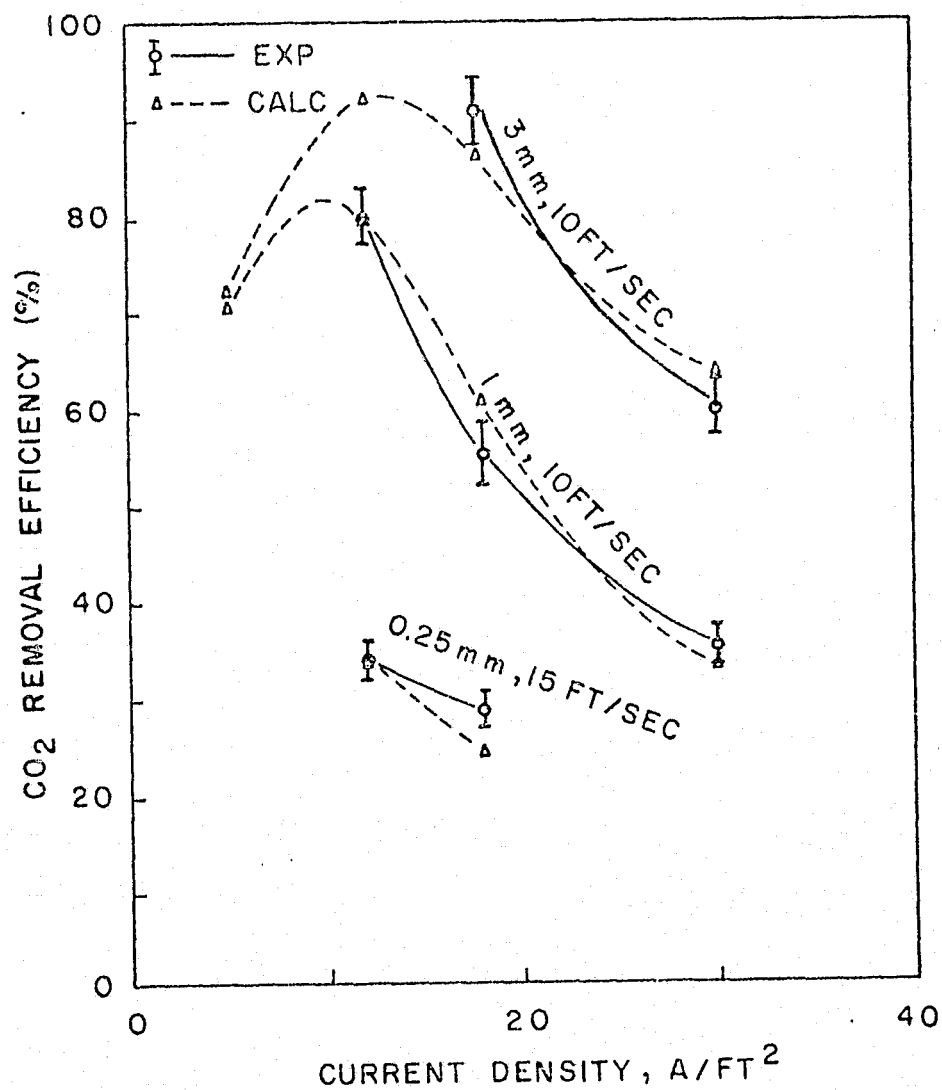


Fig. 11 Test Data Compared with Simulation Results if the CO₂ Flux is Proportional to [OH] and the Air-Catholyte Area is Dependent on Current Density, Analytical Cell, Air Inlet Temp. = 70°F, Air Dew Point = 50°F

To explain this we must reconsider the nature of the chemical reaction between CO_2 and OH^- ions, which is typical of ion-molecule reactions (Frost and Pearson, 1961). The dependence of the rate constant on the ionic strength of the solution as given by equation [2-6] is resolved into the following equation:

$$\log k = \log k^\circ + (\ell_{\text{CO}_2} + \ell_{\text{OH}} - \ell_{\text{I}})\mu \quad [6-23]$$

where the ℓ terms stand for the dependence of the activity coefficient of the corresponding species on the ionic strength. The subscript I represents the activated complex which is probably formed as a reaction intermediate. It is interesting to note the similarity between this equation and equation [2-10] which describes a completely different phenomenon, i.e., the solubility of a gas in an electrolytic solution. It is the term ℓ_{OH} which we need to reconsider here. This term results from the assumption that the activity coefficient of an ion is represented by the following equation:

$$\log \gamma_j = -0.5809 z_j^2 \mu^{1/2} / (1 + 0.3291 L \mu^{1/2}) + \ell_j \mu \quad [6-24]$$

This equation is a modified form of the Debye-Huckel equation which is assumed to apply for both the OH^- ions and the activated complex. In the case of NMe_4OH the activity coefficients in their solutions increases sharply with concentration which results in some dependence of their activity coefficients on C_2 as calculated for the multicomponent catholyte by equation [6-9]. The activity coefficient of

the activated complex is probably of the same order of magnitude as that of NMe_4HCO_3 which does not change much with concentration. The result is that the term $(\lambda_{\text{OH}^-} - \lambda_{+})$ is dependent to some extent on C_2 which results in the dependence of k_1 on C_2 . The remaining effect of the ionic strength on the rate constant is accounted for by the term λ_{CO_2} which is represented by the following equation (Frost and Pearson, 1961).

$$\log \gamma_{\text{CO}_2} = \lambda_{\text{CO}_2} \mu \quad [6-25]$$

The activity coefficient of CO_2 in an electrolytic solution is also represented by the following equation (Harned and Owen, 1958):

$$\lambda_{\text{CO}_2} = H/H^\circ \quad [2-26]$$

Combining these equations with equation [2-11] provides an easy method to predict the effect of the ionic strength on the reaction rate constant.

The dependence of the gas-electrolyte interface area on the apparent current density (current per unit electrode geometric area) is less clearly understood. It is known that the equilibrium of the electrolyte meniscus within the electrode pores depends upon the pressure differential between the gas and electrolyte, the capillary forces, and the electroosmotic forces. In regions of high current densities close to the current collector screen, the electroosmotic forces push the electrolyte towards the air side while the capillary

forces force the electrolyte back into the matrix structure in regions of low current density remote from the current collector screen. It is believed that any factor which increases the drop-off in current density remote from the current collector screen, such as increasing the cathode electronic resistance by increasing its porosity, significantly increases the CO_2 removal efficiency (Huddleston and Aylward, 1973). This may explain the change of the air-catholyte interface area with current densities as required to simulate the experimental data.

The CO_2 removal efficiency in the full-scale cell tests were significantly lower than those obtained with the analytical cell at the same conditions. The possible effect of the H_2 flow rate and pressure and the cell temperature were investigated experimentally. It was found that these parameters have little effect on the CO_2 removal efficiency (Huddleston and Aylward, 1973). The mathematical model correctly predicts this lack of sensitivity.

The difference between the air flow rates in the analytical and full-scale cells has little effect on the CO_2 removal efficiency at the baseline conditions ($P_{\text{CO}_2} = 1\text{-}3 \text{ mm Hg}$). The only apparent difference between the analytical and full-scale cells is the geometric configuration of the cell electrodes as shown in Fig. 12. Both cells have the same air path length but the width of the electrodes in the full-scale cell is 24 times of that in the analytical cell. It seems that this results in a difference in the current density distribution

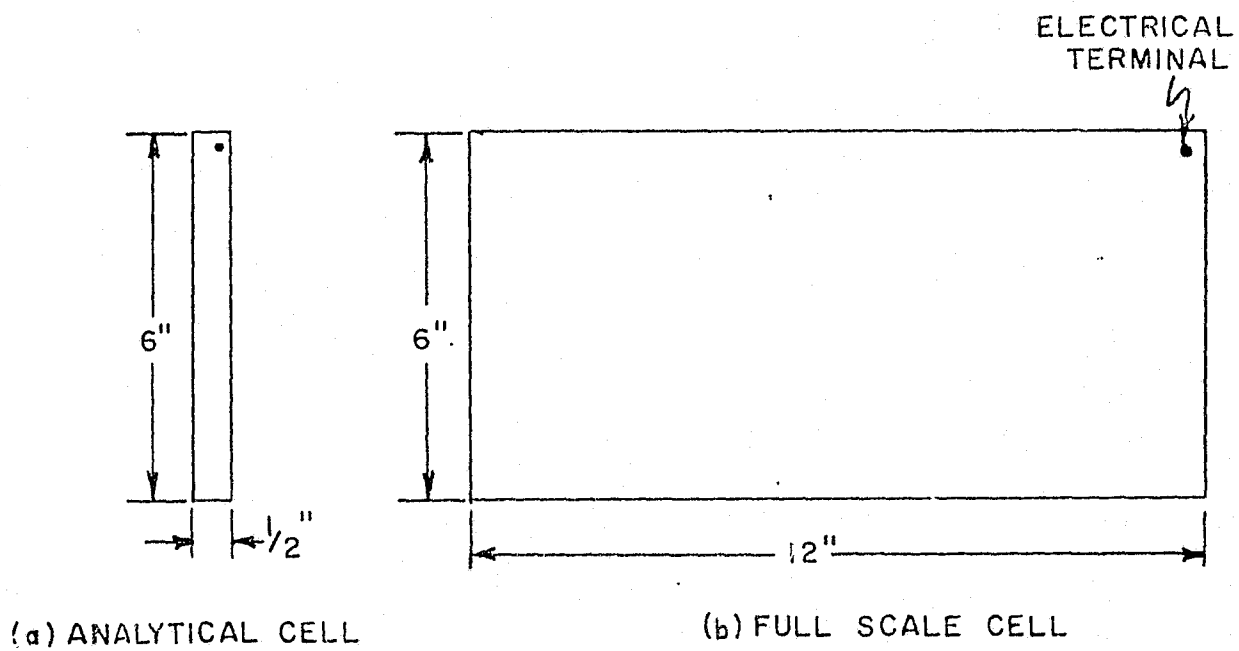


Fig. 12 Electrodes of the Analytical and Full-Scale Cells

in the cathode with a corresponding change in the balance between the electroosmotic and capillary forces which directly affect the gas-electrolyte interface.

The variation of the air-catholyte interface area, as shown in Fig. 11 was empirically fit by the following equations using the method of Churchill and Usagi (1974):

For the analytical cell

$$S_c/S_c^* = 3.70 - 3.35/[1 + (0.06 I)^{-8}]^{0.5} \quad [6-28]$$

for the full-scale cell

$$S_c/S_c^* = 1.37 - 1.24/[1 + (0.06 I)^{-8}]^{0.5} \quad [6-29]$$

These equations represent the relative values of S_c at a given current density compared to that at a characteristic current density chosen arbitrarily at 18 A/ft^2 with the analytical cell. The absolute values of S_c cannot be obtained after making the assumption that N_{5T} is proportional to C_{2c} . Instead, the parameter $(\tilde{N}_{5T}/\tilde{C}_{2c})$ can be calculated which is directly proportional to S_c . The variation of S_c with current density can then be accounted for in the mathematical model by multiplying the parameter $(\tilde{N}_{5T}/\tilde{C}_{2c})$ by the appropriate ratio (Appendix A).

The magnitude of S_a cannot be calculated accurately from the test data because the value of C_2 and C_3 at the anode cannot be determined experimentally with sufficient accuracy. However, the calculated CO_2

transfer rate and the concentration of C_1 at the anode are almost independent of the chosen value of S_a . Thus, it is possible to use an approximate value of S_a in the mathematical model ignoring any possible change with current density or with any other relevant parameter. The concentration of the hydroxyl ions can be estimated from the pH measurements of the bicarbonate solutions (Abdel-Salam, 1974) after assigning a reasonable value to the activity coefficients of the OH^- ions. The calculations are shown in detail in Appendix A.

CHAPTER VII

MODEL PREDICTIONS

Introduction

This chapter compares the performance of the concentrator with that of the model over a wide range of the operating variables. It also predicts the performance of the cell when one of the design parameters, e.g. the matrix thickness, is changed from the used value. The limits of stable cell operation in low humidity environments can be determined from the concentration distribution obtained by the model.

Effect of P_{CO_2}

At a constant current density, increasing P_{CO_2} in the inlet cabin air increases the CO_2 removal rate. This is apparent from Figs. 13 and 14 which compare the experimental and calculated rates for the analytical and full-scale cells. The increase is rather sharp in the low P_{CO_2} region becoming much slower as P_{CO_2} rises above the design baseline condition (3 mm Hg).

In the low P_{CO_2} region (< 0.25 mm Hg) the process is gas-phase mass-transfer controlled and the increase of N_{5T} is approximately

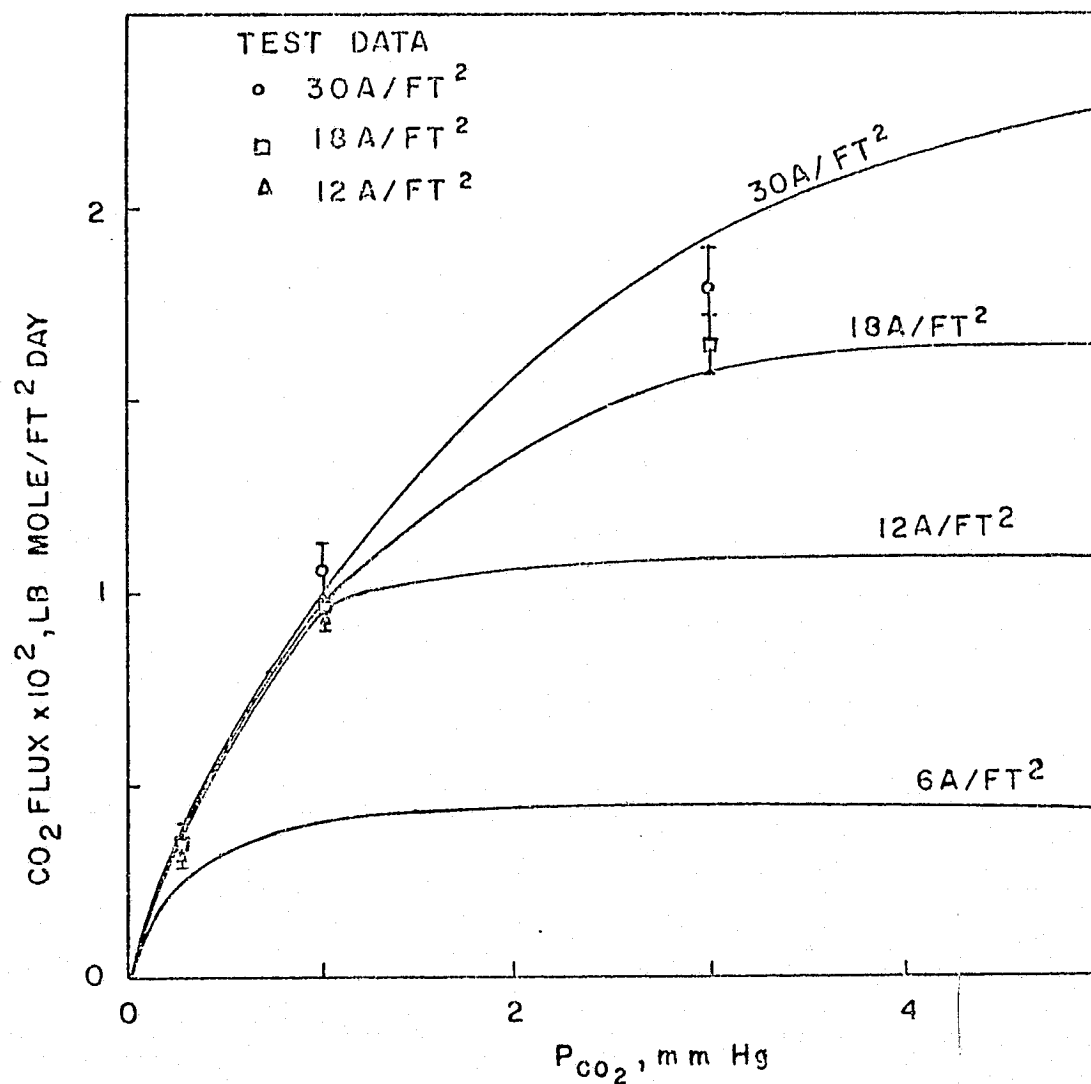


Fig. 13 Effect of P_{CO_2} at the Air Inlet on the CO₂ Removal Rate in the Analytical Cell (the solid lines represent Simulation Results)

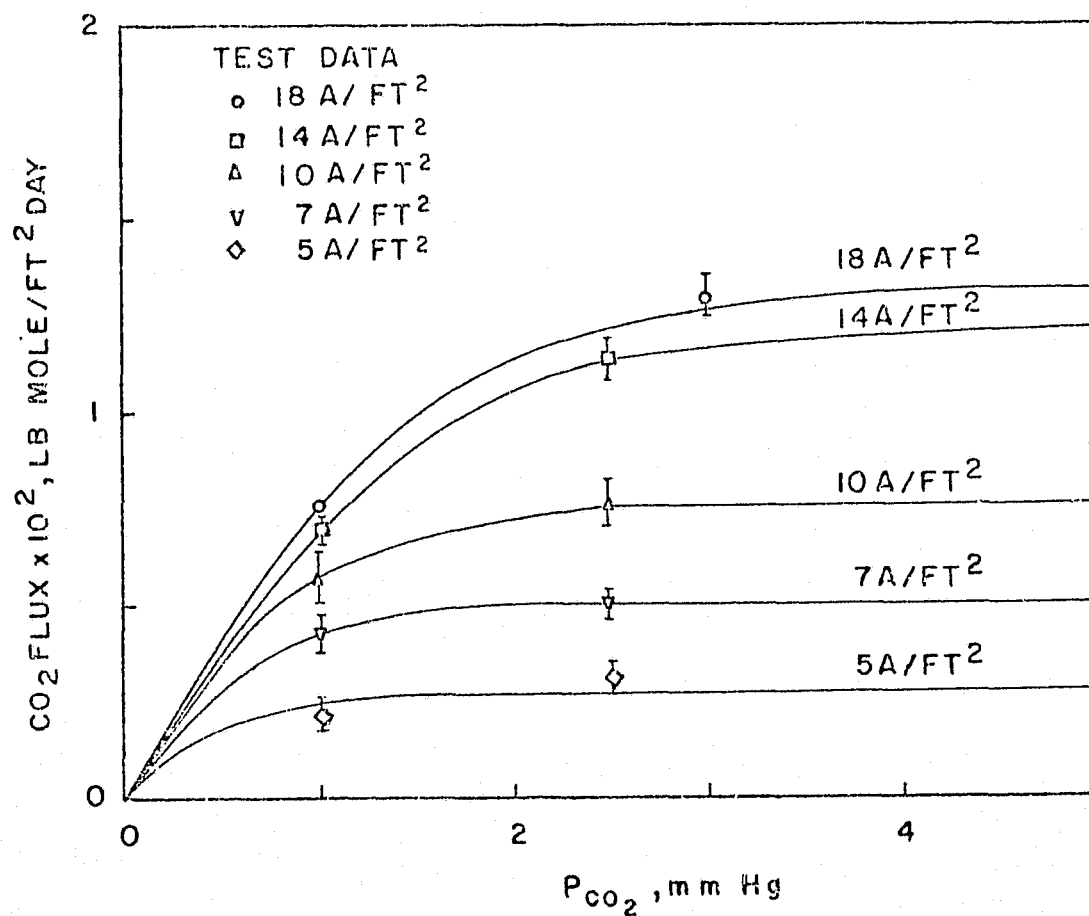


Fig. 14 Effect of P_{CO_2} in the Inlet Air on the CO_2 Removal Rate in the Full-Scale Cell (the solid lines represent Simulation Results)

linear with P_{CO_2} as is evident from equation [4-4]. As P_{CO_2} level increases the ionic transport in the matrix zone becomes the controlling step. In this zone the current is carried by the CO_3^{2-} , HCO_3^- , and OH^- ions. Increasing the CO_2 removal rate at a constant current density results in a lower fraction of the current carried by OH^- ions. A lower OH^- flux results in a smaller concentration gradient across the matrix which means a lower OH^- concentration at the cathode since there is no significant change in the anolyte pH. Figure 15 compares the calculated OH^- concentration at the cathode in the analytical cell at a current density of 18 A/ft^2 with the pH measurements obtained at different inlet P_{CO_2} . Although these measurements are crude for this purpose, not only because of the low accuracy of the measurements but also because taking a representative sample of the catholyte is hard to achieve, they show the same trend as predicted by the model.

Effect of Current Density

For the same value of P_{CO_2} , increasing the current density increases the CO_2 flux. However, the CO_2 removal efficiency (current efficiency), which is proportional to the ratio between N_{5T} and I , has a maximum value at a certain optimum current density. The optimum current density is higher for higher inlet P_{CO_2} . This is shown in Figs. 11 and 16 for the analytical and full-scale cells.

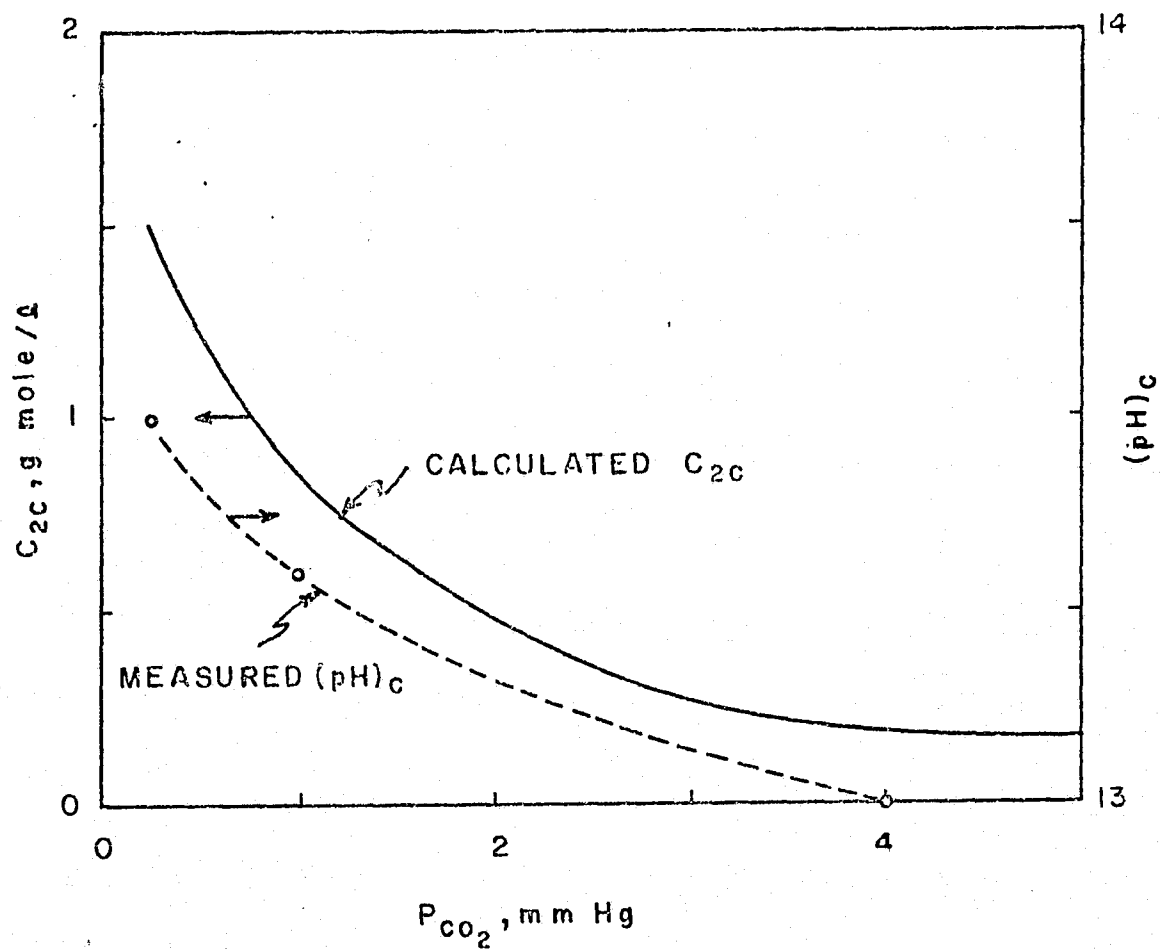


Fig. 15 Effect of P_{CO_2} on the Hydroxyl Ion Concentration in the Catholyte of the Analytical Cell

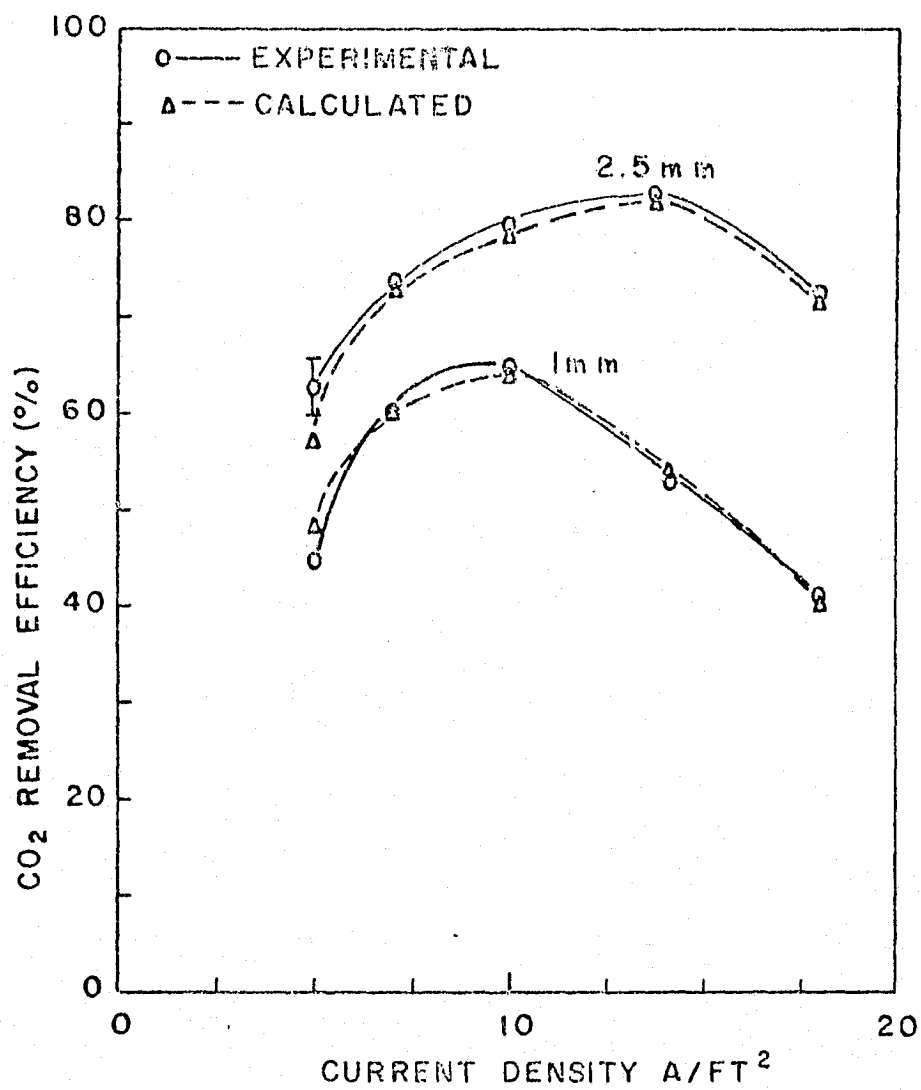


Fig. 16 CO₂ Removal Efficiency in the Full Scale Cell

This dependence of the current efficiency on current density is related to the OH^- concentration in the catholyte. Increasing I is accompanied by increase in C_{2c} , which, although increasing the rate of CO_2 absorption reaction, also increases the OH^- flux in the matrix zone. The current efficiency is proportional to the ratio between $(N_1+N_3+N_5)$ and $(N_1+N_2+2N_3)$. Although these sums increase with current density, their ratio has a certain maximum at a certain C_{2c} value. This optimum concentration is also dependent on $(P_{5c})_I$. The calculated values of C_{2c} at P_{CO_2} of 1 mm Hg for the analytical cell are compared with the measured pH values in Fig. 17.

Effect of Air Velocity

The effect of air velocity on the CO_2 removal rate is shown in Fig. 18 for the analytical cell. The calculated values are compared with the experimental values. Because of the gas-phase mass-transfer limitations in the low P_{CO_2} region, increasing the air velocity increases the CO_2 removal rate in that region. This is also evident from the lowering of the catholyte pH with the increase in air velocity (Fig. 19). At higher P_{CO_2} the ionic transport becomes more important, and hence, the increase in air velocity has no significant effect in that region.

Effect of Matrix Thickness and Compression

The matrix thickness and compression are chosen on the basis of the internal cell resistance and other mechanical considerations. How-

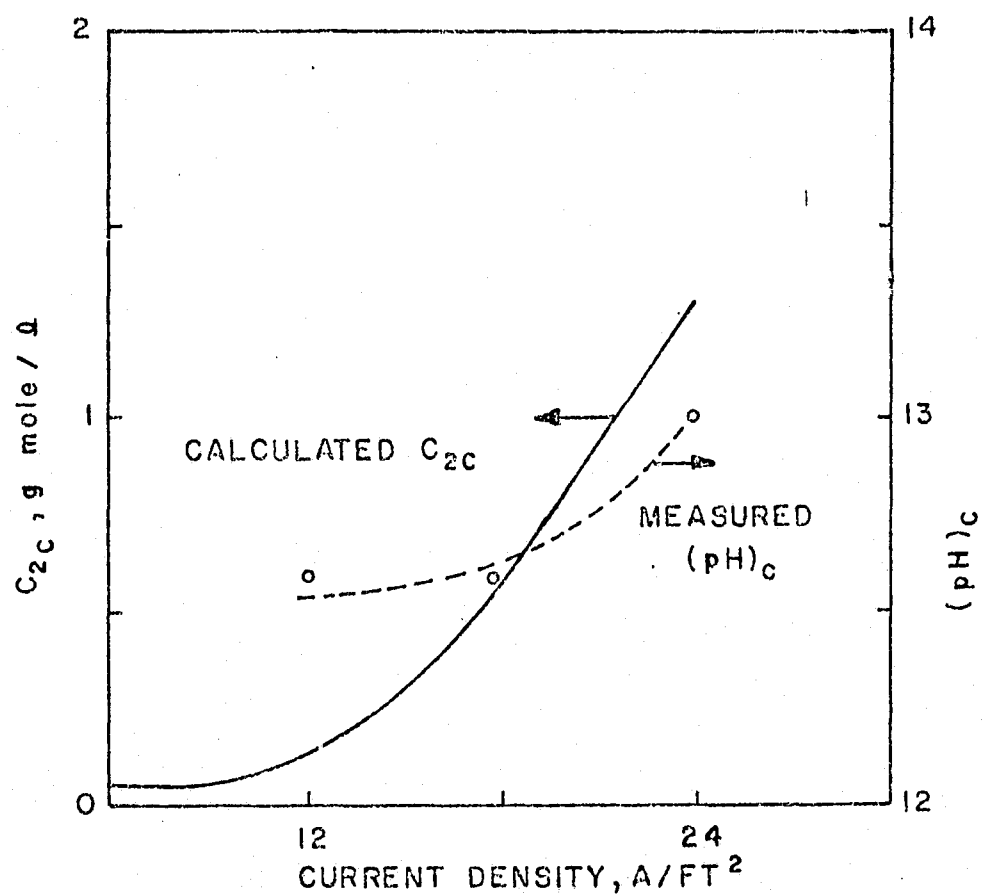


Fig. 17 Effect of Current Density on the Hydroxyl Ion Concentration in the Catholyte of the Analytical Cell

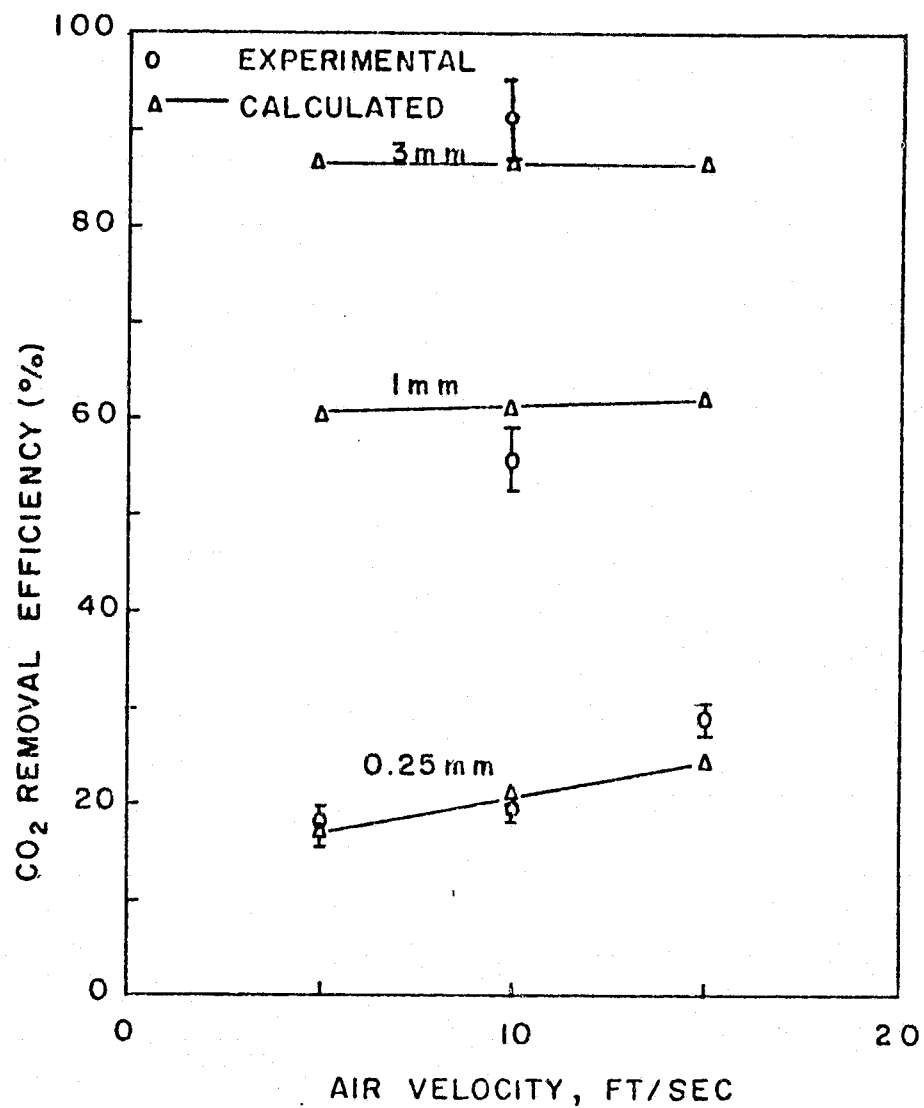


Fig. 18 Effect of Air Velocity on the CO₂ Removal Efficiency in the Analytical Cell

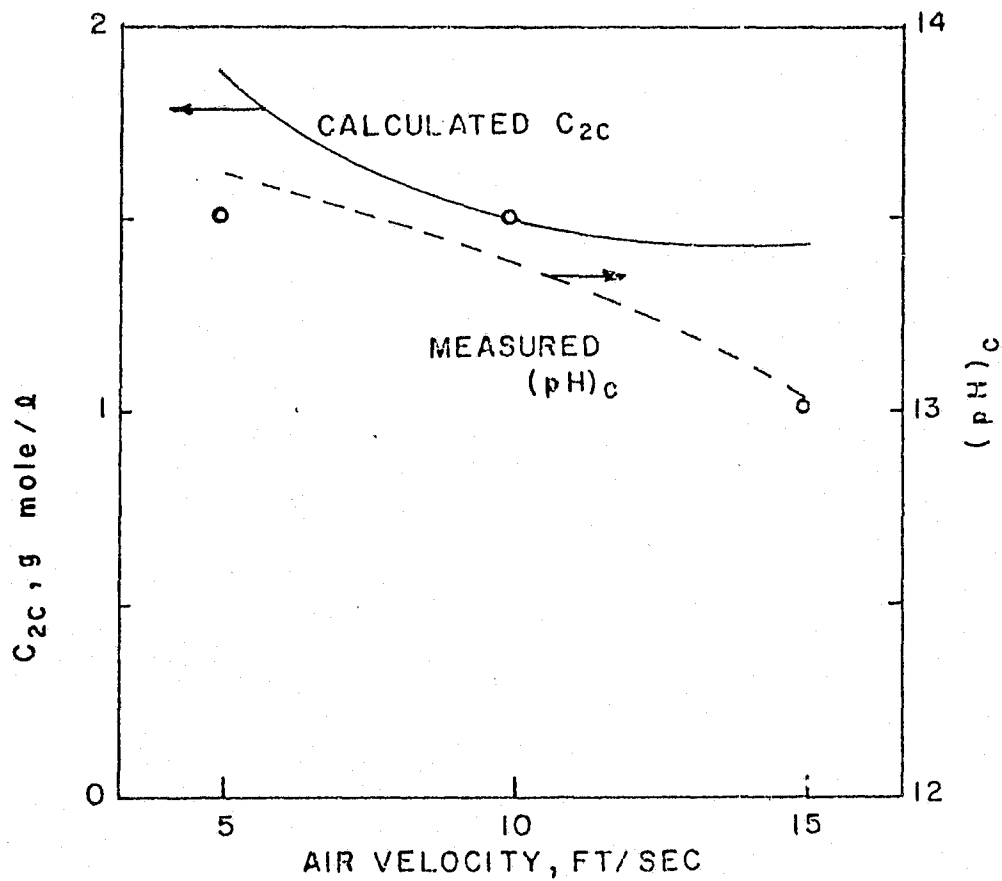


Fig. 19 Effect of Air Velocity on the Hydroxyl Ion Concentration in the Catholyte of the Analytical Cell

ever, it is desirable to predict the effect of changing the matrix thickness and compression on the CO_2 removal rate. Figure 20 shows the effect of changing the matrix thickness at the same compression. Increasing the matrix thickness increases the CO_2 removal rate up to a certain limit after which the CO_2 rate decreases. The initial increase is attributed to the decrease in back diffusion of the HCO_3^- ions from the anode to the cathode. The effect of increasing the matrix thickness on increasing the selectivity of the OH^- ions as charge carriers, which have higher mobilities and diffusion coefficients than the other ions, becomes apparent beyond a certain thickness which explains the decrease in the CO_2 removal rates afterwards.

The same reasoning can explain the effect of matrix compression which is shown in Fig. 21. Of course, the increase of the CO_2 removal rates on increasing the matrix thickness or compression in the region around design values is at the expense of the internal cell resistance and on the anolyte pH which affects the anode overvoltage. Any change in these parameters should also consider these effects on the power requirements.

Effect of Air Relative Humidity and Temperature

The model predicts a slight increase of the CO_2 removal efficiencies as the air relative humidity decreases. Test data show no significant effect of this parameter beyond the experimental error limits. This predicted change may be because the change of the electrolyte surface

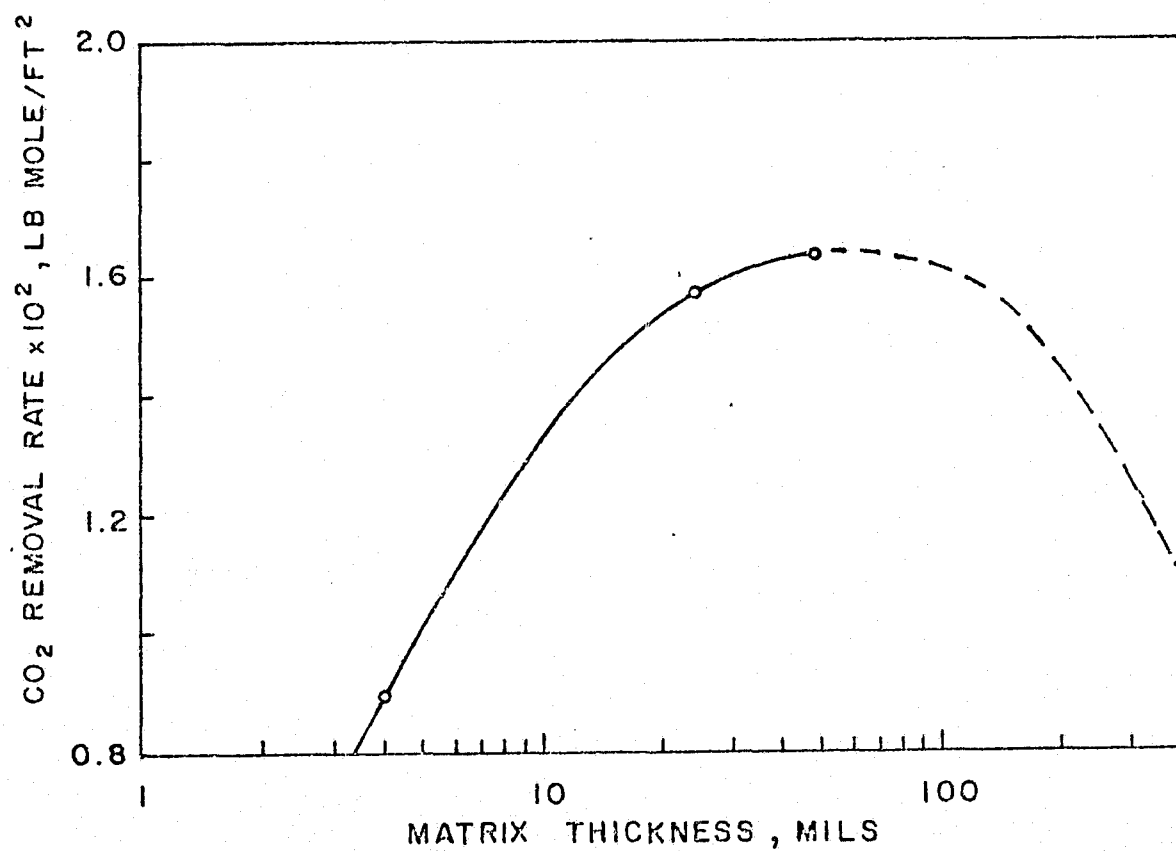


Fig. 20 Effect of Matrix Thickness on the CO₂ Removal Rate in the Analytical Cell

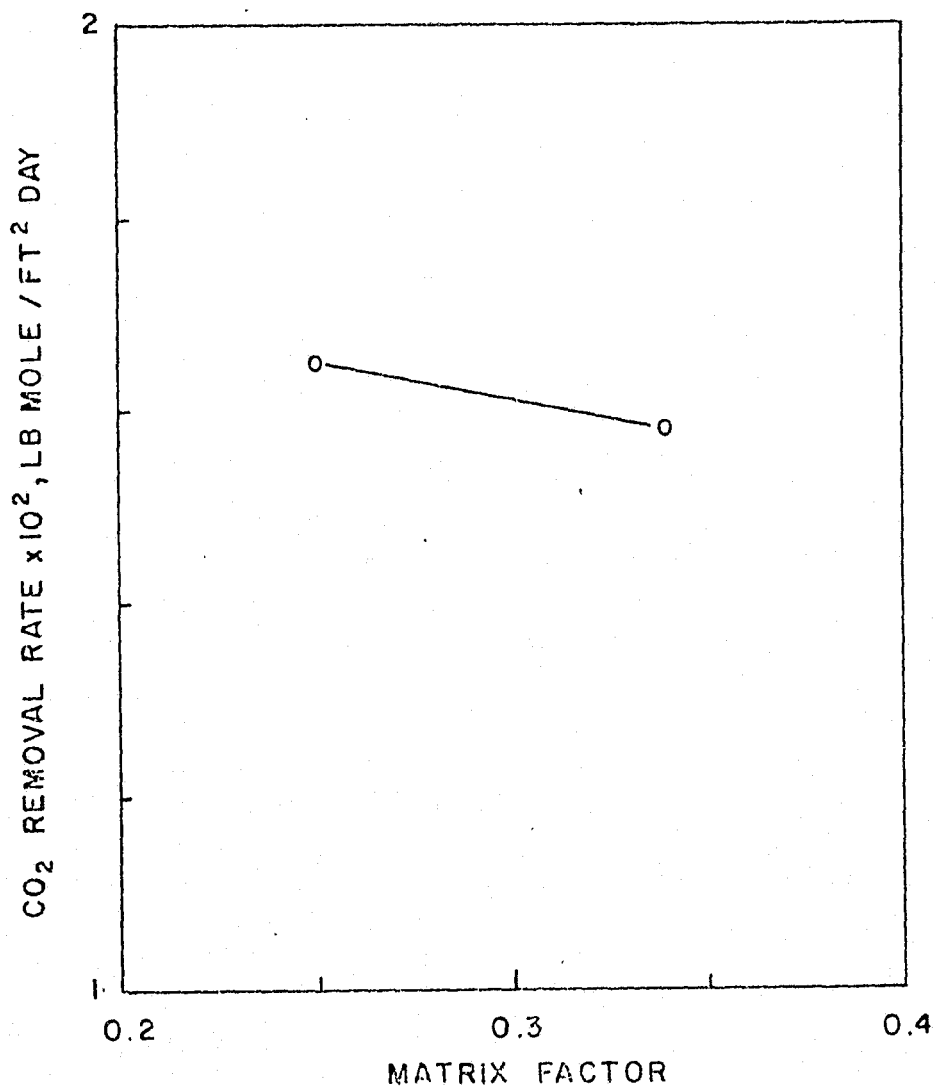


Fig. 21 Effect of Matrix Compression on the CO₂ Removal Rate in the Analytical Cell

tension with concentration is another factor to be considered in determining the gas-electrolyte interface area. Obviously, this cannot be accounted for here because of the empirical nature of the determination of the gas-electrolyte interface area and the lack of quantitative correlation with surface tension.

Temperature also has little effect on the CO_2 removal efficiency over a limited range. The effect of increasing the reaction rate constants k_i and the diffusivity of CO_2 in the catholyte with temperature seems to be counteracted by the decrease in the selectivity of the CO_3^{2-} as charge carrier, as the viscosity of the electrolyte decreases in the matrix zone.

More important is the change of the electrolyte concentration as the difference between the cell temperature and inlet air dew point increases. It is important that the concentration of the electrolyte at any point does not reach the solubility limit; otherwise the concentrator undergoes what is known as "cell drying" which causes the hydrogen to cross over from the anode chamber to the cathode chamber. Since the catholyte consists mostly of $(\text{NMe}_4)_2\text{CO}_3$ and the anolyte of NMe_4HCO_3 , the pure component solubilities can be used to check on that condition. Figure 22 shows the distribution of the concentration of the electrolyte at different points in the concentrator at air temperature of 70°F and dew point of 60°F. The cell temperature and water content of the air stream at any point along the air path is

determined by the current density, air flow rate, and cell voltage. As seen from Fig. 22 no precipitation is predicted in the concentrator at any point. Still at a lower air humidity, precipitation may commence at one or the other point in the concentrator. It is clear from Fig. 22 that precipitation could commence at the cathode rather than the anode because of the low solubility of $(\text{NMe}_4)_2\text{CO}_3$ compared with that of NMe_4HCO_3 . In the example of the computer output shown in Appendix B this precipitation is indicated at the cathode.

Effect of H_2 Flow Rate and Anode Active Area

The effect of changing the H_2 flow rate and the anode active area were investigated. No significant change of the CO_2 removal efficiency resulted on changing their values by several orders of magnitude. A slight decrease in the anolyte calculated pH was obtained on decreasing either the H_2 flow rate or the anode active area. The effect of the H_2 flow rate is the same as obtained experimentally (Huddleston and Aylward, 1973).

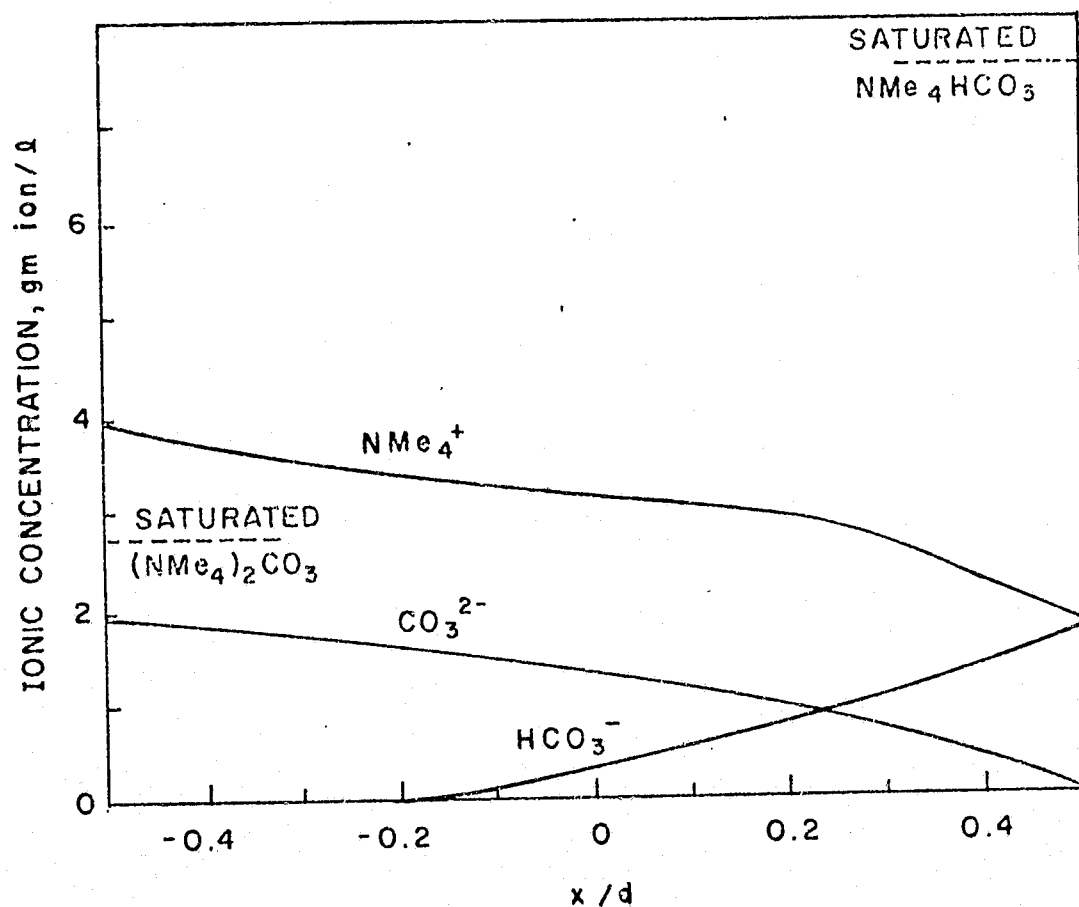


Fig. 22 The Concentration Distribution of the CO_3^{2-} , HCO_3^- and NMe_4^+ in the Analytical Cell at the Following Conditions: $P_{\text{CO}_2} = 4$ mm Hg, Current Density = 18 A/ft^2 , Air Velocity = 10 ft/sec , Air Temp. = 70°F , Air Dew Point = 60°F

CHAPTER VIII

CONCLUSIONS AND RECOMMENDATIONS

A mathematical model has been developed for simulating the steady-state performance in electrochemical CO_2 concentrators which utilize $(\text{NMe}_4)_2\text{CO}_3$ (aq.) electrolyte. This electrolyte which accommodates a wide range of air relative humidity is most suitable for one-man air revitalization systems. The model is based on the solution of coupled non-linear ordinary differential equations derived from mass transport and rate equations for the processes which take place in the cell. The boundary conditions are obtained by solving the mass and energy transport equations. A shooting-method is used to solve the differential equations.

The present model displays two different features from the previous model of the Cs_2CO_3 units (Lin and Winnick, 1974). It has been found that better fitting of test data is obtained if the CO_2 flux across the cell, N_{5T} , is proportional to the concentration of the hydroxyl ions in the catholyte, C_{2c} , rather than the square root of this concentration. It is known that in concentrated solutions the value of k_1 depends somehow on the activity coefficients of the reacting OH^- ions. The mean ionic activity coefficients of NMe_4OH obtained from vapor pressure measurements increase much more rapidly with concentration than those of alkali hydroxides.

This may explain the dependence of N_{5T} on C_{2C} rather than $(C_{2C})^{1/2}$. The second important difference between the two models is that the assumption of a constant air-catholyte interface area, S_c , at all current densities could not be extended to the present model. It was necessary to assume that the true interface area decreases with current density and that the decrease is more pronounced in the intermediate region (10-20 ASF). It was also necessary to use different values of S_c for the analytical and full-scale cells to simulate the test data. It seems that the relatively open structure of the new cathodes used in these cells promotes the role played by the electro-osmotic forces in changing the electrolyte equilibrium within the cathode pores. These forces are dependent on the current-density and this may explain the dependence of S_c on the current density.

The model has confirmed the importance of the cathode design and catholyte pH in determining the CO_2 removal efficiency; other factors being of little importance in that respect. The CO_2 removal rate increases with current density but the current efficiency has a maximum value at a certain current density. The optimum current density is dependent on the value of P_{CO_2} . The increase of the CO_2 removal rate with current density is more apparent as P_{CO_2} increases. At low values of P_{CO_2} (≤ 0.25 mm) the removal rate is significantly increased as the air velocity increases. However, the increase in the removal rate is rather limited at these low levels of P_{CO_2} . To attain the atmospheric CO_2 concentration level (0.25 mm Hg) inside the cabin

rather than the baseline design level (3 mm Hg), the number of the HDC cells must be approximately increased four to five times to remove the same amount of CO_2 .

In addition to calculating the CO_2 transfer rate at any set of specified conditions, the model also calculates the concentration distribution of all the important molecular species. These concentrations are difficult to measure experimentally because of the small dimensions of the cell. These calculations are important in several ways. First they can indicate if there is any precipitation expected in the cell under certain conditions. The concentration overpotential in the electrolyte can be estimated from the concentration distribution of the $(\text{NMe}_4)^+$ ion. The OH^- concentration at the cathode and the anode can also be helpful in estimating, in an approximate way, the electrode overpotential. From these components it may become possible to estimate the cell voltage beforehand and to understand the factors which contribute to a low cell voltage.

The capability of the model lies in the fact that it is derived from fundamental mass and energy transport equations with the parameters required by the model either independently measured or assigned reasonable values on the basis of previously developed equations. This gives us more confidence in extrapolation to off-design conditions than any empirical model. The only parameter that could not be obtained independently from test data was the air-catholyte interface area. The variation of this area with current density was easily identified

C.2

since the other parameters were fixed. With the growth of our understanding of the nature of porous electrodes and the equilibrium between the gas and electrolyte within the electrode pores, a method may be developed to estimate this parameter from measurable properties such as electrode porosity, pore diameter, and electrolyte properties. In that case a completely self-independent model can be developed which does not depend in any way on test data.

Any attempt to improve the removal efficiency should concentrate on the cathode design and the factors which increase the gas-electrolyte interface area. The geometric configuration of the electrodes may have an important effect in that respect as is shown by the test data of the analytical cell compared with the full-scale cell. The search for new electrolytes to accommodate wide ranges of air humidity should concentrate on higher members of the tetraalkylammonium carbonate series. Increasing the size of the NR_4^+ radical is accompanied by an increase in γ_+ for the carbonate according to the model of the activity coefficients presented in Chapter VI. It should be expected that the higher members will have lower water activity, and thus, a greater value of water vapor pressure lowering. Further investigation of new electrolytes should concentrate on tetraethyl-, tetrapropyl- and tetrabutylammonium carbonates.

NOMENCLATURE

a	activity
A	electrode area, ft^2
B	viscosity coefficient defined by equation [6-8], ℓ/gmole
c	constant in equation [2-10], ℓ/gmole
C	molar concentration in electrolyte, $\text{lb mole}/\text{ft}^3$
d	matrix thickness, mils
D	diffusion coefficient or molecular diffusivity, ft^2/hr
E	cell potential, V
f	compression factor in equation [5-1]
F	Faraday's constant, 96,487 C/eq
g	constant in equation [2-6]
G	parameter defined by equation [4-33]
h	mass-transfer coefficient, ft/hr
H	Henry's Law constant of CO_2 in electrolyte, $\text{mm ft}^3/\text{lb. mole}$
ΔH_R	heat of formation of water vapor, cal/gmole
I	current density, A/ft^2
J	mechanical heat equivalent, 4.184 J/cal
k	reaction rate constant, $\text{ft}^3/\text{lb. mole hr}$
K	equilibrium constant, $\text{ft}^3/\text{lb. mole}$
ℓ	constant in equation [2-6], ℓ/gmole
L	ionic radius, \AA
m	molality, gmole/kg
M	molecular weight of solvent

- N molar flux, lb mole/ft² day
- p constant in equation [2-17]
- P partial pressure, mm Hg
- q constant in equation [2-17]
- Q rate of heat generation, BTU/hr
- r local rate of reaction, lb mole/ft³ hr
- R universal gas constant, 555 mm ft³/lb mole °R
- s partial molar entropy of hydration, gibbs/gmole
- S gas-electrolyte area per unit of electrode geometric area, ft²/ft²
- T cell temperature, °K
- u electrical mobility, lb mole ft²/J sec
- v average molar bulk velocity of bulk solution, ft/sec
- V volumetric gas flowrate, ft³/hr
- \bar{V} partial molar volume of ion, cm³/gmole
- x coordinate dimension between electrodes, ft
- X electric field, V/cm
- z ionic charge
- Z mole fraction

Greek letters

- α matrix labyrinth factor
- β empirical parameter, equation [5-1]
- γ activity coefficient
- Γ reduced activity coefficient, defined by equation [6-10]

- Δ difference between CO_2 partial pressure in the gas phase and at gas-electrolyte interface, mm Hg.
- ∇ specific interaction coefficients in equation [A-4], ℓ/gmole
- δ_1 smaller side of rectangular air channel, ft
- δ_2 larger side of rectangular air channel, ft
- δ_3 length of air channel, ft
- ϵ matrix porosity
- η viscosity of solution, centipoise
- λ ionic equivalent conductance, mhos cm/eq
- μ ionic strength of solution, gmole/ℓ
- ν number of ions in solution per one molecule of electrolyte
- ξ hydration number
- τ matrix tortuosity
- ϕ osmotic coefficient
- Φ electrical potential, V
- ψ function defined by equation [4-40]
- χ ratio between the apparent molar volume of electrolyte and molar volume of water

Superscripts

- \dagger gas-electrolyte interface
- \sim equilibrium value
- \leftarrow backward reaction
- $^\circ$ infinite dilution
- $*$ characteristic value

~ dimensionless

Subscripts

a	anode
c	cathode
el	electrostatic
G	gas
h	hydration
I	gas inlet
j	ionic species
L	liquid
m	multicomponent
so	salting out
st	structural
T	total
0	gas outlet
1	HCO_3^-
2	OH^-
3	CO_3^{2-}
4	NMe_4^+
5	CO_2
6	H_2O
i	reaction [2-1]
ii	reaction [2-2]
iii	reaction [2-3]

iv reaction [2-4]

+ cation

- anion

+ activated complex in equation [6-23]

BIBLIOGRAPHY

- (1) Abdel-Salam, O.E., 1974, unpublished.
- (2) Astarita, G., "Mass Transfer with Chemical Reaction", Elsevier, New York, 1967.
- (3) Austin, L.G., in "Handbook of Fuel Cell Technology", Berger, C., ed., Prentice-Hall, New Jersey, 1968, pp. 1-211.
- (4) Aylward, J.R., Intermediate Report No. NAS 9-13679, NASA Johnson Space Center, Dec. 1974.
- (5) Aylward, J.R., IR & D Status Report, Hamilton Standard Division of United Aircraft Corporation, Feb. 1975.
- (6) Bhatia, R.N., K.E. Gubbins, and R.D. Walker, Trans. Faraday Soc., 64, 2091 (1968).
- (7) Bockris, J.O'M., and S. Srinivasan, "Fuel Cells: Their electrochemistry", McGraw-Hill, New York, 1969, pp. 247-284.
- (8) Churchill, S.W., and R. Usagi, Ind. Eng. Chem., Fundam., 13, 39 (1974).
- (9) Crane, R.L., and R.W. Klopfenstein, J. Assoc. Comput. Machinery, 12, 227 (1965).
- (10) Desnoyers, J.E., and B.E. Conway, J. Phys. Chem., 68, 2305 (1964).
- (11) Desnoyers, J.E., M. Arél, G. Perron, and C. Jolicoeur, ibid, 73, 3346 (1969).
- (12) Desnoyers, J.E., and G. Perron, J. Solution Chem., 1, 199 (1972).
- (13) Edsall, J.T., "Carbon Dioxide, Carbonic Acid and Bicarbonate Ion: Physical Properties and Kinetics of Interconversion", NASA SP-188, Aug. 1968.
- (14) Frost, A.A., and R.G. Pearson, "Kinetics and Mechanism: a Study of Homogeneous Chemical Reactions", 2nd ed., Wiley, New York-London, 1961, pp. 150-152.
- (15) Glueckauf, E., Trans. Faraday Soc., 51, 1235 (1955).

- (16) Gurney, R.W., "Ionic Processes in Solutions", Dover, New York, 1962.
- (17) Harned, H.S., and B.B. Owen, "The Physical Chemistry of Electrolytic Solutions", 3rd ed., Reinhold, New York, 1958, pp. 758.
- (18) Huddleston, J.C., and J.R. Aylward, Final Report No. NAS 9-11830, NASA Manned Space Center, May 1972.
- (19) Huddleston, J.C., and J.R. Aylward, Final Report No. NAS 9-12920, NASA Johnson Space Center, Sept. 1973.
- (20) (a) Huddleston, J.C., and J.R. Aylward, 16th Progress Report No. NAS 9-13679, NASA Johnson Space Center, April 1975.
(b) Huddleston, J.C., and J.R. Aylward, 17th Progress Report No. NAS 9-13679, NASA Johnson Space Center, May 1975.
(c) Huddleston, J.C., and J.R. Aylward, Final Report No. NAS 9-13679, NASA Johnson Space Center, June 1975.
- (21) Keller, H.B., "Numerical Methods for Two Point Boundary Value Problems", Blaisdell, Waltham, Mass., 1968.
- (22) Kern, D.M., J. Chem. Educ., 37, 14 (1960).
- (23) Knudsen, T.G., and D.L. Katz, "Fluid Dynamics and Heat Transfer", McGraw-Hill, New York, 1958, p. 388.
- (24) Lakshminarayanan, N., "Transport Phenomena in Membranes", Academic Press, New York-London, 1969.
- (25) Levien, B.J., J. Australian Chem., 18, 1161 (1965).
- (26) Lietzke, M.H., and R.W. Stoughton, J. Phys. Chem., 66, 508 (1962).
- (27) Lietzke, M.H., R.W. Stoughton, and R.M. Fuoss, Proc. Natl. Acad. Sci., U.S., 59, 39 (1968).
- (28) Lin, C.H., and J. Winnick, Ind. Eng. Chem., Process Des. Develop. 13, 63 (1974).
- (29) Lin, C.H., M. Heinemann, and R.M. Angus, *ibid*, 13, 261 (1974).
- (30) Lindenbaum, S., and G.E. Boyd, J. Phys. Chem., 68, 911 (1964).
- (31) Mackie, J.S., and P. Meares, Proc. Roy. Soc. (London), A232, 498 (1955).

- (32) Markin, V.S., A.A. Chernenko, Yu. A. Chizmadzhev, and Yu. G. Chirkov, in "Fuel Cells: Their Electrochemical Kinetics", Bagotskii, V.S., and Yu. B. Vasil'ev, ed., Trans. from Russian, Consultant Bureau, New York, 1966, pp. 21-33.
- (33) Marshall, R.D., F.H. Schubert, and J.N. Carlson, Final Report No. NAS 2-6478, NASA Ames Research Center, Aug. 1973.
- (34) McManamey, W.J., and J.M. Woollen, *AIChE J.*, 19, 667 (1973).
- (35) Meissner, H.P., and C.K. Kusik, *ibid*, 18, 294 (1972).
- (36) Meissner, H.P., and J.W. Tester, *Ind. Eng. Chem., Process Des. Develop.*, 11, 128 (1972).
- (37) Millero, F.J., *Chem. Rev.*, 71, 147 (1971).
- (38) Morén, C., *J. Electrochem. Soc.*, 122, 500 (1975).
- (39) Neff, G.W., *Anal. Chem.*, 42, 1579 (1970).
- (40) Newman, J., "Electrochemical Systems", Prentice-Hall, New Jersey, 1973, p. 217.
- (41) Nysing, R.A.T.O., and K. Kramers, *Europ. Symp. Chem. React. Eng.*, 1st, Amsterdam (1957).
- (42) Perry, R.H., C.H. Chilton, and S.D. Kirkpatrick, ed., "Chemical Engineers Handbook", 4th ed, McGraw-Hill, New York, 1963.
- (43) Pethybridge, A.D., and J.E. Prue, *Chem. Soc., Annual Report*, 65A, 129 (1968).
- (44) Pinsent, B.R.W., L. Pearson, and F.J.W. Roughton, *Trans. Faraday Soc.*, 52, 1512 (1956).
- (45) Prue, J.E., A.J. Read, and G. Romeo, *ibid*, 67, 420 (1971).
- (46) Randles, J.E.B., *Adv. Electrochem. Electrochem. Eng.*, 3, 1 (1963).
- (47) Roberts, S.M., and J.S. Shipman, "Two-Point Boundary Value Problems: Shooting Methods", American Elsevier, New York, 1972.
- (48) Robinson, R.A., and R.H. Stokes, "Electrolyte Solutions", 2nd ed., Butterworths, London, 1959.

- (49) Russell, C.R., Final Report No. NAS 9-12920, NASA Johnson Space Center, March 1973.
- (50) Srinivasan, S., and E. Gileadi, in "Handbook of Fuel Cell Technology", Berger, C., ed., Prentice-Hall, New Jersey, 1968, pp. 219-357.
- (51) Stokes, R.H., and R.A. Robinson, J. Amer. Chem. Soc., 70, 1870 (1948).
- (52) Stokes, R.H., and R.A. Robinson, *ibid*, 53, 301 (1957).
- (53) Van Krevelen, D.W., and P.J. Hoftijzer, Chim. Ind., XXI em Congres Int. Chim. Ind., 168 (1948).
- (54) Wen, W.Y., in "Water and Aqueous Solutions", Horne, R.A., ed., Wiley-Interscience, New York, 1972, Chap. 6.
- (55) Wen, W.Y., S. Saito, and C. Lee, J. Phys. Chem., 70, 1244 (1966).
- (56) Wheeler, A., Advances in Catalysis, 3, 249 (1951).
- (57) Winnick, J., R.D. Marshall, and F.H. Schubert, Ind. Eng. Chem., Process Des. Develop., 13, 59 (1974).
- (58) Wishaw, B.F., and R.H. Stokes, J. Amer. Chem. Soc., 76, 2065 (1954).

APPENDIX A

DETAILED CALCULATIONS

Activity Coefficients

Table 1 contains the activity coefficients of tetramethylammonium halides used in interpolation in the concentration range from 0.1m to 1.5m (the iodide forms a saturated solution at 0.2715m).

TABLE 1

ACTIVITY COEFFICIENTS OF TETRAMETHYLAMMONIUM HALIDES AT 25°C

m	NMe ₄ F	NMe ₄ Cl	NMe ₄ Br	NMe ₄ I
0.1	0.795	0.746	0.7203	0.6985
0.2	0.776	0.683	0.6450	0.6136
0.3	0.778	0.644	0.5976	
0.4	0.787	0.617	0.5637	
0.5	0.802	0.597	0.5375	
0.6	0.823	0.580	0.5160	
0.7	0.846	0.566	0.4974	
0.8	0.873	0.556	0.4827	
0.9	0.902	0.546	0.4688	
1.0	0.931	0.539	0.4582	
1.2	0.998	0.527		
1.4	1.077	0.520		
1.5			0.4432	

The electrostatic, hydration, and mutual salting-out terms for these halides were calculated using equations [6-4], [6-5], and the modified forms of equations [6-6] and [6-7]. The hydration numbers used were the same as suggested by Glueckauf (1955), 0.9 for Cl^- , Br^- , and I^- , 1.8 for F^- , and 0.0 for NMe_4^+ . The partial molal volumes tabulated by Millero (1971) were also used. Table 2 shows these calculated terms and the term $\log \gamma_{st}$ obtained by subtraction from $\log \gamma_{\pm}$.

The term $(B_j - 0.0025 \bar{V}_j)$ used in interpolation was calculated from the values of B_j and \bar{V}_j shown in Table 3 for the ions in question. These values of $(-\log \gamma_{st})$ were plotted against the term $(B_j - 0.0025 \bar{V}_j)$, for the halides and then used to calculate the same terms for $(\text{NMe}_4)_2\text{CO}_3$, NMe_4HCO_3 , and NMe_4OH as shown in Fig. 23. In the case of NMe_4OH the activity coefficients exceeded unity. Thus it was inappropriate to use the activities as a measure of ion density. Instead, the Debye-Huckel term was calculated using the ionic strength as a measure of the ion density with the ion size parameters calculated with the following equation of Stokes and Robinson (1957):

$$L_j = 0.613 (\bar{V}_j + 18 \epsilon_j)^{1/3} \quad [\text{A-1}]$$

and

TABLE 2
TERMS IN EQUATION [6-3] FOR THE NMe_4 -HALIDES

m	$\log \gamma_{el}$	$\log \gamma_h$	$\log \gamma_{so}$	$\log \gamma_{st}$
NMe_4F				
0.1	-0.0991	0.0138	0.0054	-0.0197
0.2	-0.1233	0.0274	0.0105	-0.0247
0.3	-0.1390	0.0408	0.0159	-0.0267
0.4	-0.1509	0.0540	0.0214	-0.0285
0.5	-0.1605	0.0670	0.0272	-0.0294
0.6	-0.1689	0.0798	0.0336	-0.0291
0.7	-0.1761	0.0925	0.0402	-0.0292
0.8	-0.1826	0.1049	0.0475	-0.0288
0.9	-0.1885	0.1171	0.0552	-0.0286
1.0	-0.1938	0.1292	0.0633	-0.0298
1.2	-0.2033	0.1528	0.0814	-0.0318
1.4	-0.2117	0.1758	0.1024	-0.0345
NMe_4Cl				
0.1	-0.0943	0.0089	0.0062	-0.0481
0.2	-0.1145	0.0177	0.0113	-0.0801
0.3	-0.1268	0.0262	0.0160	-0.1065
0.4	-0.1357	0.0345	0.0204	-0.1289
0.5	-0.1483	0.0427	0.0247	-0.1431
0.6	-0.1540	0.0507	0.0288	-0.1621
0.7	-0.1530	0.0585	0.0328	-0.1855
0.8	-0.1572	0.0661	0.0368	-0.2006
0.9	-0.1608	0.0736	0.0407	-0.2163
1.0	-0.1642	0.0809	0.0446	-0.2297
1.2	-0.1699	0.0950	0.0542	-0.2557
1.4	-0.1749	0.1085	0.0603	-0.2779

TABLE 2 - Continued

m	$\log \gamma_{el}$	$\log \gamma_h$	$\log \gamma_{so}$	$\log \gamma_{st}$
NMe ₄ Br				
0.1	-0.0924	0.0104	0.0063	-0.0668
0.2	-0.1114	0.0206	0.0113	-0.1109
0.3	-0.1228	0.0305	0.0156	-0.1469
0.4	-0.1308	0.0402	0.0197	-0.1781
0.5	-0.1371	0.0497	0.0234	-0.2056
0.6	-0.1421	0.0589	0.0270	-0.2312
0.7	-0.1463	0.0679	0.0304	-0.2553
0.8	-0.1500	0.0767	0.0337	-0.2767
0.9	-0.1531	0.0854	0.0368	-0.2981
1.0	-0.1560	0.0938	0.0400	-0.3167
1.5	-0.1590	0.1332	0.0580	-0.3856
NMe ₄ I				
0.1	-0.0903	0.0127	0.0063	-0.0845
0.2	-0.1136	0.0250	0.0113	-0.1403

TABLE 3

IMPORTANT PARAMETERS OF THE IONS

Ion	B	$\bar{V}^\circ, \text{cm}^3 \text{mol}^{-1}$	s, gibbs mol^{-1}	$L, \text{\AA}$	ξ
F ⁻	0.155	4.2	3.0	1.36	1.8
Cl ⁻	0.014	23.2	18.5	1.81	0.9
Br ⁻	-0.021	30.1	24.6	1.95	0.9
I ⁻	-0.060	41.6	31.4	2.16	0.9
CO ₃ ²⁻	0.171	6.5	-2.0	1.99	
HCO ₃ ⁻	-0.040	28.8	28.0	1.33	
OH ⁻	0.181	1.4	2.8	1.33	
NMe ₄ ⁺	0.099	84.2		3.47	0.0

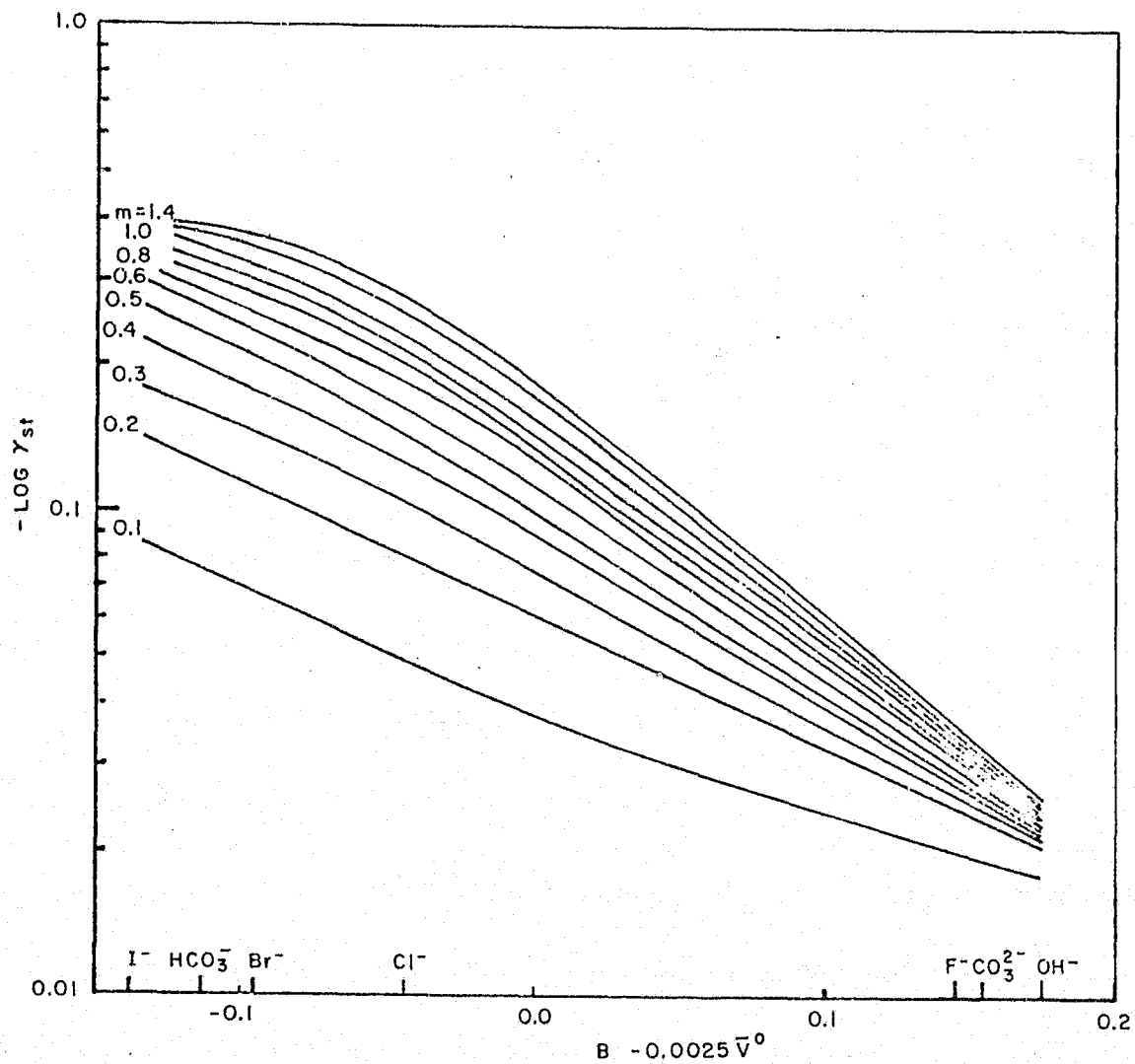


Fig. 23 The $-\log \gamma_{st}$ Term in Equation [6.3] for Tetramethylammonium Electrolytes at 25°C

$$L = L_+ + L_- \quad [A-2]$$

The hydration numbers of $(NMe_4)_2CO_3$, NMe_4HCO_3 , and NMe_4OH were chosen so that the experimental osmotic coefficient data at the lowest concentrations agree with the value obtained by the equation (Robinson and Stokes, 1959)

$$\phi = 1 + (1/m) \int_0^m m \, d \ln \gamma \quad [A-3]$$

The values obtained for these electrolytes are 1.5, 0, and 6.4, respectively. The small hydration number obtained for NMe_4HCO_3 may be attributed to a higher degree of association than that expected by simple structural arguments. The calculated activity coefficient terms for the three electrolytes are shown in Table 4 while the experimental and calculated osmotic coefficients and the derived activity coefficients are shown in Table 5.

For concentrations below 0.1m, the activity coefficients can be calculated by the Guggenheim equation

$$\log \gamma_{\pm} = -0.5809 |z_+ z_-| \mu^{1/2} / (1 + \mu^{1/2}) + \nabla_{ij} \mu \quad [A-4]$$

where ∇_{ij} is the specific interaction coefficient between ions i

TABLE 4
OSMOTIC AND ACTIVITY COEFFICIENTS OF
(NMe₄)₂CO₃, NMe₄HCO₃, AND NMe₄OH AT 25°C

m	ϕ_{exp}	ϕ_{calc}	γ	m	ϕ_{exp}	ϕ_{calc}	γ
(NMe ₄) ₂ CO ₃							
0.1		0.726	0.578	1.202	1.377		0.975
0.2		0.823	0.548	1.603	1.857		1.88
0.3		0.877	0.545	2.060	2.417		4.38
0.4		0.924	0.555	2.584	2.974		11.3
0.5		0.967	0.573	3.205	3.434		28.6
0.534	0.981	0.981	0.579	3.934	4.027		90.5
0.848	1.108		0.685	4.808	4.326		230
NMe ₄ HCO ₃							
0.1		0.811	0.685	1.307	0.604	0.614	0.286
0.2		0.792	0.589	1.852	0.801		0.313
0.3		0.767	0.526	2.469	1.012		0.375
0.4		0.743	0.479	3.175	1.158		0.443
0.5		0.720	0.441	3.989	1.323		0.552
0.6		0.700	0.410	4.938	1.405		0.648
0.7		0.680	0.383	6.061	1.518		0.797
0.8		0.662	0.360	7.407	1.547		0.913
0.9		0.645	0.340	9.054	1.619		1.10
1.0		0.629	0.322	11.111	1.688		1.35
1.2		0.614	0.296				
NMe ₄ OH							
0.1		0.926	0.863	1.221	1.505		2.21
0.2		1.008	0.916	1.939	1.702		3.55
0.3		1.113	1.042	2.747	1.982		6.30

TABLE 4 - Continued

m	ϕ_{exp}	ϕ_{calc}	γ	m	ϕ_{exp}	ϕ_{calc}	γ
NMe ₄ OH							
0.4		1.183	1.166	3.663	2.366		13.0
0.5		1.252	1.312	4.710	2.722		27.3
0.5783	1.320	1.320	1.463	5.917	3.198		68.7

TABLE 5

THE TERM $\text{LOG } \gamma_{\text{st}}$ FOR THE HYDROXIDES AT 25°C

	LiOH	NaOH	KOH	CsOH	NMe ₄ OH
L_+	0.6 Å	0.95 Å	1.33 Å	1.65 Å	3.47 Å
m					
0.1	-0.0694	-0.0416	-0.0253	-0.0091	-0.0179
0.2	-0.1130	-0.0724	-0.0436	-0.0270	-0.0201
0.3	-0.1579	-0.1038	-0.0624	-0.0463	-0.0211
0.4	-0.2033	-0.1366	-0.0803	-0.0638	-0.0218
0.5	-0.2501	-0.1712	-0.0975	-0.0816	-0.0223

and j. From the calculated activity coefficients of (NMe₄)₂CO₃, NMe₄HCO₃, and NMe₄OH the ∇_{ij} coefficients were found to be 0.439, -0.420, and 0.583 mole⁻¹, respectively. For comparison the ∇_{ij} value for NMe₄OH is 0.5 ± 0.1 mole⁻¹ as obtained by cell measurements (Prue et al., 1971).

According to the structural hydration model (Desnoyers et al., 1969), the activity coefficients of alkali and tetra-

methylanmonium electrolytes with the same anion vary in a systematic manner as the cation size increases. Table 5 shows the calculated $\log \gamma_{st}$ term for the hydroxides which exhibit that systematic change.

To test the accuracy of this method, the activity coefficients of Na_2CO_3 were calculated by adding the electrostatic hydration, mutual salting-out and structural terms, calculated as described earlier. Since the CO_3^{2-} and OH^- ions are very similar in their structural effects (Fig. 23), it is reasonable to use the values of $\log \gamma_{st}$ of NaOH in Table 5 for Na_2CO_3 . The calculated activity coefficients are compared with the experimental values in Table 6. These values agree within $\pm 5\%$.

TABLE 6
ACTIVITY COEFFICIENTS OF Na_2CO_3 AT 25°C

m	$\gamma_{\text{calc.}}$	$\gamma_{\text{exp.}}$
0.1	0.489	0.466
0.2	0.406	0.394
0.3	0.357	0.356
0.4	0.319	0.332
0.5	0.288	0.313

Characteristic Parameters

Table 7 contains the characteristic parameters used in calculations.

Table 7

CHARACTERISTIC PARAMETERS

C^* , lb mol/l	0.4495
D^* , ft ² /hr	1×10^{-5}
d^* , mils	30
γ_T	7.7

Equilibrium and Henry's Law Constants

The concentrations of the different spaces used in calculating the average equilibrium constants are shown in Table 8. These concentrations are approximately the same as obtained at the base conditions ($P_{CO_2} = 3$ mm Hg, $I = 18A/ft^2$, and inlet air dewpoint = 60°F). Table 8 also contains the factors which should be multiplied by K_i^o

Table 8

AVERAGE CONCENTRATIONS AND EQUILIBRIUM CONSTANTS

	C_1	C_2	C_3	K_i/K_i^o	K_{ii}/K_{ii}^o	H/H^o
	g mole/l					
Cathode Zone	0.003	0.5	1.80	33	8.1	1.686
Matrix Zone	-	-	-	20	4.5	-
Anode Zone	1.8	10^{-6}	0.018	7.1	0.85	1.190

Diffusion Coefficients and Mobilities

Table 9 contains the values of λ° and D° for the different ions at infinite dilution. Table 10 shows the calculated diffusion coefficients and Table 11 shows the calculated equivalent conductivity.

TABLE 9
EQUIVALENT CONDUCTANCES AND DIFFUSION COEFFICIENTS
AT INFINITE DILUTION AND 25°C

Ion	$\lambda^\circ, \text{cm}^2 \Omega^{-1} \text{equiv}^{-1}$	$D^\circ \times 10^5, \text{cm}^2/\text{sec}$
CO_3^{2-}	69.3	0.922
HCO_3^-	44.5	1.185
OH^-	198.3	5.278
NMe_4^+	44.9	1.196

TABLE 10
DIFFUSION COEFFICIENTS AT 25°C

m	C	$1 + \frac{d\lambda n\gamma}{d\lambda n m}$	η/η°	$D \times 10^5, \text{cm}^2/\text{sec}$	$D^- \times 10^5, \text{cm}^2/\text{sec}$
$(\text{NMe}_4)_2\text{CO}_3$					
0.1	0.0982	0.913	1.12	0.887	0.752
0.2	0.193	0.960	1.21	0.863	0.731
0.5	0.461	1.083	1.46	0.807	0.731
1.0	0.846	1.905	1.91	1.085	0.919
2.0	1.482	4.772	3.15	1.648	1.397
3.0	1.969	5.718	7.47	0.833	0.706
4.0	2.360	6.552	12.1	0.589	0.499

TABLE 10 - Continued

m	C	$1 + \frac{d\ln\gamma}{d\ln m}$	η/η°	$D \times 10^5, \text{cm}^2/\text{sec}$	$D^- \times 10^5, \text{cm}^2/\text{sec}$
NMe_4HCO_3					
0.1	0.100	0.820	1.07	0.912	0.908
0.2	0.195	0.752	1.08	0.829	0.826
0.5	0.472	0.610	1.18	0.615	0.612
1.0	0.895	0.465	1.37	0.404	0.402
2.0	1.638	1.649	1.69	1.161	1.156
3.0	2.229	1.730	2.25	0.915	0.911
4.0	2.740	1.787	3.09	0.688	0.685
5.0	3.176	1.850	4.04	0.545	0.543
10.0	4.660	2.100	11.8	0.212	0.211
NMe_4OH					
0.1	0.0991	1.035	1.03	1.958	5.302
0.2	0.196	1.240	1.07	2.270	6.147
0.5	0.480	1.571	1.24	2.469	6.686
1.0	0.917	1.685	1.37	2.397	6.491
2.0	1.711	2.510	2.08	2.352	6.369
3.0	2.357	3.333	2.78	2.337	5.329

TABLE 11
EQUIVALENT CONDUCTANCES AT 25°C

$(\text{NMe}_4)_2\text{CO}_2$		NMe_4HCO_3		NMe_4OH	
C	Λ	C	Λ	C	Λ
0.49	55.8	0.35	63.7	0.55	193
0.74	46.4	0.72	53.5	1.11	166
0.99	37.9	1.12	44.6	1.67	137
1.26	29.0	1.50	38.7	2.23	112
1.52	22.2	1.90	33.3	2.81	83.1
1.69	17.3	2.32	28.8	3.39	66.7
2.06	11.3	2.72	25.4	3.98	47.2

TABLE 11 - Continued

$(\text{NMe}_4)_2\text{CO}_3$		NMe_4HCO_3		NMe_4OH	
C	Λ	C	Λ	C	Λ
2.33	7.36	3.15	21.4		
2.61	4.12	3.57	17.1		
2.92	1.87	4.02	12.8		
		4.45	9.64		
		4.90	7.16		

The diffusion coefficients and mobilities (as well as the increase in mobilities for a ten degree Fahrenheit increase) of each anion were fit to polynomials in concentration of sixth degree. The coefficients of these polynomials are given in Table 11. The viscosities were approximated by a single polynomial of fourth degree such that at any point the viscosity is given by

$$\eta = \eta(C_1 + C_2 + 2C_3) \quad [\text{A-5}]$$

The fitting equation is

$$\eta = 0.8937 - 1.00938 C + 2.37864 C^2 - 1.13294 C^3 + 0.17625 C^4 \quad [\text{A-6}]$$

The change of viscosity with temperature is assumed to be proportional to that of water.

Cathode and Anode Active Areas

Instead of calculating the magnitudes of the cathode active areas, the dimensionless parameters $(\hat{N}_{5T}/\hat{C}_{5C})$ was calculated. This parameter is proportional to \hat{C}_{2C} which should also give the same value

TABLE 12
COEFFICIENTS OF THE POLYNOMIALS USED IN CALCULATING
THE IONIC DIFFUSION COEFFICIENTS AND MOBILITIES

Parameter	c^0	c^1	c^2	c^3	c^4	c^5	c^6
CO_3^{2-}							
$D \times 10^5, \text{ cm}^2/\text{sec}$	0.90718	-1.10333	-0.29669	4.80487	-4.31020	1.25519	-0.10134
$u F^2$	34.395	-47.222	27.566	5.098	-14.045	5.796	-0.754
$\Delta u F^2$	2.437	0.380	-2.072	0.199	0.890	-0.435	0.060
HCO_3^-							
$D \times 10^5, \text{ cm}^2/\text{sec}$	1.22224	-3.13108	4.17542	-1.85812	0.23239	0.02796	-0.00587
$u F^2$	44.392	-45.917	40.410	-21.182	6.027	-0.875	0.051
$\Delta u F^2$	2.415	1.739	-2.139	0.712	-0.069	-0.007	0.001
OH^-							
$D \times 10^5, \text{ cm}^2/\text{sec}$	5.13441	5.60765	-6.31471	1.45324	1.28160	-0.74001	0.10685
$u F^2$	198.110	-100.195	59.105	-17.696	-3.231	2.461	-0.309
$\Delta u F^2$	14.653	-4.307	4.263	-2.789	0.285	0.155	-0.028

of \hat{N}_{5T} as calculated from the differential equations which represent the mass transfer processes in the matrix zone. By trial and error the correct value of \hat{C}_{2c} was obtained in each case from which the value of $(\hat{N}_{5T}/\hat{C}_{5c}\hat{C}_{2c})$ was calculated. As this parameter is presumably constant at a given current density and total ionic strength, an average value was calculated for each current density and air dew point. For example, the average value of this dimensionless parameter at 18ASF and 60°F for an inlet dew point in the analytical cell is 2.820×10^6 . The relative change of this parameter with current density is the same as that of cathode active area (Fig. 10).

To calculate the value of S_a we can use the experimental value of CO_2 flux obtained for the full-scale cell at a current density of 18A/ft², P_{CO_2} of 3mm Hg, and V_a of 600 cm³/min. Equation [4-32] gives a value of 0.004775 gmole/l for C_{5a} . Previous measurement of the pH in the NMe_4HCO_3 solutions at a concentration of 1.8 gmole/l under constant pressure of CO_2 was 8.21g (Abdel-Salem, 1974). Assuming that the pH of the solution measures the hydrogen ion activity and the activities of hydroxyl ions are the same as those of NMe_4OH at this low concentration, then the ratio C_1/C_2K_i at the anode is 0.006508 gmole/l. From equation [4-42] the value of the dimensionless parameter $[\hat{K}_a\hat{D}_5(\hat{C}_2 + G)]^{1/2}$ in that case is 1440 units. Increasing the value of this parameter by several times has only little effect on the calculated CO_2 removal rate. Therefore this value is used throughout.

APPENDIX B

COMPUTER PROGRAM

Calculation of the heat, water, and CO_2 transport in the cell are performed by the attached computer program. The program consists of a main program and several subroutines. The calculations for any set of conditions proceed as follows:

- (1) The subroutine ENERGY calculates the temperature of each subcell and the catholyte concentration. The subroutine LAGRAN is used in interpolation from the table of vapor pressure data for $(\text{NMe}_4)_2\text{CO}_3$ solutions. (The interpolation is based on the method of Lagrange. The calculated temperature, catholyte concentration, and outlet air dew point depend on the current density, cell voltage, and air flow rate together with the inlet air temperature and dew point. These parameters must be specified for each case.
- (2) An initial guess of the CO_2 flux is made. This is used to calculate the CO_2 concentration in the catholyte which is then used to calculate the OH^- concentration in the catholyte. From this information the concentrations of CO_3^{2-} and HCO_3^- are obtained at $\bar{x} = -1/2$.
- (3) With the guessed value of the CO_2 flux the differential equations [4-34] and [4-35] are integrated using subroutine CRANE. The derivatives are evaluated in each step by the subroutine DERIV. The subroutine DIN calculates the ionic mobilities and diffusion coefficients. The subroutine DATAI is used to calculate the equilibrium constants at the cell temperature. From the calculated CO_3^{2-} and HCO_3^- concentrations at the anode the anode CO_2 flux is calculated and compared with the

guessed cathode flux.

(4) The boundary condition at the anode is satisfied when the calculated anode flux is within 5% of the guessed value at the cathode. This results in an error of no more than 0.01% in the calculated CO_2 flux. Convergence is obtained more rapidly if the initial guess and upper and lower limits for the flux are reasonable. For any set of operating conditions the initial guess can be obtained approximately from Figs. 11 and 16. This reduces the computer time considerably.

(5) When the boundary conditions are satisfied the concentration distribution across the matrix is obtained for all the ionic species. If the concentration exceeds the solubility limit at any point a warning is issued to that effect. It is sufficient to check the catholyte and anolyte and not the entire matrix.

The program is written in FORTRAN G1 language. The calculations were carried out on IBM 360 machine. The attached listing shows calculations for four cases using different operating conditions. In one case precipitation is indicated when a high current density (30A/ft^2) is combined with a low air relative humidity.

C THIS PROGRAM PERFORMS CALCULATIONS FOR THE MATHEMATICAL MODEL WHICH
 C SIMULATES HEAT, WATER AND CARBON DIOXIDE TRANSFER IN ELECTROCHEMICAL
 C CO2 CONCENTRATOR(ONE MAN AIR REVITALIZATION SYSTEM)
 C THESE CELLS USE TMAC ELECTROLYTE
 C
 C THE INPUT PARAMETERS REQUIRED BY THE PROGRAM ARE AS FOLLOWS
 C /INPUT/ IS A LIST OF PARAMETERS RELATED TO THE CO2 TRANSFER
 C IC=IDENTIFICATION NUMBER , 1 FOR THE ANALYTICAL CELL AND 2 FOR THE
 C FULL-SCALE CELL
 C PCO2A= ANODE SIDE PCO2, INLET VALUE USED HERE, MM HG
 C BLFALL= LOWER BOUND FOR TI OF ALL SUBCELLS
 C BUFALL=UPPER BOUND FOR TI OF ALL SUBCELLS
 C NTSC= NO. OF TOTAL SUBCELLS
 C CURENT= CURRENT DENSITY OF THE CONCENTRATOR
 C PCO2IN= CATHODE (AIR) SIDE INLET PCO2, MM HG
 C TI= TRANSFER INDEX, LB. CO2 TRANSFERRED PER LB. C2 CONSUME, HERE A GUESSED
 C VALUE FOR THE FIRST SUBCELL IS USED FOR INPUT
 C TRANSFER INDEX OF 2.75 CORRESPONDS TO 100% CO2 CURRENT EFFICIENCY
 C XD= DISTANCE BETWEEN ELECTRODES, MILS.
 C CFM= AIR FLOW RATE, CUBIC FT. PER MINUTE PER CELL(FULL-SCALE BASIS)
 C = (AIR VELOCITY,FT/SEC) X 1.52
 C TIN= INLET AIR TEMP.
 C TDEWIN= INLET AIR DEW POINT TEMP.
 C ALL TEMPERATURES ARE IN DEGREE F
 C VOLT= VOLTAGE OF THE CELL, VOLTS
 C VHV=HYDROGEN FLOW RATE,FT3/MIN.CELL(FULL-SCALE BASIS)
 C
 C DESCRIPTIONS OF IMPORTANT INTERMEDIATE PARAMETERS
 C XP(N)= X-COORDINATE OF THE N-TH NODE AT WHERE THE VALUES OF CONCENTRATIONS
 C ARE SAVED
 C DXP= DISTANCE BETWEEN NODES
 C NSC= THE NO. OF THE SUBCELL BEING SIMULATED
 C FLUX= FLUX OF SUBCELL CO2 TRANSFER
 C BUFLUX= UPPER BOUND FOR FLUX
 C BLFLUX= LOWER BOUND FOR FLUX

```

C H= INITIAL INTEGRATION STEP FOR CRANE
C Y(1)= FIRST DEPENDENT VARIABLE IN CRANE, C1
C Y(2)= SECOND DEPENDENT VARIABLE IN CRANE, C3
C F(1)= DERIVATIVE OF Y(1)
C F(2)= DERIVATIVE OF Y(2)
C
C OUTPUT OF THE MAIN PROGRAM - WHAT THE MAIN PROGRAM CALCULATES
C C1= BICARBONATE ION CONCENTRATION
C C2= HYDROXYL ION CONCENTRATION
C C3= CARBONATE ION CONCENTRATION
C C4=TMA ION CONCENTRATION
C PCO2A=OUTLET PCO2 OF ANODE SIDE
C CO2 REMOVAL RATE ,CO2 REMOVAL EFFICIENCY,CO2 TRANSFER INDEX
C
C
C DIMENSION XP(101),C1(101),C3(101),F1(101),F2(101),CSCATH(40),
C .TELEC(40),XPP(101)
C DIMENSION UIR(4),DIR(5),D(5)
C LOGICAL DONT,ENDCNX,OKPC
C REAL*8 X,Y,F,PREC,XHAT,H,FLUX,CURRENT,FLUX1,BLFAH,BLFLUX,BUFLUX,
C *BUF,TFLUX,RFLUX,BFLUX
C COMMON /CRANEC/X,Y(40),F(40),PREC,XHAT,H,N,NB(40),MIN,INIT,DGNT,
C *ENDCNX,OKPC
C COMMON EQK2M,EQK1M,EQK2C,EQK2A,EQK1A,EQK1C,CKDS,AKD,HC,HA,VELC,
C *VELA,HENRYC,HENRYA,RAK,PKC,CFM,IC
C COMMON /BLK1/FACMAT,TVISF,TEMPD
C COMMON /BLK2/CURRENT,FLUX,C4,DTA2,V1,V2,V3,V4
C COMMON /BLK3/VHV
C NAMELIST/INPUT/IC,PCO2A,BLFAH,BUFAH,NTSC,CURRENT,PCO2IN,TI,XD,
C * CFM,VHV,TIN,TDEWIN,VCLT
C THE FOLLOWING IS NECESSARY TO AVOID THE INTERRUPTION OF CRANE SUBROUTINE
C WHEN SOME VALUES EXCEED THE LIMITS OF MACHINE COMPUTATION (THESE VALUES
C DO NOT AFFECT THE RESULTS BUT ARRISE WHEN SOME TESTS ON THE ERRORS ARE
C MADE)
C CALL ERRSET (207,300,-1)

```

ORIGINAL PAGE IS
OF POOR QUALITY

```

      CALL ERRSET (208,300,-1)
      CALL ERRSET (209,300,-1)
1  READ(5,INFUT,END=9999)
      IF(IC .EQ. 1)WRITE(6,1111)
1111 FORMAT('1',10X,' ANALYTICAL CELL AT THE FOLLOWING CONDITIONS :')
      IF(IC .EQ. 2)WRITE(6,1112)
1112 FORMAT('1',10X,' FULL SCALE CELL AT THE FOLLOWING CONDITIONS :')
      WRITE(6,1113)PCO2IN,CURRENT,XD,CFM,TIN,TDEWIN
1113 FORMAT('0',10X,39(1H*)/10X,' INLET AIR PCO2 = ',3X,F6.2,3X,' MM HG
1  '/10X,' CURRENT DENSITY = ',3X,F6.2,3X,' A /FT2 '/10X,
2  ' MATRIX THICKNESS=',4X,F6.2,3X,' MILS '/10X,
3  ' AIR FLOW RATE   = ',3X,F6.2,3X,' FT3/MIN '/10X,
4  ' AIR TEMPERATURE = ',3X,F6.2,3X,' DEG. F '/10X,
5  ' AIR DEW POINT   = ',3X,F6.2,3X,' DEG. F ')
      WRITE(6,1114)
1114 FORMAT('0',10X,' OTHER CONDITIONS : ')
      WRITE(6,1115)VOLT,VHV,FCC2A
1115 FORMAT('0',10X,'CELL VOLTAGE      = ',3X,F6.2,3X,' VOLT '/10X,
2  ' HYDROGEN RATE    = ',3X,F6.2,3X,' FT3/MIN '/10X,
3  ' ANODE PCO2IN     = ',3X,F6.2,3X,' MM HG '/10X,40(1H*))
      CALL ENERGY(NTSC,VOLT,CURRENT,TIN,TDEWIN,CFM,TELEC,CSCATH)
C  THE FOLLOWING STATEMENTS SPECIFY THE MATRIX FACTOR AND THE FACTOR WHICH
C  SHOULD BE MULTIPLIED BY THE AIR - CATHOLYTE AREA TO ACCOUNT FOR THE EFFECT
C  OF THE CURRENT DENSITY
C  FACMAT= THE MATRIX LABYRINTH FACTOR
C  ACAR =AIR-CATHOLYTE AREA FACTOR
      FACMAT=.34
      IF(IC .EQ. 2)GO TO 111
      ACAR=3.70-3.35/(1.+(1./ .06/CURRENT)** 8.))**.5
      GO TO 112
111 ACAR=1.37-1.24/(1.+(1./ .06/CURRENT)** 8.))**.5
112 CONTINUE
      XD=XD/30.
      DXF=XD/50.
      XP(1)=-XD/2.

```

ORIGINAL PAGE IS
 OF POOR QUALITY

```

      DO 3 KP=2,51
      XP(KP)=XP(KP-1)+DXP
3     CONTINUE
C     CURENT IS NONDIMENSIONLIZED AND THE GUESSED FIRST SUBCELL TI IS
C     CONVERTED INTO FLUX
      CURENT=0.04576*CURENT
      FLUX=TI/5.5*CURENT
      BLFLUX=BLFALL*CURENT/5.5
      BUFLUX=BUFALL*CURENT/5.5
      N=2
      NSC=1
      R=0.
      LL=1
C     THE CATHOLYTE TMAC CONCENTRATIONS OBTAINED FROM THE SUBROUTINE ENERGY ARE
C     NON-DIMENSIONLIZED
4     C4C=CSCATH(NSC)/7.2
      CALL DATA1(TELEC(NSC))
      VELC=VELC*NTSC
      VELA=VELA*NTSC
C     PCO2 IS NON-DIMENSIONLIZED
      PCO2IN=PCO2IN*HENRYC
      PCO2A=PCO2A*HENRYA
      WRITE(6,401) BUFLUX,BLFLUX
401  FORMAT('0',10X,'UPPER FLUX LIMIT= ',G12.6/10X,' LOWER FLUX LIMIT=
1',G12.6//)
      IT=0
      H=XD/1.0E5
5     C5C=PCO2IN*1.E6-FLUX/VELC/(1.-EXP(-HC/VELC))*1.E6
      C5A=PCO2A+FLUX/VELA/(1.-EXP(-HA/VELA))
C     CORRECTION TO INCLUDE THE EFFECT OF IGNIC STRENGTH ON REACTION RATE CONSTANT
C     CO2 DIFFUSIVITY, AND HENRY'S LAW CONSTANT
      CKD=2.820*ACAR*SQRT((5.1/VISCCS(C4C*7.2)*TVISF)**.47*
1 10.**(.063*(3.6-7.2*C4C)))*CKDS
      C2C=FLUX/CKD/C5C
      C3C=(C4C-C2C)/(2.+EQK2C/C2C)

```

```

      C1C=EQK2C/C2C*C3C
C   INITIALIZE Y(1) AND Y(2) FOR DERIV AND CRANE
7   Y(1)=EQK2M*C3C/C2C
      Y(2)=C3C
      IF(C1C .LT. 0.) GO TO 24
      K=0
      X=-XD/2.
      XHAT=XD/2.
      DONT=.FALSE.
      MIN=3
      PREC=5.
      FLUX1=FLUX
      WRITE(6,700) FLUX
700  FORMAT('-',10X,47(1H-)/10X,' THE INITIAL FLUX AT THE CATHODE IS ',
      1G12.6/10X,48(1H-))
      H=XD/1.0E5
      ENDONX=.TRUE.
      INIT=0
      CALL DERIV
      XX=-.5
      WRITE(6,701) XX,Y(1),Y(2),C4
701  FORMAT('//10X,' X =',G12.6,3X,'C1C =',G12.6,3X,'C3C =',G12.6,3X,'C4
      1C =',G12.6)
      XN=X
      C1(1)=C1C
      C3(1)=C3C
      F1(1)=F(1)
      F2(1)=F(2)
      C1N=C1C
      C3N=C3C
      F1N=F(1)
      F2N=F(2)
      KP1=2
8   CONTINUE
      IF(Y(1))88,88,803

```

```

88 LL=LL+1
   IF(LL .NE. 3)GO TO 881
   FLUX=TI*CURENT*1.1/5.5
   GO TO 5
881 IF(LL .GT. 7)GO TO 41
   GO TO 24
803 IF(Y(2))89,89,805
89 LL=LL+1
   IF(LL .NE. 3)GO TO 882
   FLUX=BLFALL*CURENT/5.5
   GO TO 5
882 IF(LL .GT. 7)GO TO 41
   GO TO 26
805 CONTINUE
   CALL CRANE
9   XO=XN
   C10=C1N
   C30=C3N
   F10=F1N
   F20=F2N
   XN=X
   C1N=Y(1)
   C3N=Y(2)
   F1N=F(1)
   F2N=F(2)
   IF(X.LT.XP(KP1) .OR. KP1 .EQ. 51) GO TO 13
   KP2=KP1+1
10  IF(X.LT.XP(KP2)) GO TO 11
   IF(KP2 .EQ. 51) GO TO 11
   KP2=KP2+1
   GO TO 10
11  KP2=KP2-1
   DO 12 KP=KP1,KP2
   SLOP=(XP(KP)-XO)/(XN-XO)
C   EVALUATING AND SAVING VALUES OF C1 AND C3 AT THE NODES

```

ORIGINAL PAGE IS
OF POOR QUALITY


```

      C3(KP)=C30+(C3N-C30)*SLOP
      C1(KP)=C10+(C1N-C10)*SLOP
      F1(KP)=F10+(F1N-F10)*SLOP
      F2(KP)=F20+(F2N-F20)*SLOP
12    CONTINUE
      KP1=KP2+1
13    CONTINUE
      K=K+1
      IF(MOD(K,1000) .EQ. 0) WRITE(6,14) K,X
14    FORMAT(/ /10X,' INTEGRATION STEP NUMBER =',G12.6,5X,'X =',G12.6)
      IF(K .GT. 2000) GO TO 39
      IF((X+H/2.) .LT. XHAT) GO TO 8
20    CONTINUE
      XP(51)=X
      C1(51)=Y(1)
      C3(51)=Y(2)
      XX=.5
      WRITE(6,2000)XX,Y(1),Y(2),C4,K
2000  FORMAT(/ /10X,' X =',G12.6,3X,'C1A =',G12.6,3X,'C3A =',G12.6,3X,'C4
1A =',G12.6//10X,' THE INTEGRATION ROUTINE TOOK',I4,' + 1 STEPS')
      C1A=Y(1)
      C3A=Y(2)
      IF(C1A) 24,24,21
21    IF(C3A) 26,26,22
22    C2A=EQK2A*C3A/C1A
C    TEST IF THE ANODE BOUNDARY CONDITION IS SATISFIED
      G=FLUX-1440.*(EQK1A*C1A*1.E6/(C2A*1.E6)-C5A)
      CRIT = DABS(G/FLUX)
      IF(CRIT .LT. 0.05) GO TO 31
      WRITE(6,2200) G,CRIT
2200  FORMAT(/ /10X,' GUESSED CATHODE FLUX - CALC. ANODE FLUX IS',3X,G12.
16,3X,'DIFF./FLUX =',G12.6)
      IF(G) 26,31,24
24    BUFLUX=FLUX
      GO TO 27

```

```

26   BLFLUX=FLUX
C   HALF INTERVAL TO DETERMINED NEWLY GUESSED FLUX
27   FLUX=(BLFLUX+BUFLUX)/2.
    IF(DABS(FLUX-FLUX1) .LT. .0000001)GO TO 36
29   IT=IT+1
    IF(IT-50) 5,5,36
31   CONTINUE
    WRITE(6,3101)
3101 FORMAT('0',10X,69(1H=))
    WRITE(6,3100)
3100 FORMAT(/18X,'X',13X,'C1',13X,'C2',13X,'C3',13X,'C4')
    WRITE(6,3102)
3102 FORMAT('0',10X,69(1H-))
    DO 32 IP=1,51
    XPP(IP)=XP(IP)/XD
    EGK2 =EGK2M
    IF(IP .EQ. 1)EQK2=EQK2C
    IF(IP .EQ. 51)EQK2=EQK2A
    C4=C1(IP)+2.*C3(IP)+EGK2*C3(IP)/C1(IP)
    CR1=C1(IP)*7.2
    CR3=C3(IP)*7.2
    CR2=EQK2 *C3(IP)/C1(IP)*7.2
    CR4=C4*7.2
    CALL DIN(CR1,CR2,CR3,CR4,DIR,UIR)
    IF(IP .EQ. 1) GO TO 311
    IF(MOD(IP, 10) .NE. 1) GO TO 32
311  WRITE(6,3104)XPP(IP),CR1,CR2,CR3,CR4
3104 FORMAT(/12X,5(G12.6,3X))
    IF(IP .EQ. 1 .AND. CR4 .GE. 5.4)WRITE(6,3111)
3111 FORMAT(/10X,' **WARNING** PRECIPITATION EXPECTED AT CATHODE')
    IF(IP .EQ. 51 .AND. CR4 .GE. 7.3)WRITE(6,3112)
3112 FORMAT(/10X,' **WARNING** PRECIPITATION EXPECTED AT ANODE')
32   CONTINUE
    WRITE(6,3103)
3103 FORMAT('0',10X,69(1H-))

```

ORIGINAL PAGE IS
 OF POOR QUALITY

```

C   R IS THE ACCUMULATED SUBCELL FLUX
33   R=R+FLUX
      PCO2A=(PCO2A+FLUX/VELA)/HENRYA
      PCO2IN=(PCO2IN-FLUX/VELC)/HENRYC
      WRITE(6,3300) NSC,FLUX
3300  FORMAT(/10X,' FLUX FOR SUBCELL NUMBER',I3,' IS ',G12.6)
      IF(NSC .GE. NTSC) GO TO 35
      NSC=NSC+1
      BUF=FLUX*1.05
      IF(NSC .GT. 2) GO TO 34
      RFLUX=FLUX
      FLUX=FLUX*0.98
      GO TO 4
34   TFLUX=RFLUX
      RFLUX=FLUX
      FLUX=(2.*FLUX-TFLUX)*0.98
      GO TO 4
35   TI=5.5*R/CURRENT/FLOAT(NTSC)
      CCCC=R*.0431/FLOAT(NTSC)
      CCCD=CCCC*44.
      WRITE(6,3502)CCCC,CCCD
3502  FORMAT('0',10X,'CO2 REMOVAL RATE = ',G12.6,3X,' LB MOL/FT2.DAY */2
17X,' = ',G12.6,3X,' LB /FT2.DAY')
      WRITE(6,3500) TI,PCO2A
3500  FORMAT(/10X,' TRANSFER INDEX =',G12.6,3X,'CO2 ANODE PRESSURE =',G
112.6)
      EFF=TI*100./2.75
      WRITE(6,3501)EFF
3501  FORMAT(/10X,' CO2 REMOVAL EFFICIENCY = ',3X,F5.2,3X,' % ')
      GO TO 40
36   CCNTINUE
C   IF ANY OF THE FOLLOWING STATEMENTS IS PRINTED OUT TRY TO USE NEW INITIAL
C   VALUES FOR TI
      WRITE(6,3600) CRIT
3600  FORMAT(/' NON CONVERGENCE',3X,'CRIT =',G14.8)

```

```
      GO TO 40
39  WRITE(6,3900)
3900 FORMAT(// ' TOO MANY R-K STEPS ,STOP CALCULATIONS' )
      GO TO 40
41  WRITE(6,4100)
4100 FORMAT(// ' INITIAL VALUES OUTSIDE RANGE,USE NEW GUESSED VALUES '//
1  IN THAT CASE THE USER IS ADVISED TO USE CLOSE VALUES OF TI ,BUFAL
2L,BLFALL,GOOD INITIAL GUESS CAN BE OBTAINED FROM FINAL REPORT NASA
39-12526(FEB.1976) ' )
40  GO TO 1
9999 STOP
      END
```

```

SUBROUTINE DERIV
DIMENSION D(5),U(4),FRT(3)
LOGICAL DONT,ENDONX,OKPC
REAL*8 X,Y,F,PREC,XHAT,H,FLUX,CURRENT
COMMON /CRANEC/X,Y(40),F(40),PREC,XHAT,H,N,NB(40),MIN,INIT,DONT,
*ENDONX,OKPC
COMMON EQK2,EQK1M
COMMON /BLK2/CURRENT,FLUX,C4,DTA2,V1,V2,V3,V4
CR1=Y(1)*7.2
CR2=Y(2)*7.2*EQK2/Y(1)
CR3=Y(2)*7.2
CR4=CR1+CR2+2.*CR3
C4=Y(1)+2.*Y(2)+Y(2)*EQK2/Y(1)
CALL DIN(CR1,CR2,CR3,CR4,D,U)
DO 50 II=1,3
FRT(II)=U(II)*D(4)/U(4)
50 CONTINUE
W1=D(1)+FRT(1)*(Y(1)-EQK2*Y(2)/Y(1))/C4
W2=2.*Y(2)*(1.-EQK2*Y(2)/Y(1)**2)*FRT(3)/C4
W3=(2.*Y(1)+EQK2)*FRT(1)/C4
W4=D(3)+2.*FRT(3)*(1.-Y(1)/C4)
V1=W1+W2+D(5)*2.*EQK1M/EQK2*Y(1)/Y(2)
V2=W3+W4-D(5)*EQK1M/EQK2*(Y(1)/Y(2))**2
V3=W1+2.*W2+FRT(2)*EQK2*Y(2)/Y(1)/C4*(1.-EQK2*Y(2)/Y(1)**2)
V3=V3-D(2)*EQK2*Y(2)/Y(1)**2
V4=W3+2.*W4+D(2)*EQK2/Y(1)+FRT(2)*EQK2*(1.-Y(1)/C4)/Y(1)
DTA2=V1*V4-V2*V3
FLUXX=FLUX-CURRENT*(Y(1)+Y(2)-Y(1)*U(1)/U(4)-2*Y(2)*U(3)/U(4))/2.
1 /7.7
CURNT=CURRENT-CURRENT*(Y(1)+Y(2)*EQK2/Y(1)+2.*Y(2)-Y(1)*U(1)/U(4)
1 -4.*Y(2)*U(3)/U(4)-Y(2)*EQK2/Y(1)*U(2)/U(4))/2./7.7
F(1)=(CURNT*V2-FLUXX*V4)/DTA2
F(2)=(FLUXX*V3-CURNT*V1)/DTA2
RETURN
END

```

```

      SUBROUTINE DIN(CR1,CR2,CR3,CR4,D,U)
C   THIS SUBROUTINE EVALUATED DIFFUSIVITIES D AND MOBILITIES U FOR GIVEN
C   CONCENTRATIONS
C   CR'S ARE CONCENTRATIONS IN MOLE/LITER
C   THE NUMBERS ASSOCIATED WITH THE D'S AND U'S ARE CORRESPOND TO THAT WITH C'S
      DIMENSION D(5),U(4),DC1(7),DC2(7),DC3(7),UC1(7),UCT1(7),
      *UC2(7),UC3(7),UCT3(7),VISR(3),UCT2(7)
      COMMON /BLK1/FACMAT,TVISF,TEMPD
      DATA DC1/1.22223653,-3.13108479,4.17542244,-1.85811884,
1 .2323907,.02796468,-.00586895/
      DATA DC2/5.13441054,5.60764899,-6.31470563,1.45324064,
1 1.28159542,-.74000812,.10684605/
      DATA DC3/.90717802,-1.10332668,-.29668964,4.80486975,
1 -4.31019978,1.25519037,-.10133989/
      DATA UC1/44.39165773,-45.91748832,40.40956334,-21.182183598
* 6.02671557,-.87455289,.05072426/
      DATA UCT1/2.41549965,1.73864338,-2.13873683,.71171359,
*-.06922713,-.0069561,.001212/
      DATA UC2/198.10978722,-100.19543755,59.10497144, -17.69603863,
* -3.23141665,2.46134103,-.3091231/
      DATA UCT2/14.6534768,-4.30708816,4.26289263,-2.78870985,
* .28474868,.15513752,-.02804015/
      DATA UC3/34.3951439,-47.22174887,27.5656625,5.09830616,
1 -14.04491884,5.79626865,-.75395075/
      DATA UCT3/2.43698943,.38048952,-2.07248995,.19862643,
1 .8900114,-.43544587,.05981754/
      CR1=AMIN1(CR1,14.4)
      CR2=AMIN1(CR2,14.4)
      CR3=AMIN1(CR3,14.4)
      CR4=AMIN1(CR4,14.4)
      CR1=AMAX1(CR1,.1E-7)
      CR2=AMAX1(CR2,.1E-7)
      CR3=AMAX1(CR3,.1E-7)
      CR4=AMAX1(CR4,.1E-7)
      VISM=VISCOS(CR4)

```

DO 58 J=1,3
 C(J)=0.
 U(J)=0.
 58 CONTINUE
 VISR(1)=VISCOS(CR1)/VISM*TVISF
 VISR(2)=VISCOS(CR2)/VISM*TVISF
 VISR(3)=VISCOS(2.*CR3)/VISM*TVISF
 C D(1) IS EVALUATED AT T=77 F IN PURE SOL*N
 DO 61 I=1,7
 E(1)=D(1)+DC1(I)*CR1** (I-1)
 61 CONTINUE
 C D(2) IS EVALUATED AT T=77 F IN PURE SOL*N
 DO 62 I=1,7
 D(2)=D(2)+DC2(I)*CR2** (I-1)
 62 CONTINUE
 C D(3) IS EVALUATED AT T=77 F IN PURE SOL*N
 DO 63 I=1,7
 E(3)=D(3)+DC3(I)*CR3** (I-1)
 63 CONTINUE
 C D'S ARE EVALUATED AT THE CELL TEMPERATURE IN MIXTURE IN MATRIX
 DO 64 I=1,3
 D(I)=D(I)*FACMAT*VISR(I)/.258
 64 CONTINUE
 D(4)=(CR1*1.2/1.18*D(1)+CR2*1.2/5.25*D(2)+2.*CR3*1.2/.923*
 *D(3))/CR4
 D(5)=1.8*0.9375/VISM*TVISF*FACMAT/.258
 C U(1) IS EVALUATED AT THE CELL TEMPERATURE IN PURE SOL*N
 DO 65 I=1,7
 U(1)=U(1)+(UC1(I)+UCT1(I)*TEMPD)*CR1** (I-1)
 65 CONTINUE
 C U(1) IS EVALUATED IN MIXTURE IN MATRIX
 U(1)=U(1)*VISR(1)/TVISF*FACMAT
 C U(2) IS EVALUATED AT T=77 F IN PURE SOL*N
 DO 66 I=1,7
 U(2)=U(2)+(UC2(I)+UCT2(I)*TEMPD)*CR2** (I-1)

ORIGINAL PAGE IS
 OF POOR QUALITY

```

66  CONTINUE
C    U(2) IS EVALUATED AT THE CELL TEMPERATURE IN MIXTURE IN MATRIX
    U(2)=U(2)*VISR(2)*FACMAT
C    U(3) IS EVALUATED AT THE CELL TEMPERATURE IN PURE SOLID
    DO 67 I=1,7
    U(3)=U(3)+(UC3(I)+UCT3(I)*TEMPD)*CR3** (I-1)
67  CONTINUE
C    U(3) IS EVALUATED IN MIXTURE IN MATRIX
    U(3)=U(3)*VISR(3)/TVISF*FACMAT
    U(4)=(CR1*44.9/44.5*U(1)+CR2*44.9/198.0*U(2)+2.*CR3*44.9/
    *34.7*U(3))/CR4
    RETURN
    END

```


SUBROUTINE DATAI(TCELL)

C
C THIS SUBPROGRAM INITIALIZED THE DIMENSIONLESS PHYSICAL AND CHEMICAL PARATERS
C NEEDED FOR SIMULATIONS
C FOR PROCEDURES OF NON-DIMENSIONLIZATION, SEE THE INTERNAL NOTE REFERRED
C TCELL IS THE ELECTROLYTE TEMPERATURE
C EQK2C= K2 IN THE CATHODE ZONE
C EQK2M= EQUILIBRIUM CONSTANT K2 IN THE BULK ELECTROLYTE ZONE
C EQK2A= K2 IN THE ANODE ZONE
C EQK1M= EQUILIBRIUM CONSTANT K1 IN THE BULK ELECTROLYTE ZONE
C EQK1C= K1 IN THE CATHODE ZONE
C EQK1A= K1 IN THE ANODE ZONE
C CKDS= SQUARE ROOT OF KCD5 IN THE CATHODE ZONE AT A GIVEN C4
C AKD= = SQUARE ROOT OF KAD5 IN THE ANODE ZONE
C HA= HYDROGEN ZONE MASS TRANSFER COEFFICIENT FOR CO2
C HC= AIR ZONE MASS TRANSFER COEFFICIENT FOR CO2
C VELA= HYDROGEN FLOW RATE
C VELC= AIR FLOW RATE
C HENRYC= HENRY CONSTANT FOR THE CATHODE ZONE
C HENRYA= HENRY CONSTANT FOR THE ANODE ZONE
C RAK= THE FACTOR B DEFINED IN THE NOTE
C PKC= TEMPERATURE FACTOR USED FOR CALCULATING PH
C TVISF= TEMPERATURE EFFECT ON THE VISCOSITY OF ELECTROLYTE
C TEMPD= TEMPERATURE EFFECT ON SOME DIFFUSIVITIES
C CKDS= TEMPERATURE EFFECT OF REACTION RATE CONSTANT
C
C DIMENSION T(14),VISCDW(14)
C COMMON EQK2M,EQK1M,EQK2C,EQK2A,EQK1A,EQK1C,CKDS,AKD,HC,HA,VELC,
C *VELA,HENRYC,HENRYA,RAK,PKC,CFM,IC
C COMMON /BLK1/FACMAT,TVISF,TEMPD
C COMMON /BLK3/VHV
C THE DATA OF WATER VISCOSITY AT DIFFERENT TEMPERATURE
C DATA T/40.,45.,50.,55.,60.,65.,70.,75.,77.,80.,85.,90.,95.,100./
C DATA VISCDW/1.546,1.439,1.307,1.21,1.122,1.044,.9753,.9135,
C *.8904,.8577,.8071,.7612,.7194,.6812/

```

C   TEMPERATURE IN CENTIGRADE
      TK=(TCELL-32.)/1.8
      HEN=(0.981035+0.042102*TK+3.198135E-4*TK**2)*1.E4
C   TEMPERATURE IN KELVIN
      TK=TK+273.18
C   EVALUATION OF REACTION RATE CONSTANT
      REACK=10.**{13.635-(2895./TK)}
      TEMPD=(TCELL-75.)/10.
      PKW=4471.33/TK-6.0846+.017053*TK
      PK1=3404.71/TK-14.8435+0.032786*TK-PKW
      PK2=2902.39/TK-6.4980+0.02379*TK-PKW
      IF(TCELL .GT. T(1)) GO TO 71
      TVISF=.8904/((VISCOW(2)-VISCOW(1))/(T(2)-T(1))*(TCELL-T(1))+
      *VISCOW(1))
      RETURN
71   DO 72 J=2,14
      IF(TCELL .GT. T(J)) GO TO 72
      J1=J-1
      J2=J
      GO TO 73
72   CONTINUE
      J1=13
      J2=14
73   TVISF=.8904/((VISCOW(J2)-VISCOW(J1))/(T(J2)-T(J1))*(TCELL-T(J1))+
      *VISCOW(J1))
      AW=0.75
      PKC=PKW+ALOG10(7.2/AW)
      EQK1=10.**PK1
      EQK2=10.**PK2
      EQK1C=EQK1/238.
      EQK1M=EQK1/144.
      EQK1A=EQK1/51.
      EQK2C=EQK2/58.
      EQK2M=EQK2/32.
      EQK2A=EQK2/6.1

```

```
HENRYC=1./HEN/1.686/7.2  
HENRYA=1./HEN/1.190/7.2  
HC=(2.3952+.1885*CFM)*HEN  
VELC=1.365*CFM*HEN  
FA=5.60*HEN  
VELA=.02366*HEN *VHV/0.067  
CKDS=SQRT(REACK/((10.**((13.635-(2895./298.))))))  
RETURN  
END
```

```
      FUNCTION VISCOS(CS)
C     THIS SUBPROGRAM EVALUATES THE ELECTROLYTE VISCOSITY FOR GIVEN CR4
      VISCOS=.8937      -1.0093842*CS+2.37863884*CS**2-1.13294407*
      *CS**3+.17625416*CS**4
      RETURN
      END
```

```

      SUBROUTINE ENERGY(NTSC,VOLT,CURRENT,TIN,TDEWIN,CFM,TELEC,CSCATH)
C     THIS SUBPROGRAM SIMULATES THE HEAT AND WATER TRANSFER IN THE CELL
C
C     WVP(I) IS THE WATER VAPOR PRESSURE OF PURE WATER AT TEMP. T(I)
C     SVP(I,J) IS THE VAPOR PRESSURE OF TMAC SOLUTION WITH CR4=2*CS(J) AT TEMP.
C     T(I)
C     RH07= DENSITY OF AIR, LB/FT**3
C     CP= HEAT CAPACITY OF AIR, BTU/LB-F
C     AJ= CONVERSION FACTOR, JOULE/CAL
C     FR= HEAT OF REACTION FOR H2(G) + 1/2O2(G) = H2O(G), CAL/G-MOLE
C     F= FARADAY'S CONSTANT, AMPS-SEC/G-EQUIVALENT
C
C     DUCTS=NO. OF CHANNELS IN AIR COMPARTMENT
C     XAC= LENGTH OF THE AIR CHANNEL, FT
C     YAC= WIDTH OF THE CHANNEL, FT
C     ZAC= HEIGHT OF THE CHANNEL, FT
C     LIMNU= LIMIT NUSSELT NO.
C     AREA= ACTIVE ELECTRODE AREA, FT**2
C     AREAMT= MASS TRANSFER AREA, FT**2
C     AREAHT= HEAT TRANSFER AREA, FT**2
C     AREACS= AIR CHANNEL CROSS-SECTIONAL AREA, FT**2
C     W= AIR MASS FLOW RATE, LB/HR
C     I= CURRENT, AMPS
C     N6= MOLAR RATE OF WATER PRODUCTION, LB-MOLE/HR
C     DH= EQUIVALENT DIAMETER OF AIR CHANNEL, FT
C     QGEN= RATE OF HEAT GENERATED BY THE CELL, BTU/HR
C     PH2O= WATER PARTIAL PRESSURE IN AIR FLOW, MMHG
C     TAIR(J)= AIR TEMPERATURE IN THE SUBCELL J
C     TELEC(J)= ELECTROLYTE TEMPERATURE IN THE SUBCELL J
C     MU7= AIR VISCOSITY, LB/HR-FT
C     D57= CO2 DIFFUSIVITY IN AIR, FT**2/HR
C     D67= WATER DIFFUSIVITY IN AIR, FT**2/HR
C     SC= SCHMIDT NO.
C     PR= PRANDTL NO.
C     HTC= HEAT TRANSFER COEFFICIENT, BTU/HR-FT**2-F

```

C MTC5= MASS TRANSFER COEFFICIENT FOR CO2, FT/HR
 C MTC6= MASS TRANSFER COEFFICIENT FOR WATER, FT/HR
 C PE= ELECTROLYTE WATER VAPOR PRESSURE, MMHG
 C CSCATH(J)= CATION CONCENTRATION IN THE CATHOLYTE OF THE SUBCELL J
 C

```

REAL LIMNU,MU7,K7,I,N6
DIMENSION T(13),WVP(13),TELEC(40),CSCATH(40),SVP(13,11),CS(11),
1 JT(2),PET(2),CST(2),X(11),TAIR(41),PH2O(41),RH(11)
DATA          T/90.,85.,80.,75.,70.,65.,60.,55.,50.,45.,40.,35.,
1 30./
DATA          WVP/36.,7,30,75,26,27,22,24,18,76,15,77,13,29,11,09
1,9,22,7,7,6,30,5,17,4,23/
DATA RHO7/0.0808/, CP/0.24/, AJ/4.186/, HV/1060./, HR/-57797.9/,
1 R/555./, F/96500./
DATA RH/1...970.,949.,913.,850.,763.,658.,551.,424.,324.,30/
DATA CS/0...49.,74.,99,1.25,1.52,1.79,2.06,2.33,2.61,2.75/
DATA          SVP/36,07,30,75,26,27,22,24,18,76,15,77,13,29,11,09,
1 5*0.,35.02,29.87,25.55,21.61,18.23,15.32,12.91,10.77,5*0.,
2 34.27,29.20,24.98,21.13,17.83,14.98,12.62,10.54,5*0.,
3 32.37,28.10,24.02,20.33,17.15,14.41,12.14,10.14,5*0.,
4 30.70,26.18,22.37,18.93,15.96,13.42,11.31,9.44,5*0.,
5 27.56,23.48,20.07,16.99,14.33,12.04,10.14,8.47,5*0.,
6 23.81,20.28,17.36,14.68,12.38,10.41,8.76,7.32,5*0.,
7 19.87,16.98,14.52,12.27,10.36,8.71,7.34,6.11,5*0.,
8 15.33,13.07,11.17,9.45,7.98,6.70,5.65,4.71,5*0.,
9 11.72,9.99,8.55,7.23,6.09,5.13,4.32,3.60,5*0.,
1 9.6,7.8,6.3,5.05,4.25,3.5,2.9,2.3,5*0./
DUCTS=96.
XAC=6./12.
YAC=0.2/12.
ZAC=0.19/12.
AREA = 1.
AREAMT=YAC*XAC*DUCTS
LIMNU=2.89
AREAMT=2.0*(YAC+ZAC)*XAC*DUCTS

```

ORIGINAL PAGE IS
 OF POOR QUALITY

```

AREACS=ZAC*YAC
DH=2.*AREACS/(YAC+ZAC)
W=CFM*60.*RH07
I=CURRENT*AREA
N6=I/2./F/453.*3600.
W6=N6*18.02
QGEN=-I*(HR/2./F+VOLT/AJ)*3600./252.
TAIR(1)=TIN
CALL LAGRAN(TDEWIN,T,WVP,13,PH20IN,13,13)
PH20(1)=PH20IN
TSCN=FLOAT(NTSC)
DC 821 J=1,NTSC
TAIR(J+1)=TAIR(J)+QGEN/CP/W/TSCN
821 CONTINUE
835 DO 94 JC=1,NTSC
TAVE=(TAIR(JC)+TAIR(JC+1))/2.
MU7=((TAVE+460.)/492.)*1.5*697./((TAVE+665.)*0.01709*2.42
K7=0.0140+(TAVE-32.)/180.*0.0043
D57=.164/(2.54**2)/144.*3600.*((TAVE+460.)/537.)*1.832
D67=.256/(2.54**2)/144.*3600.*((TAVE+460.)/537.)*2.334
RED=DH*CFM/DUCTS/AREACS*RH07/MU7*60.
PR=CF*MU7/K7
SC5=MU7/RH07/D57
SC6=MU7/RH07/D67
CONST=(0.003+0.019*ZAC/YAC)*RED*PR*DH/XAC*TSCN/FLOAT(JC)
CONS5=(0.003+0.039*ZAC/YAC)*RED*SC5*DH/XAC*TSCN/FLOAT(JC)
CONS6=(0.003+0.039*ZAC/YAC)*RED*SC6*DH/XAC*TSCN/FLOAT(JC)
HTC=LIMNU*K7/DH*(1.+CONST)
MTC5=LIMNU*D57*(1.+CONS5)/DH
MTC6=LIMNU*D67*(1.+CONS6)/DH
TELEC(JC)=TAVE+QGEN/HTC/AREAHT/TSCN
TELEC(JC)=AMAX1(TAIR(JC+1),TELEC(JC))
PH20(JC+1)=(PH20(JC)/(TAIR(JC)+460.)+N6/TSCN*R/CFM/60.)*
1 (TAIR(JC+1)+460.)
PH20AV=(PH20(JC)+PH20(JC+1))/2.

```

```

      PE=PH2CAV+N6*R*(TAVE+460.)/AREAMT/MTC6
      PE=AMAX1(PH2CAV,PE)
C     USE LAGRANGIAN INTERPOLATION TO DETERMINE WVP AT TELEC(JC)
      CALL LAGRAN(TELEC(JC),T,WVP,13,WVPTE,13,13)
C     CALCULATE WATER ACTIVITY, AW, OF THE CATHCLYTE IN THE SUBCELL
      AW=PE/WVPTE
      IF(TELEC(JC) .LT. 90.) GO TO 111
      WVPTE=36.11*EXP(.0318*(TELEC(JC)-90.))
      AW=PE/WVPTE
      CALL LAGRAN(AW,RH,CS,11,CSE,11,11)
      GO TO 93
111 CONTINUE
C     DETERMINE A SET OF T(JT(1)) AND T(JT(2)) SUCH THAT JT(1)=JT(2)-1 AND THAT
C     T(JT(1)), TELEC(JC), T(JT(2)) ARE IN DESCENDING ORDER
      DO 85 J=1,12
      IF(T(J) .LT. TELEC(JC)) GO TO 86
85 CONTINUE
      J=J+1
86 JT(1)=J-1
      JT(2)=J
      IF(JT(1) .GT. 0) GO TO 88
      PET(1)=WVP(1)*AW
      DO 87 L=1,11
      X(L)=SVP(1,L)
87 CONTINUE
      CALL LAGRAN(PET(1),X,CS,11,CSE,11,11)
      GO TO 93
88 IF(JT(2) .LE. 12) GO TO 90
      PET(2)=WVP(12)*AW
      DO 89 L=1,11
      X(L)=SVP(12,L)
89 CONTINUE
      CALL LAGRAN(PET(2),X,CS,11,CSE,11,11)
      GO TO 93
C     DETERMINE THE CATION CONCENTRATIONS OF A CARBONATE SOLUTION WITH WATER

```

ORIGINAL PAGE IS
OF POOR QUALITY


```

C   ACTIVITY AW AT THE TEMPERATURES T(JT(1)) AND T(JT(2))
90 DO 92 J=1,2
    JTJ=JT(J)
    PET(J)=WVP(JTJ)*AW
    DO 91 L=1,11
        X(L)=SVP(JTJ,L)
91 CONTINUE
    CALL LAGRAN(PET(J),X,CS,11,CST(J),11,11)
92 CONTINUE
    J1=JT(1)
    J2=JT(2)
C   INTERPOLATE FOR CATION CONCENTRATION OF THE CATHOLYTE AT TELEC(JC)
    CSE=CST(1)+(CST(2)-CST(1))/(T(J2)-T(J1))*(TELEC(JC)-T(J1))
93 CSCATH(JC)=CSE*2.
94 CONTINUE
    PH2DOU=PH2O(NTSC+1)
    CALL LAGRAN(PH2DOU,WVP,T,13,TDEWOU,13,13)
    WRITE(6,9400) TDEWOU
9400 FORMAT(' ',10X,'OUTLET AIR D.P. = ',3X,F6.2,3X,' DEG. F ')
    WRITE(6,9401)
9401 FORMAT('0',10X,' NO. OF SUBCELL    TAIRIN    TAIRCUT    TELEC    P
1H2OIN    PH2OOUT    CSCATH')
    DO 95 JC=1,NTSC
        WRITE(6,9402) JC,TAIR(JC),TAIR(JC+1),TELEC(JC),PH2O(JC),PH2C(JC+1)
        1,CSCATH(JC)
9402 FORMAT(16X,I2,11X,5(F6.2,4X),F6.2)
95 CONTINUE
    RETURN
    END

```

```

SUBROUTINE LAGRAN(XA,X,Y,N,ANS,NX,NY)
C THIS IS A LAGRANGIAN INTERPOLATION ROUTINE
DIMENSION X(NX),Y(NY)
SUM=0.
DO 3 I=1,N
PROD=Y(I)
DO 2 J=1,N
A=X(I)-X(J)
IF(A) 1,2,1
1 E=(XA-X(J))/A
PRCD=PROD*E
2 CONTINUE
3 SUM=SUM+PROD
ANS=SUM
RETURN
END

```

ORIGINAL PAGE IS
OF POOR QUALITY

```

SUBROUTINE CRANE
IMPLICIT REAL*8(A-H,D-Z)
C
C  HELP IS LOGICAL VARIABLE SET TRUE IN DERIV WHEN
C  A DISCONTINUITY OCCURS AND IT IS NECESSARY TO DECREASE THE TIME
C  INCREMENT AND RESTART THE INTEGRATION BEFORE CONTINUING.
C  THE Y AND F ARRAYS AND X ARE RESET TO THEIR LAST GOOD VALUES
C  AND INIT SET EQUAL TO ZERO BEFORE PROCEEDING WITH NEW H.
C  THE ARGUMENTS OF THIS SUBROUTINE ARE ALL CONTAINED IN THE FOLLOW-
C  ING COMMON STATEMENT, LABELED CRANEC. DRIVER PROGRAM MUST CONFORM
C  IN ORDER AND DIMENSIONS WITHIN COMMON/CRANEC/, THOUGH NOT NECES-
C  SARY IN THE NAMES OF THE VARIABLES.
C
C  LOGICAL IONT,INDONX,IKPC,IELP
C  COMMON /CRANEC/X,Y(40),F(40),PREC,XHAT,H,N,NB(40),MIN,INIT,IGNT,
C  *INDONX,IKPC
C  IELP=.FALSE.
C
C  MEANING OF THE ARGUMENTS ARE AS FOLLOWS
C
C  X  THE INDEPENDENT VARIABLE.
C  Y  ARRAY OF DEPENDENT VARIABLES, 40 MAXIMUM.
C  F  ARRAY OF DERIVATIVES, FUNCTIONS OF X AND THE Y VECTOR.
C  H  STEP SIZE IN X. MUST BE NON-ZERO. USUALLY MAY BE ALTERED
C  INTERNALLY BY CRANE, AFTER FIRST BEING SET + OR - EXTERNALLY.
C  N  THE NO. OF Y S AND F S IN THE SYSTEM. USUALLY THE NO. ALSO
C  OF COUPLED ORDINARY DIFF. EQUNS.
C  NB  AN ARRAY OF FLAGS. IF +, HOLD ABSOLUTE TRUNCATION ERROR EST.
C  BELOW A SPECIFIED LIMIT =10.**(-PREC)
C  IF 0, DITTO FOR RELATIVE TRUNCATION ERROR ESTIMATE.
C  IF -, DISREGARD THE TRUNC. ERROR. EST.
C  FOR THE Y S WHOSE FLAGS ARE NEGATIVE.
C  MIN  THE MINIMUM NO. OF STEPS BETWEEN OCCASIONS FOR DOUBLING H.
C  THE VALUE OF MIN MAY NOT EXCEED 10, NOR BE LESS THAN 3.
C  INIT  SET TO ZERO BEFORE FIRST CALL, CAUSING THE SR TO INITIALIZE
C  ITSELF. THEREAFTER, INIT IS BUMPED INTERNALLY, EACH STEP.

```

CRAN0010

CRAN0020

CRAN0030

CRAN0040

CRAN0050

CRAN0060

CRAN0080

CRAN0090

CRAN0100

CRAN0120

CRAN0130

CRAN0140

CRAN0150

CRAN0160

CRAN0170

CRAN0180

CRAN0190

CRAN0200

CRAN0210

CRAN0220

CRAN0230

CRAN0240

CRAN0250

CRAN0260

C DONT A FLAG WHICH IF TRUE FORBIDS ANY CHANGE IN H TO BE MADE
 C INTERNALLY BY THE SR. (UNLESS ENDCNX=T)
 C PREC A POSITIVE CONST. APPROXIMATELY EQUAL TO THE NO. OF SIGNIFI- CRAN0290
 C CANT DECIMAL DIGITS OF LOCAL PRECISION. (BASED ON TRUNCATIONCRAN0300
 C ERROR ESTIMATES MADE INTERNALLY. EFFECTIVE ONLY IF DONT=T.)
 C ENDCNX A FLAG WHICH IF SET TRUE IN CALLING ROUTINE AND ACCOMPANIED
 C BY A VALUE OF XHAT .GT. X AT INIT=0 FOR H .GT. 0. (OR XHAT
 C .LT. X IF H .LT. 0.) WILL ENABLE SR TO RETURN TO CALLING
 C PROGRAM WITH X=XHAT AND ENDCNX SET FALSE AS A FLAG TO THIS
 C EFFECT. DONT WILL BE IGNORED IN THIS INSTANCE.
 C XHAT VALUE OF X, IDEPENDENT SEGMENT, AT WHICH A DISCONTINUITY
 C OCCURS. USED IN CONJUNCTION WITH ENDCNX TO HAVE X=XHAT AT END
 C OF A STEP.
 C OKPC A FLAG TO INDICATE THAT AT LEAST ONE PREDICTOR-CORRECTOR STEP
 C WHICH SATISFIES THE ERROR CRITERIA HAS BEEN TAKEN.
 C
 C THE PARTICULAR PREDICTOR-CORRECTOR ALGORITHM IS THAT PUBLISHED CRAN0320
 C BY CRANE AND KLOPFENSTEIN IN J.A.C.M. VOL 12, PAGES 227-241, APRILCRAN0330
 C 1965. IT IS OF FOURTH ORDER, I.E., TRUNCATION ERRORS ARE OF ORDERCRAN0340
 C H^{**5} . THE ALGORITHM WAS DEVELOPED TO MAXIMIZE THE RANGE OF STEP CRAN0350
 C SIZE CONSISTENT WITH ABSOLUTE STABILITY, AND IN A LOOSER SENSE, TOCRAN0360
 C HAVE A GOOD RANGE OF RELATIVE STABILITY. THESE RANGES, EXPRESSED CRAN0370
 C AS H, NORMALIZED BY MULTIPLYING BY PARTIAL DERIV OF $Y(=G(X,Y))$ WITHCRAN0380
 C RESPECT TO Y, ARE CRAN0390
 C FOR ABSOLUTE, $C.GE.HBAR.GE.(-2.4809)$ CRAN0400
 C FOR RELATIVE, $INFINITY.GE.HBAR.GE.(-.446)$ CRAN0410
 C THE STARTING PROCEDURE IS THE RUNGE-KUTTA VARIANT PUBLISHED BY CRAN0420
 C S. GILL, CAMB. PHIL. SOC. PROC., 47, PS6,(1951) CRAN0430
 C CRAN0440
 C CRAN0450
 C TO USE THIS ROUTINE, A SUBROUTINE CALLED DERIV MUST BE PREVI-CRAN0460
 C DED WHICH USES LABELED COMMON/CRANEC/AND CALCULATES THE F VECTOR. CRAN0470
 C THE FIRST CALL OF CRANE WILL ONLY OBTAIN F S, AND SET INIT=1. EACH CRAN0480
 C SUBSEQUENT CALL WILL ADVANCE ONE STEP AND UPDATE X,Y AND F, EXCEPTCRAN0490
 C THAT AFTER THREE STEPS, CRANE MAY HALVE H AND RETURN TO INITIAL CRAN0500
 C CONDITIONS WITH INIT=4. (THIS BEHAVIOR WILL RECUR UNTIL PRECISIONCRAN0510

```

C      IS SATISFIED ACCORDING TO AN ERROR ESTIMATE AFTER THREE STEPS.) CRAN0520
C      CRAN0530
C      PRIOR TO FIRST CALL, SET INIT X AND Y AND DEFINE THE VALUES CRAN0540
C      OF THE NB VECTOR, ALSO DEFINE VALUES OF N,MIN,INIT(=0),IDCNT, AND CRAN0550
C      PREC. PREC SHOULD ADVISEDLY BE FROM 2.5 TO 7. (NOT NECESSARILY CRAN0560
C      AN INTEGER), THOUGH THERE WILL BE NO EFFECT IF IDCNT.NE.0 CRAN0570
C      CRAN0580
C      PRINTOUT AND TERMINATION ARE NOT ACCOMPLISHED BY CRANEC ENDTNCRAN0590
C      CRAN0600
C      DO NOT CHANGE X,Y,F,N OR H EXTERNALLY UNLESS YOU SET INIT=0, CRAN0610
C      EXTERNALLY. HOWEVER, NB AND PREC MAY BE CHANGED AT ANY TIME. SET- CRAN0620
C      TING INIT.LT.0 WILL RESULT IN INHIBITING INCREASE IN H FOR MIN CRAN0630
C      STEPS, BUT WILL PERMIT DECREASES IN H. INIT WILL BE POSITIVE ON CRAN0640
C      EXITTING CRANE AGAIN. CRAN0650
C      DIMENSION Q(40),Y1(40),Y0(40),F0(40),F1(40),F2(40),F3(40),F4(40), CRAN0660
C      IF5(40),Y2(40),E(10),Y3(40),Y4(40),Y5(40) CRAN0670
C      EQUIVALENCE( Y5(1),Q(1)),(R,T) CRAN0680
C      Y5 AND Q ARE NOT BOTH NEEDED AT THE SAME INSTANT. CRAN0690
C      DATA VNU /1.5258556E-05/
C      VNU MAXIMUM ROUND OFF ERROR ON UNIVAC 1108 CALCULATED BY
C      V=ALPHA*BASE**((1-IT) WHERE ALPHA = 1. FOR ROUNDING MACHINE
C      AND .5 FOR TRUNCATING MACHINE. BASE IS THE NUMBER BASE FOR
C      MACHINE (2 FOR 1108). IT IS NUMBER OF DIGITS IN MANTISSA OF
C      THE WORD IN MEMORY ( 27 FOR 1108 ).
C      FIRST EXECUTABLE NEXT CRAN0710
C
C***** *****
      IF(INIT)1,2,3 CRAN0720
1  INIT=0 CRAN0730
   E(MIN)=10. CRAN0740
2  IF ( N .GT. 0 .AND. N .LE. 40 ) GO TO 5
   WRITE(6,200)
200 FORMAT(54HON WAS NOT A POSITIVE INTEGER.LT.40, ON CALLING CRANE.) CRAN0790
   CALL EXIT CRAN0800
5  IF ( MIN .LT. 3 ) MIN=3

```

```
IF ( MIN .GT. 10 ) MIN=10
IF ( INDX .AND. (XHAT-X)/H .LT. 0. ) GO TO 2040
BETA =-DLOG10(VNU)*.9
70 IF ( PREC-BETA ) 11,13,12
12 PREC = BETA
11 IF ( PREC .LT. 2. ) PREC=4.
C STATEMENT 11 ASSUMES THAT THE OVERSIGHT OF SPECIFYING NO PRECI- CRAN0900
C SIGN, OR PRECISION BELOW 2.0 DECIMALS, SHOULD CALL FOR 4 DECIMALS, CRAN0910
C VIA INTERNAL CORRECTION. ALSO, PREC ABOVE MACHINE ACCURACY IS
C REDUCED TO MACHINE ACCURACY.
13 PRECN=PREC CRAN0930
T=10.**(-PREC) CRAN0940
BOUNDB=T*16.21966 CRAN0950
BCUNDA=T*.05 CRAN0960
BOUND=BOUNDA*FLOAT(MIN) CRAN0970
IF( INIT)1155,1155,16 CRAN0980
1155 CALL DERIV CRAN0990
IF ( IELP) GO TO 2000
ASSIGN 18 TO KT
C*****RUNGE-KUTTA SETUP
17 K=0 CRAN1000
IF ( INDX .AND. (XHAT-X)/(4.*H) .LE. 1. ) H=(XHAT-X)/4.
ASSIGN 55 TO IS CRAN1010
H1=.5*H CRAN1020
KBC=3 CRAN1030
IKPC = .FALSE.
GO TO KT, (18,20)
C IF PROGRAM HAS BACKED UP TO START OF A R-K GO TO 18.
C IF PROGRAM HAS BACKED UP TO LAST PC THEN GO TO 20.
C THIS WILL PERMIT PRINTOUT TO 'START OVER'.
C ALSO FIRST CALL WITH INIT=0 WILL ALSO PASS THRU 18.
C*****END R-K SETUP
C THIS IS THE NORMAL CALL OF DERIV WITH A NEW PC Y VECTOR, HENCE
C A USEABLE VALUE OF F IF HELP=FALSE.
15 CALL DERIV CRAN1050
```

IF (IELP) GO TO 52	
18 INIT=1+INIT	CRAN1060
IF (INDCNX .AND. DABS((XFAT-X)/XHAT) .LT. VNU *10.)	
. INDCNX=.FALSE.	
19 IF (IKPC .OR. INIT .EQ. 1) RETURN	
C THE ABOVE IS THE ONLY RETURN FROM INTODE. NEXT IS REACHED WHEN	CRAN1080
C INIT EXCEEDS 0.	CRAN1090
C*****	*****
C	
3 IF (PREC - PRECN) 70,16,70	
16 IF (IONT .AND. IKPC) GO TO 213	
IF (IKPC) GO TO 212	
C	
20 K=4	CRAN1120
213 DO 22 I=1,N	CRAN1130
F3(I)=F2(I)	CRAN1140
F2(I)=F1(I)	CRAN1150
F1(I)=F0(I)	CRAN1160
F0(I)=F(I)	CRAN1170
Y3(I)=Y2(I)	CRAN1180
Y2(I)=Y1(I)	CRAN1190
Y1(I)=Y0(I)	CRAN1200
22 Y0(I)=Y(I)	CRAN1210
IF (KBC .EQ. 0 .OR. IONT) GO TO 23	
24 KBC=KBC-1	CRAN1230
XN=X+H	CRAN1240
X=X+H1	CRAN1250
RX=.292893219	CRAN1260
ASSIGN 33 TO KS	CRAN1270
C***** START OF ONE RK STEP	*****
37 DO 29 I=1,N	CRAN1280
AK=H*F(I)	CRAN1290
GO TO KS,(33,34,30)	CRAN1300
33 Y(I)=Y(I)+0.5*AK	CRAN1310
Q(I)=AK	CRAN1320

GC TO 29	CRAN1330
30 $Y(I) = (-Q(I) - Q(I) + AK) * .166666667 + Y(I)$	CRAN1340
GO TO 29	CRAN1350
34 $R = RX * (AK - Q(I))$	CRAN1360
$Q(I) = ((R + R + R) - RX * AK) + Q(I)$	CRAN1370
$Y(I) = Y(I) + R$	CRAN1380
29 CONTINUE	CRAN1390
GO TO (1551, 224, 219, 251), K	CRAN1400
219 $RX = 1.70710678$	CRAN1410
GO TO 1551	CRAN1420
251 ASSIGN 34 TO KS	CRAN1430
GO TO 1551	CRAN1440
224 ASSIGN 30 TO KS	CRAN1450
$X = XN$	CRAN1460
1551 CALL DERIV	CRAN1470
IF (IELP) GO TO 2020	
C THIS CALL OF DERIV IS DURING R-K ONLY	
36 $K = K - 1$	CRAN1480
IF(K)18,18,37	CRAN1490
C***** END OF ONE RK STEP	*****
C DELTAX IS DONE. THE CODING IS A BIT COMPLEX IN ORDER TO MINIMIZE	CRAN1510
C THE LOOP BEGINNING AT 37 IS EXCTD 4 TIMES BEFORE ONE STEP IN	CRAN1500
C MULTIPLICATIONS AND INDEXING. IT IS EQUIVALENT TO SLOWER CODE.	CRAN1520
C AS FOLLOWS... DO 36 J=1,4 WHEREIN J=5-K	CRAN1530
C DO 29 I=1,N+1	CRAN1540
C $AK(I,J) = DELTAX * F(I)$	CRAN1550
C $R(I,J) = A(J) * AK(I,J) - B(J) * Q(I)$	CRAN1560
C $Y(I) = Y(I) + R(I,J)$	CRAN1570
C $Q(I) = Q(I) + 3. * R(I,J) - C(J) * AK(I,J)$	CRAN1580
C 29 $X = Y(N+1)$	CRAN1590
C CALL DERIV (X,Y,F)	CRAN1600
C 36 CONTINUE	CRAN1610
C RETURN	CRAN1620
C ACC. TO S. GILL, CAMB. PHIL. SCC., PROC., 47,P96 (1951), THE	CRAN1630
C VALUES OF A, B , AND C ARE BEST....	CRAN1640

C	A(J)=0.5,1.-SQRTF(.5),1.+SQRTF(.5),1./6.	J=1,4	CRAN1650
C	B(J)=1. ,1.-SQRTF(.5),1.+SQRTF(.5),1./3.	J=1,4	CRAN1660
C	C(J)=0.5,1.-SQRTF(.5),1.+SQRTF(.5),0.5	J=1,4	CRAN1670
C			CRAN1680
C			
C	FOLLOWING IS REACHED FROM STMT 16 WHEN KBC=0, AFTER PRED-CORR		CRAN1690
C	INITIALIZATION IS COMPLETE.		CRAN1700
212	IF (INDONX .AND. (XHAT-X)/(4.*H) .LT. 1.) GO TO 17		
	IF (E(MIN) .GT. BOUNDA) GO TO 28		
100	DO 4 I=2,MIN		CRAN1750
4	E(1)=E(1)+E(I)		CRAN1760
	IF(E(1)-BOUND)38,28,28		CRAN1770
C	28 IS USUAL. 38 IS PREPARE TO DOUBLE DELTAX.		CRAN1780
28	DO 39 I=1,N		CRAN1790
	F5(I)=F4(I)		CRAN1800
	F4(I)=F3(I)		CRAN1810
	F3(I)=F2(I)		CRAN1820
	F2(I)=F1(I)		CRAN1830
	F1(I)=F0(I)		CRAN1840
	F0(I)=F (I)		CRAN1850
	Y5(I)=Y4(I)		CRAN1860
	Y4(I)=Y3(I)		CRAN1870
	Y3(I)=Y2(I)		CRAN1880
	Y2(I)=Y1(I)		CRAN1890
	Y1(I)=Y0(I)		CRAN1900
	Y0(I)=Y (I)		CRAN1910
39	Y(I)=1.547652*Y(I)+2.017204*Y2(I)-1.867503*Y1(I)-.697353*Y3(I)+S*		CRAN1920
	1(.985508124*F(I)+.895121303*F2(I)-.351589071*F3(I)-F1(I))		CRAN1930
40	X=X+H		CRAN1940
	CALL DERIV		CRAN1950
	IF (IELP) GO TO 2030		
C	THIS CALL OF DERIV IS FIRST WITH PREDICTED Y VECTOR AND MAY BE		
C	REACHED WITH LAST STEP OF AN R-K STEP HENCE UNCHECKED OR WITH		
C	LAST STEP A GOOD PC.		
42	DO 10 I=2,MIN		CRAN1960

10	E(I-1)=E(I)	CRAN1970
	E(MIN)=0.	CRAN1980
	DO 43 I=1,N	CRAN1990
	T=Y0(I)+AK*(9.*F(I)+19.*F0(I)+F2(I)-5.*F1(I))	CRAN2000
	PMC=Y(I)-T	CRAN2010
C	AT THIS POINT, PMC IS PREDICTOR-CORRECTOR	CRAN2020
	IF (IONT) GO TO 43	
72	IF(NB(I))43,44,47	CRAN2040
44	IF (Y(I))46,43,46	CRAN2050
46	PMC=PMC/Y(I)	CRAN2060
47	IF(DABS(PMC)-E(MIN))43,43,48	CRAN2070
48	E(MIN)=DABS(PMC)	CRAN2080
43	Y(I)=T	CRAN2090
C	HERE, E(MIN) IS THE MAX. TRUNC. ERROR EST., ABS. OR REL., OVER I	CRAN2100
C	WHILE THIS REST OF E ARE ITS PREDECESSORS.	CRAN2110
	IF(E(MIN)-BOUNDB)50,50,51	CRAN2120
50	GO TO IS,(15,55)	CRAN2130
C	15 IS NORMAL AND CALLS DERIV, JUMPING TO 18 TO STEP INIT+1,RETURN	CRAN2140
C	55 IS REACHED FIRST STEP AFTER A SEQUENCE OF RKG STEPS.(CRD 0510)	CRAN2150
C	WHEN LARGEST ERROR EXCEEDS BOUND, STMT 51 IS A BRANCH GOVERNED	CRAN2160
C	BY WHETHER THIS IS ON FIRST P-C STEP OR NOT. 52 IS NORMAL.	CRAN2170
51	IF (.NOT. IKPC) GO TO 59	
C	52 IS REACHED WHEN LARGEST ERROR EXCEEDS BOUND, FNCTN OF PRECISN.	CRAN2190
52	X=X-H	CRAN2200
	DO 54 I=1,N	CRAN2210
	Y(I)=Y0(I)	CRAN2220
54	F(I)=F0(I)	CRAN2230
	ASSIGN 20 TO KT	
53	IF (IONT) GO TO 1000	
	H=.625*H	CRAN2240
	IELP = .FALSE.	
C	NOTE - ALL STEP SIZE REDUCTIONS GO THRU HERE	
C	EXCEPT CN ENDONX INITIATED REDUCTION.	
	GO TO 17	CRAN2250
C	RETURN TO 17 SETS UP RKG INITIALIZATION	CRAN2260

55	IKPC = .TRUE.	
	ASSIGN 15 TO IS	CRAN2280
	GO TO 5	CRAN2300
C		
C	ABOVE SEQUENCE COMPLETES INITIALIZATION OF PRED-CORR ROUTINE.	CRAN2310
C	NEXT, FAILURE OF FIRST TEST AFTER RKG SEQUENCE CAUSES BACKUP 3	CRAN2320
C	STEPS.	CRAN2330
59	X=X-4.*H	CRAN2340
	DO 60 I=1,N	CRAN2350
	Y(I)=Y3(I)	CRAN2360
60	F(I)=F3(I)	CRAN2370
61	ASSIGN 18 TO KT	
	GO TO 53	CRAN2380
C	THE FOLLOWING SETS UP DOUBLING DELTX	CRAN2400
C	REFER TO CARD 1130 FOR RETURN TO RKG INITIALIZATION.	CRAN2390
38	H=2.*H	CRAN2410
	DO 64 I=1,N	CRAN2420
	F2(I)=F3(I)	CRAN2430
	F3(I)=F5(I)	CRAN2440
	F0(I)=F(I)	CRAN2450
	Y2(I)=Y3(I)	CRAN2460
	Y3(I)=Y5(I)	CRAN2470
64	Y0(I)=Y(I)	CRAN2480
C	23 IS REACHED AFTER 3 RKG STEPS, I E WHEN KBC=0. (REF. STTMT 22)	CRAN2490
23	AK=.04166666667*H	CRAN2500
	E(MIN)=10.	CRAN2510
	S=H*2.03169	CRAN2520
	DO 62 I=1,N	CRAN2530
C	SAME AS STATEMENT 39	
62	Y(I)=1.547652*Y(I)+2.017204*Y2(I)-1.867503*Y1(I)-.697353*Y3(I)+S*	CRAN2540
	1(.98550E124*F(I)+.895121303*F2(I)-.351589671*F3(I)-F1(I))	CRAN2550
	GO TO 40	CRAN2560
C	ABOVE CALLS DERIVATIVE WITH FIRST PREDICTED Y VECTOR.	CRAN2570
C		
2020	K = 3-KBC	

```

      X      =XN- K*H
      GO TO (2021,2022,2023),K
2021 DO 2024 I=1,N
      F(I)   = F0(I)
2024 Y(I)   = Y0(I)
      GO TO 61
2022 DO 2025 I=1,N
      F(I)   = F1(I)
2025 Y(I)   = Y1(I)
      GO TO 61
2023 DO 2026 I=1,N
      F(I)   = F2(I)
2026 Y(I)   = Y2(I)
      GO TO 61
C
2030 IF ( IKPC ) GO TO 52
      GO TO 59
C
1000 WRITE (6,1001)
1001 FORMAT ('0THE USE OF A FIXED STEP SIZE (DONT=TRUE) IS INCOMPATIBLE
. WITH USE OF HELP IN DERIV AND IS GENERALLY USELESS.'/' RUN ABORTE
.D.')
      CALL EXIT
C
2000 WRITE(6,2001)
2001 FORMAT('0 CRANE WAS CALLED WITH INITIAL VALUES UNACCEPTABLE TO DER
.IV. CASE ABORTED.')
      CALL EXIT
C
2040 INDONX = .FALSE.
      WRITE(6,2041)
2041 FORMAT('0VALUES OF ENDONX, XHAT, X, AND H ARE NOT COMPATIBLE.
.. RUN ABORTED.')
      CALL EXIT
      END

```

CRAN2580

ANALYTICAL CELL AT THE FOLLOWING CONDITIONS :

INLET AIR PCO2 = 4.00 MM HG
 CURRENT DENSITY = 30.00 A /FT2
 MATRIX THICKNESS= 25.00 MILS
 AIR FLOW RATE = 10.00 FT3/MIN
 AIR TEMPERATURE = 70.00 DEG. F
 AIR DEW POINT = 40.00 DEG. F

OTHER CONDITIONS :

CELL VOLTAGE = 0.30 VOLT
 HYDROGEN RATE = 0.07 FT3/MIN
 ANODE PCO2IN = 0.0 MM HG

OUTLET AIR D.P. = 42.61 DEG. F

NO. OF SUBCELL	TAIRIN	TAIROUT	TELEC	PH2OIN	PH2OCUT	CSCATH
1	70.00	72.80	73.34	6.30	6.54	5.57
2	72.80	75.59	76.78	6.54	6.77	5.47
3	75.59	78.39	79.90	6.77	7.01	5.29

UPPER FLUX LIMIT= .698880
 LOWER FLUX LIMIT= .374400

 THE INITIAL FLUX AT THE CATHODE IS .499200

X = -.500000 C1C = .196621D-04 C3C = .335602 C4C = .773765

X = .500000 C1A = .491241D-01 C3A = .127676D-06 C4A = .491244E-01

THE INTEGRATION ROUTINE TOOK 267 + 1 STEPS

GUESSED CATHODE FLUX - CALC. ANODE FLUX IS -335.884 DIFF./FLUX = 672.844

THE INITIAL FLUX AT THE CATHODE IS .599040

X = -.500000 C1C = .136394D-04 C3C = .317050 C4C = .773762

THE INITIAL FLUX AT THE CATHODE IS .549120

X = -.500000 C1C = .163770D-04 C3C = .326912 C4C = .773764

THE INITIAL FLUX AT THE CATHODE IS .549120

X = -.500000 C1C = .163770D-04 C3C = .326912 C4C = .773764

ORIGINAL PAGE IS
OF POOR QUALITY

THE INITIAL FLUX AT THE CATHODE IS .524160

X = -.500000 C1C = .179413D-04 C3C = .331390 C4C = .773764

THE INITIAL FLUX AT THE CATHODE IS .511680

X = -.500000 C1C = .187807D-04 C3C = .333528 C4C = .773764

X = .500000 C1A = .205002 C3A = .467484D-05 C4A = .205011

THE INTEGRATION ROUTINE TOOK 235 + 1 STEPS

GUESSED CATHODE FLUX - CALC. ANODE FLUX IS -159.230 DIFF./FLUX = 311.190

THE INITIAL FLUX AT THE CATHODE IS .517920

X = -.500000 C1C = .183559D-04 C3C = .332467 C4C = .773764

X = .500000 C1A = .126244D-04 C3A = .136551 C4A = .338095

THE INTEGRATION ROUTINE TOOK 72 + 1 STEPS

ORIGINAL PAGE IS
OF POOR QUALITY

GUESSED CATHODE FLUX - CALC. ANODE FLUX IS .993074 DIFF./FLUX = 1.91743

THE INITIAL FLUX AT THE CATHODE IS .514800

X = -.500000 C1C = .185670D-04 C3C = .333000 C4C = .773764

X = .500000 C1A = .246460 C3A = .349104D-01 C4A = .316282

THE INTEGRATION ROUTINE TOOK 130 + 1 STEPS

GUESSED CATHODE FLUX - CALC. ANODE FLUX IS .956083 DIFF./FLUX = 1.85719

THE INITIAL FLUX AT THE CATHODE IS .513240

X = -.500000 C1C = .186735D-04 C3C = .333264 C4C = .773765

X = .500000 C1A = .239710 C3A = .107936D-04 C4A = .239732

THE INTEGRATION ROUTINE TOOK 225 + 1 STEPS

GUESSED CATHODE FLUX - CALC. ANODE FLUX IS -93.8911 DIFF./FLUX = 182.938

THE INITIAL FLUX AT THE CATHODE IS .514020

X = -.500000 C1C = .186202D-04 C3C = .333132 C4C = .773764

X = .500000 C1A = .262050 C3A = .250806D-04 C4A = .262101

THE INTEGRATION ROUTINE TOOK 220 + 1 STEPS

GUESSED CATHODE FLUX - CALC. ANODE FLUX IS -47.8095 DIFF./FLUX = 93.0109

THE INITIAL FLUX AT THE CATHODE IS .514410

X = -.500000 C1C = .185936D-04 C3C = .333066 C4C = .773764

X = .500000 C1A = .275288 C3A = .657292D-04 C4A = .275419

THE INTEGRATION ROUTINE TOOK 190 + 1 STEPS

GUESSED CATHODE FLUX - CALC. ANODE FLUX IS -19.5612 DIFF./FLUX = 38.0265

THE INITIAL FLUX AT THE CATHODE IS .514605

X = -.500000 C1C = .185803D-04 C3C = .333033 C4C = .773764

X = .500000 C1A = .282327 C3A = .291471D-03 C4A = .282910

THE INTEGRATION ROUTINE TOOK 161 + 1 STEPS

GUESSED CATHODE FLUX - CALC. ANODE FLUX IS -3.88692 DIFF./FLUX = 7.55321

THE INITIAL FLUX AT THE CATHODE IS .514702

X = -.500000 C1C = .185736D-04 C3C = .333016 C4C = .773764

X = .500000 C1A = .272965 C3A = .102860D-01 C4A = .293537

THE INTEGRATION ROUTINE TOOK 134 + 1 STEPS

GUESSED CATHODE FLUX - CALC. ANODE FLUX IS .857809 DIFF./FLUX = 1.66661

THE INITIAL FLUX AT THE CATHODE IS .514654

X = -.500000 C1C = .185770D-04 C3C = .333024 C4C = .773764

X = .500000 C1A = .282932 C3A = .124643D-02 C4A = .285425

THE INTEGRATION ROUTINE TOOK 142 + 1 STEPS

GUESSED CATHODE FLUX - CALC. ANODE FLUX IS -.157754

DIFF./FLUX = .306524

THE INITIAL FLUX AT THE CATHODE IS .514678

X = -.500000

C1C = .185753D-04

C3C = .333020

C4C = .773764

X = .500000

C1A = .279280

C3A = .469985D-02

C4A = .288680

THE INTEGRATION ROUTINE TOOK 134 + 1 STEPS

GUESSED CATHODE FLUX - CALC. ANODE FLUX IS .691097

DIFF./FLUX = 1.34277

THE INITIAL FLUX AT THE CATHODE IS .514666

X = -.500000

C1C = .185761D-04

C3C = .333022

C4C = .773764

X = .500000

C1A = .281706

C3A = .251683D-02

C4A = .286740

THE INTEGRATION ROUTINE TOOK 137 + 1 STEPS

ORIGINAL PAGE IS
OF POOR QUALITY

GUESSED CATHODE FLUX - CALC. ANODE FLUX IS .424902 DIFF./FLUX = .825588

THE INITIAL FLUX AT THE CATHODE IS .514660

X = -.500000 C1C = .185766D-04 C3C = .333023 C4C = .773764

X = .500000 C1A = .282556 C3A = .168239D-02 C4A = .285921

THE INTEGRATION ROUTINE TOOK 142 + 1 STEPS

GUESSED CATHODE FLUX - CALC. ANODE FLUX IS .141105 DIFF./FLUX = .274171

THE INITIAL FLUX AT THE CATHODE IS .514657

X = -.500000 C1C = .185768D-04 C3C = .333024 C4C = .773764

X = .500000 C1A = .282792 C3A = .142038D-02 C4A = .285633

THE INTEGRATION ROUTINE TOOK 140 + 1 STEPS

=====

X	C1	C2	C3	C4
---	----	----	----	----

-.500000	.737946E-04	.775425	2.39777	5.57104
----------	-------------	---------	---------	---------

WARNING PRECIPITATION EXPECTED AT CATHODE

-.299999	.178827E-03	.447020	1.84811	4.14341
----------	-------------	---------	---------	---------

-.999989E-01	.255907E-03	.278618	1.64838	3.57563
--------------	-------------	---------	---------	---------

.100001	.568852E-03	.116606	1.53351	3.18419
---------	-------------	---------	---------	---------

.300001	.515143	.104352E-03	1.24278	3.00081
---------	---------	-------------	---------	---------

.500000	2.03610	.113971E-05	.102268E-01	2.05655
---------	---------	-------------	-------------	---------

FLUX FOR SUBCELL NUMBER 1 IS .514657

UPPER FLUX LIMIT= .514660

LOWER FLUX LIMIT= .514654

THE INITIAL FLUX AT THE CATHODE IS .504364

X = -.500000 C1C = .210294D-04 C3C = .327879 C4C = .760133

X = .500000 C1A = .201070 C3A = .402115D-05 C4A = .201070

THE INTEGRATION ROUTINE TOOK 255 + 1 STEPS

GUESSED CATHODE FLUX - CALC. ANODE FLUX IS -180.414 DIFF./FLUX = 357.706

THE INITIAL FLUX AT THE CATHODE IS .509512

X = -.500000 C1C = .206246D-04 C3C = .326998 C4C = .760133

X = .500000 C1A = .197939 C3A = .868866D-01 C4A = .371716

THE INTEGRATION ROUTINE TOOK 129 + 1 STEPS

GUESSED CATHODE FLUX - CALC. ANODE FLUX IS 1.39459 DIFF./FLUX = 2.73710

THE INITIAL FLUX AT THE CATHODE IS .506938

X = -.500000 C1C = .208259D-04 C3C = .327440 C4C = .760133

ORIGINAL PAGE IS
OF POOR QUALITY

X = .500000 C1A = .241159 C3A = .990317D-05 C4A = .241178

THE INTEGRATION ROUTINE TOOK 222 + 1 STEPS

GUESSED CATHODE FLUX - CALC. ANODE FLUX IS -104.796 DIFF./FLUX = 206.724

THE INITIAL FLUX AT THE CATHODE IS .508225

X = -.500000 C1C = .207250D-04 C3C = .327220 C4C = .760133

X = .500000 C1A = .269390 C3A = .275996D-04 C4A = .269445

THE INTEGRATION ROUTINE TOOK 204 + 1 STEPS

GUESSED CATHODE FLUX - CALC. ANODE FLUX IS -46.1474 DIFF./FLUX = 90.8012

THE INITIAL FLUX AT THE CATHODE IS .508868

X = -.500000 C1C = .206747D-04 C3C = .327109 C4C = .760133

X = .500000 C1A = .287258 C3A = .163542D-03 C4A = .287585

THE INTEGRATION ROUTINE TOOK 173 + 1 STEPS

GUESSED CATHODE FLUX - CALC. ANODE FLUX IS -7.72239

DIFF./FLUX = 15.1756

THE INITIAL FLUX AT THE CATHODE IS .509199

X = -.500000

C1C = .206496D-04

C3C = .327054

C4C = .760132

X = .500000

C1A = .249855

C3A = .381862D-01

C4A = .326229

THE INTEGRATION ROUTINE TOOK 126 + 1 STEPS

GUESSED CATHODE FLUX - CALC. ANODE FLUX IS 1.37257

DIFF./FLUX = 2.69560

THE INITIAL FLUX AT THE CATHODE IS .509029

X = -.500000

C1C = .206622D-04

C3C = .327081

C4C = .760133

X = .500000

C1A = .284852

C3A = .576662D-02

C4A = .296385

THE INTEGRATION ROUTINE TOOK 129 + 1 STEPS

GUESSED CATHODE FLUX - CALC. ANODE FLUX IS 1.14740

DIFF./FLUX = 2.25409

ORIGINAL PAGE IS
OF POOR QUALITY

THE INITIAL FLUX AT THE CATHODE IS .508949

X = -.500000 C1C = .206684D-04 C3C = .327095 C4C = .760133

X = .500000 C1A = .289450 C3A = .391825D-03 C4A = .290234

THE INTEGRATION ROUTINE TOOK 149 + 1 STEPS

GUESSED CATHODE FLUX - CALC. ANODE FLUX IS -2.46487 DIFF./FLUX = 4.84307

THE INITIAL FLUX AT THE CATHODE IS .508989

X = -.500000 C1C = .206653D-04 C3C = .327088 C4C = .760133

X = .500000 C1A = .289761 C3A = .112358D-02 C4A = .292008

THE INTEGRATION ROUTINE TOOK 146 + 1 STEPS

GUESSED CATHODE FLUX - CALC. ANODE FLUX IS .504884E-01 DIFF./FLUX = .991936E-01

THE INITIAL FLUX AT THE CATHODE IS .508969

X = -.500000 C1C = .206669D-04 C3C = .327092 C4C = .760133

X = .500000 C1A = .289823 C3A = .593342D-03 C4A = .291010

THE INTEGRATION ROUTINE TOOK 144 + 1 STEPS

GUESSED CATHODE FLUX - CALC. ANODE FLUX IS -1.15821 DIFF./FLUX = 2.27561

THE INITIAL FLUX AT THE CATHODE IS .508979

X = -.500000 C1C = .206661D-04 C3C = .327090 C4C = .760133

X = .500000 C1A = .289888 C3A = .797143D-03 C4A = .291483

THE INTEGRATION ROUTINE TOOK 143 + 1 STEPS

GUESSED CATHODE FLUX - CALC. ANODE FLUX IS -.504570 DIFF./FLUX = .991338

THE INITIAL FLUX AT THE CATHODE IS .508984

X = -.500000 C1C = .206657D-04 C3C = .327089 C4C = .760133

X = .500000 C1A = .289870 C3A = .894847D-03 C4A = .291660

THE INTEGRATION ROUTINE TOOK 146 + 1 STEPS

GUESSED CATHODE FLUX - CALC. ANODE FLUX IS -.296205 DIFF./FLUX = .581953

THE INITIAL FLUX AT THE CATHODE IS .508986

X = -.500000 C1C = .206655D-04 C3C = .327089 C4C = .760133

X = .500000 C1A = .289823 C3A = .101488D-02 C4A = .291853

THE INTEGRATION ROUTINE TOOK 135 + 1 STEPS

GUESSED CATHODE FLUX - CALC. ANODE FLUX IS -.948888E-01 DIFF./FLUX = .186427

THE INITIAL FLUX AT THE CATHODE IS .508988

X = -.500000 C1C = .206654D-04 C3C = .327088 C4C = .760133

X = .500000 C1A = .289808 C3A = .104231D-02 C4A = .291893

THE INTEGRATION ROUTINE TOOK 134 + 1 STEPS

ORIGINAL PAGE IS
OF POOR QUALITY

GUESSED CATHODE FLUX - CALC. ANODE FLUX IS -.553602E-01 DIFF./FLUX = .108765

THE INITIAL FLUX AT THE CATHODE IS .508988

X = -.500000 C1C = .206653D-24 C3C = .327088 C4C = .760133

X = .500000 C1A = .289785 C3A = .108642D-22 C4A = .291958

THE INTEGRATION ROUTINE TCOK 138 + 1 STEPS

=====

X	C1	C2	C3	C4
---	----	----	----	----

-.500000	.820913E-04	.762733	2.35504	5.47289
----------	-------------	---------	---------	---------

WARNING PRECIPITATION EXPECTED AT CATHODE

-.299999	.198256E-03	.448308	1.84439	4.13728
----------	-------------	---------	---------	---------

-.999989E-01	.288166E-03	.277216	1.65771	3.59293
--------------	-------------	---------	---------	---------

.100001	.972670E-03	.769111E-01	1.55240	3.18269
.300001	.639953	.916931E-04	1.21768	3.07541
.500000	2.08645	.947745E-06	.782220E-02	2.10210

FLUX FOR SUBCELL NUMBER 2 IS .508989

UPPER FLUX LIMIT= .508989

LOWER FLUX LIMIT= .508988

THE INITIAL FLUX AT THE CATHODE IS .493253

X = -.500000 C1C = .237996D-04 C3C = .317703 C4C = .734042

X = .500000 C1A = .182098 C3A = .270445D-05 C4A = .182104

THE INTEGRATION ROUTINE TOOK 244 + 1 STEPS

GUESSED CATHODE FLUX - CALC. ANODE FLUX IS -222.963 DIFF./FLUX = 452.024

THE INITIAL FLUX IS
- 493.253

THE INITIAL FLUX AT THE CATHODE IS .501121

X = -.500000 C1C = .230821D-04 C3C = .316463 C4C = .734042

X = .500000 C1A = .263814 C3A = .185762D-04 C4A = .263851

THE INTEGRATION ROUTINE TOOK 211 + 1 STEPS

GUESSED CATHODE FLUX - CALC. ANODE FLUX IS -66.8944 DIFF./FLUX = 133.489

THE INITIAL FLUX AT THE CATHODE IS .505055

X = -.500000 C1C = .227317D-04 C3C = .315793 C4C = .734042

X = .500000 C1A = .166977D-03 C3A = .178660 C4A = .365376

THE INTEGRATION ROUTINE TOOK 65 + 1 STEPS

GUESSED CATHODE FLUX - CALC. ANODE FLUX IS 1.78025 DIFF./FLUX = 3.52487

THE INITIAL FLUX AT THE CATHODE IS .503088

X = -.500000 C1C = .229062D-24 C3C = .316129 C4C = .734042

X = .500000 C1A = .240427 C3A = .514951D-01 C4A = .343419

THE INTEGRATION ROUTINE TOOK 122 + 1 STEPS

GUESSED CATHODE FLUX - CALC. ANODE FLUX IS 1.75607 DIFF./FLUX = 3.49058

THE INITIAL FLUX AT THE CATHODE IS .502105

X = -.500000 C1C = .229940D-24 C3C = .316297 C4C = .734042

X = .500000 C1A = .281955 C3A = .486617D-04 C4A = .282052

THE INTEGRATION ROUTINE TOOK 199 + 1 STEPS

GUESSED CATHODE FLUX - CALC. ANODE FLUX IS -23.1674 DIFF./FLUX = 56.0987

THE INITIAL FLUX AT THE CATHODE IS .502596

X = -.500000 C1C = .229500D-24 C3C = .316213 C4C = .734042

X = .500000 C1A = .292416 C3A = .219134D-03 C4A = .292854

ALL INFORMATION CONTAINED
HEREIN IS UNCLASSIFIED

THE INTEGRATION ROUTINE TOOK 168 + 1 STEPS

GUESSED CATHODE FLUX - CALC. ANODE FLUX IS -5.37424 DIFF./FLUX = 10.6930

THE INITIAL FLUX AT THE CATHODE IS .502842

X = -.500000 C1C = .229281D-04 C3C = .316171 C4C = .734042

X = .500000 C1A = .277892 C3A = .158284D-01 C4A = .309549

THE INTEGRATION ROUTINE TOOK 128 + 1 STEPS

GUESSED CATHODE FLUX - CALC. ANODE FLUX IS 1.68677 DIFF./FLUX = 3.35448

THE INITIAL FLUX AT THE CATHODE IS .502719

X = -.500000 C1C = .229391D-04 C3C = .316192 C4C = .734042

X = .500000 C1A = .294015 C3A = .116060D-02 C4A = .296336

THE INTEGRATION ROUTINE TOOK 131 + 1 STEPS

GUESSED CATHODE FLUX - CALC. ANODE FLUX IS .410857 DIFF./FLUX = .817269

THE INITIAL FLUX AT THE CATHODE IS .502658

X = -.500000 C1C = .229446D-04 C3C = .316203 C4C = .734042

X = .500000 C1A = .293633 C3A = .389906D-03 C4A = .294395

THE INTEGRATION ROUTINE TOOK 152 + 1 STEPS

GUESSED CATHODE FLUX - CALC. ANODE FLUX IS -2.37277 DIFF./FLUX = 4.72044

THE INITIAL FLUX AT THE CATHODE IS .502689

X = -.500000 C1C = .229418D-04 C3C = .316197 C4C = .734042

X = .500000 C1A = .294072 C3A = .591956D-03 C4A = .295256

THE INTEGRATION ROUTINE TOOK 142 + 1 STEPS

GUESSED CATHODE FLUX - CALC. ANODE FLUX IS -.901589 DIFF./FLUX = 1.79353

ORIGINAL PAGE IS
OF POOR QUALITY

THE INITIAL FLUX AT THE CATHODE IS .502704

X = -.500000 C1C = .229405D-04 C3C = .316195 C4C = .734042

X = .500000 C1A = .294152 C3A = .792341D-03 C4A = .295107

THE INTEGRATION ROUTINE TOOK 134 + 1 STEPS

GUESSED CATHODE FLUX - CALC. ANODE FLUX IS -.225510 DIFF./FLUX = .448594

THE INITIAL FLUX AT THE CATHODE IS .502712

X = -.500000 C1C = .229398D-04 C3C = .316193 C4C = .734042

X = .500000 C1A = .294117 C3A = .960661D-03 C4A = .296038

THE INTEGRATION ROUTINE TOOK 145 + 1 STEPS

GUESSED CATHODE FLUX - CALC. ANODE FLUX IS .125581 DIFF./FLUX = .249808

THE INITIAL FLUX AT THE CATHODE IS .502708

X = -.500000 C1C = .229401D-04 C3C = .316194 C4C = .734042

X = .500000 C1A = .294144 C3A = .872883D-03 C4A = .295890

THE INTEGRATION ROUTINE TOOK 135 + 1 STEPS

GUESSED CATHODE FLUX - CALC. ANODE FLUX IS -.407192E-01 DIFF./FLUX = .809997E-01

THE INITIAL FLUX AT THE CATHODE IS .502710

X = -.500000 C1C = .229399D-04 C3C = .316194 C4C = .734042

X = .500000 C1A = .294133 C3A = .917400D-03 C4A = .295968

THE INTEGRATION ROUTINE TOOK 129 + 1 STEPS

GUESSED CATHODE FLUX - CALC. ANODE FLUX IS .475653E-01 DIFF./FLUX = .946178E-01

THE INITIAL FLUX AT THE CATHODE IS .502709

X = -.500000 C1C = .229400D-04 C3C = .316194 C4C = .734042

X = .500000 C1A = .294138 C3A = .902101D-03 C4A = .295942

THE INTEGRATION ROUTINE TOOK 134 + 1 STEPS

=====

X	C1	C2	C3	C4

-.500000	.911273E-04	.731743	2.27660	5.28503
-.299999	.217680E-03	.445692	1.82748	4.10988
-.999989E-01	.319576E-03	.275163	1.65640	3.58828
.100001	.904061E-03	.916162E-01	1.56017	3.21285
.300001	.722812	.879197E-04	1.19705	3.11700
.500000	2.11779	.854130E-06	.649513E-02	2.13078

FLUX FOR SURCELL NUMBER 3 IS .502709

CO2 REMOVAL RATE = .219286E-01 LB MCL/FT2.DAY
= .964858 LB /FT2.DAY

ORIGINAL PAGE IS
OF POOR QUALITY

TRANSFER INDEX = 2.03840

CO2 ANODE PRESSURE = 176.350

CO2 REMOVAL EFFICIENCY = 74.12 %

ORIGINAL PAGE IS
OF POOR QUALITY

FULL SCALE CELL AT THE FOLLOWING CONDITIONS :

INLET AIR PCO2 = 1.00 MM HG
CURRENT DENSITY = 15.00 A /FT2
MATRIX THICKNESS= 10.00 MILS
AIR FLOW RATE = 10.00 FT3/MIN
AIR TEMPERATURE = 70.00 DEG. F
AIR DEW POINT = 50.00 DEG. F

OTHER CONDITIONS :

CELL VOLTAGE = 0.20 VOLT
HYDROGEN RATE = 0.07 FT3/MIN
ANODE PCO2IN = 0.0 MM HG

CUTLET AIR D.P. = 51.15 DEG. F

NO. OF SURCELL	TAIRIN	TAIRCUT	TELEC	PH2OIN	PH2OOUT	CSCATH
1	70.00	74.64	77.16	9.22	9.61	4.59

UPPER FLUX LIMIT= .249600
LOWER FLUX LIMIT= .624000D-01

THE INITIAL FLUX AT THE CATHODE IS .149760

X = -.500000

C1C = .346156D-04

C3C = .290527

C4C = .637927

X = .500000 C1A = .443485 C3A = .525495D-04 C4A = .443590

THE INTEGRATION ROUTINE TOOK 206 + 1 STEPS

GUESSED CATHODE FLUX - CALC. ANODE FLUX IS -67.2489 DIFF./FLUX = 449.045

THE INITIAL FLUX AT THE CATHODE IS .199680

X = -.500000 C1C = .158104D-04 C3C = .262691 C4C = .637918

X = .500000 C1A = .255648D-04 C3A = .236172 C4A = .534931

THE INTEGRATION ROUTINE TOOK 46 + 1 STEPS

GUESSED CATHODE FLUX - CALC. ANODE FLUX IS .719293 DIFF./FLUX = 3.60223

THE INITIAL FLUX AT THE CATHODE IS .174720

X = -.500000 C1C = .238699D-04 C3C = .279325 C4C = .637922

X = .500000 C1A = .347399 C3A = .974937D-01 C4A = .542389

THE INTEGRATION ROUTINE TOOK 116 + 1 STEPS

ORIGINAL PAGE IS
OF POOR QUALITY

GUESSED CATHODE FLUX - CALC. ANODE FLUX IS .606960 DIFF./FLUX = 3.47390

THE INITIAL FLUX AT THE CATHODE IS .162240

X = -.500000 C1C = .288295D-04 C3C = .285424 C4C = .637924

X = .500000 C1A = .454200 C3A = .140072D-03 C4A = .454480

THE INTEGRATION ROUTINE TOOK 181 + 1 STEPS

GUESSED CATHODE FLUX - CALC. ANODE FLUX IS -26.0907 DIFF./FLUX = 160.816

THE INITIAL FLUX AT THE CATHODE IS .168480

X = -.500000 C1C = .262578D-04 C3C = .282517 C4C = .637923

X = .500000 C1A = .459364 C3A = .312855D-02 C4A = .465621

THE INTEGRATION ROUTINE TOOK 127 + 1 STEPS

GUESSED CATHODE FLUX - CALC. ANODE FLUX IS -.614720 DIFF./FLUX = 3.64862

THE INITIAL FLUX AT THE CATHODE IS .171600

X = -.500000 C1C = .250421D-04 C3C = .280959 C4C = .637922

X = .500000 C1A = .401177 C3A = .529592D-01 C4A = .507097

THE INTEGRATION ROUTINE TOOK 119 + 1 STEPS

GUESSED CATHODE FLUX - CALC. ANODE FLUX IS .563100 DIFF./FLUX = 3.28147

THE INITIAL FLUX AT THE CATHODE IS .170040

X = -.500000 C1C = .256444D-04 C3C = .281747 C4C = .637923

X = .500000 C1A = .433483 C3A = .249103D-01 C4A = .403304

THE INTEGRATION ROUTINE TOOK 120 + 1 STEPS

GUESSED CATHODE FLUX - CALC. ANODE FLUX IS .475897 DIFF./FLUX = 2.79874

THE INITIAL FLUX AT THE CATHODE IS .169260

X = -.500000 C1C = .259497D-04 C3C = .282134 C4C = .637923

X = .500000 C1A = .448823 C3A = .119477D-01 C4A = .472718

THE INTEGRATION ROUTINE TOOK 122 + 1 STEPS

GUESSED CATHODE FLUX - CALC. ANODE FLUX IS .304339 DIFF./FLUX = 1.79806

THE INITIAL FLUX AT THE CATHODE IS .168870

X = -.500000 C1C = .261034D-04 C3C = .282326 C4C = .637923

X = .500000 C1A = .455125 C3A = .672517D-02 C4A = .468575

THE INTEGRATION ROUTINE TOOK 121 + 1 STEPS

GUESSED CATHODE FLUX - CALC. ANODE FLUX IS .504498E-01 DIFF./FLUX = .298749

THE INITIAL FLUX AT THE CATHODE IS .168675

X = -.500000 C1C = .261805D-04 C3C = .282421 C4C = .637923

X = .500000 C1A = .457580 C3A = .467244D-02 C4A = .466925

THE INTEGRATION ROUTINE TOOK 128 + 1 STEPS

GUESSED CATHODE FLUX - CALC. ANODE FLUX IS -.204022 DIFF./FLUX = 1.20956

THE INITIAL FLUX AT THE CATHODE IS .168772

X = -.500000 C1C = .261419D-04 C3C = .282374 C4C = .637923

X = .500000 C1A = .456429 C3A = .563984D-02 C4A = .467709

THE INTEGRATION ROUTINE TOOK 120 + 1 STEPS

GUESSED CATHODE FLUX - CALC. ANODE FLUX IS -.610741E-01 DIFF./FLUX = .361872

THE INITIAL FLUX AT THE CATHODE IS .168821

X = -.500000 C1C = .261227D-04 C3C = .282350 C4C = .637923

X = .500000 C1A = .455793 C3A = .617028D-02 C4A = .468133

THE INTEGRATION ROUTINE TOOK 120 + 1 STEPS

=====

X	C1	C2	C3	C4

-.500000	.103770E-03	.527021	2.03292	4.59296
-.299998	.350299E-03	.284884	2.04668	4.37859
-.999975E-01	.376896E-02	.269228E-01	2.08105	4.19280
.100002	1.41879	.514466E-04	1.49698	4.41281
.300002	2.27811	.201897E-04	.943290	4.16471
.500000	3.28171	.346271E-05	.444260E-01	3.37056

FLUX FOR SUBCELL NUMBER 1 IS .168821

CO2 REMOVAL RATE = .727619E-02 LB MCL/FT2.DAY
 = .320152 LB /FT2.DAY

TRANSFER INDEX = 1.35273 CO2 ANODE PRESSURE = 58.5152

CO2 REMOVAL EFFICIENCY = 49.19 %

ORIGINAL PAGE IS
OF POOR QUALITY

ANALYTICAL CELL AT THE FOLLOWING CONDITIONS :

INLET AIR PCO2 = 0.25 MM HG
 CURRENT DENSITY = 20.00 A /FT2
 MATRIX THICKNESS= 25.00 MILS
 AIR FLOW RATE = 25.00 FT3/MIN
 AIR TEMPERATURE = 70.00 DEG. F
 AIR DEW POINT = 60.00 DEG. F

OTHER CONDITIONS :

CELL VOLTAGE = 0.20 VOLT
 HYDROGEN RATE = 0.07 FT3/MIN
 ANODE PCO2IN = 0.0 MM HG

OUTLET AIR D.P. = 60.50 DEG. F

NO. OF SUBCELL	TAIRIN	TAIROUT	TELEC	PH2OIN	PH2OOUT	CSCATH
1	70.00	72.47	75.91	13.29	13.51	3.85

UPPER FLUX LIMIT= .133120
 LOWER FLUX LIMIT= .499200D-01

 THE INITIAL FLUX AT THE CATHODE IS .998400D-01

X = -.800000 C1C = .378327D-05 C3C = .143521 C4C = .534157

ORIGINAL PAGE IS
 OF POOR QUALITY

X = .500000 C1A = .312672D-05 C3A = .898357D-01 C4A = .366839

THE INTEGRATION ROUTINE TOOK 46 + 1 STEPS

GUESSED CATHODE FLUX - CALC. ANODE FLUX IS .364382 DIFF./FLUX = 3.64966

THE INITIAL FLUX AT THE CATHODE IS .748800D-01

X = -.500000 C1C = .133836D-04 C3C = .214801 C4C = .534161

X = .500000 C1A = .225412 C3A = .300666D-05 C4A = .225418

THE INTEGRATION ROUTINE TOOK 252 + 1 STEPS

GUESSED CATHODE FLUX - CALC. ANODE FLUX IS -304.186 DIFF./FLUX = 4262.32

THE INITIAL FLUX AT THE CATHODE IS .873600D-01

X = -.500000 C1C = .789772D-05 C3C = .189094 C4C = .534159

X = .500000 C1A = .308108 C3A = .221583D-04 C4A = .308153

THE INTEGRATION ROUTINE TOOK 231 + 1 STEPS

GUESSED CATHODE FLUX - CALC. ANODE FLUX IS -76.8655

DIFF./FLUX = 879.871

THE INITIAL FLUX AT THE CATHODE IS .936000D-01

X = -.500000

C1C = .570335D-05

C3C = .169997

C4C = .534158

X = .500000

C1A = .231888D-04

C3A = .172447

C4A = .393359

THE INTEGRATION ROUTINE TOOK 55 + 1 STEPS

GUESSED CATHODE FLUX - CALC. ANODE FLUX IS .341608

DIFF./FLUX = 3.64966

THE INITIAL FLUX AT THE CATHODE IS .904800D-01

X = -.500000

C1C = .676271D-05

C3C = .180261

C4C = .534158

X = .500000

C1A = .213350

C3A = .105745

C4A = .424842

THE INTEGRATION ROUTINE TOOK 109 + 1 STEPS

GUESSED CATHODE FLUX - CALC. ANODE FLUX IS .322466

DIFF./FLUX = 3.56395

ORIGINAL PAGE IS
OF POOR QUALITY

THE INITIAL FLUX AT THE CATHODE IS .889200D-01

X = -.500000 C1C = .732026D-05 C3C = .184837 C4C = .534158

X = .500000 C1A = .329858 C3A = .948240D-04 C4A = .330047

THE INTEGRATION ROUTINE TOOK 171 + 1 STEPS

GUESSED CATHODE FLUX - CALC. ANODE FLUX IS -20.3480 DIFF./FLUX = 228.835

THE INITIAL FLUX AT THE CATHODE IS .897000D-01

X = -.500000 C1C = .703906D-05 C3C = .182591 C4C = .534158

X = .500000 C1A = .296242 C3A = .365867D-01 C4A = .369416

THE INTEGRATION ROUTINE TOOK 111 + 1 STEPS

GUESSED CATHODE FLUX - CALC. ANODE FLUX IS .284160 DIFF./FLUX = 3.16789

THE INITIAL FLUX AT THE CATHODE IS .893100D-01

X = -.500000 C1C = .717905D-05 C3C = .183724 C4C = .534158

X = .500000 C1A = .335818 C3A = .424864D-03 C4A = .336668

THE INTEGRATION ROUTINE TOOK 137 + 1 STEPS

GUESSED CATHODE FLUX - CALC. ANODE FLUX IS -4.45613 DIFF./FLUX = 49.8951

THE INITIAL FLUX AT THE CATHODE IS .895050D-01

X = -.500000 C1C = .710890D-05 C3C = .183160 C4C = .534158

X = .500000 C1A = .324849 C3A = .110969D-01 C4A = .347043

THE INTEGRATION ROUTINE TOOK 119 + 1 STEPS

GUESSED CATHODE FLUX - CALC. ANODE FLUX IS .155338 DIFF./FLUX = 1.73552

THE INITIAL FLUX AT THE CATHODE IS .894075D-01

X = -.500000 C1C = .714394D-05 C3C = .183443 C4C = .534158

DELETED PAGE IS
IN YOUR COPY

X = .500000 C1A = .335626 C3A = .177566D-02 C4A = .339177

THE INTEGRATION ROUTINE TOOK 120 + 1 STEPS

GUESSED CATHODE FLUX - CALC. ANODE FLUX IS -.816599 DIFF./FLUX = 9.13345

THE INITIAL FLUX AT THE CATHODE IS .894562D-01

X = -.500000 C1C = .712641D-05 C3C = .183302 C4C = .534158

X = .500000 C1A = .331461 C3A = .546107D-02 C4A = .342383

THE INTEGRATION ROUTINE TOOK 119 + 1 STEPS

GUESSED CATHODE FLUX - CALC. ANODE FLUX IS -.359644E-01 DIFF./FLUX = .402934

THE INITIAL FLUX AT THE CATHODE IS .894806D-01

X = -.500000 C1C = .711765D-05 C3C = .183231 C4C = .534158

X = .500000 C1A = .328285 C3A = .816082D-02 C4A = .344607

THE INTEGRATION ROUTINE TOOK 117 + 1 STEPS

GUESSED CATHODE FLUX - CALC. ANODE FLUX IS .886551E-01 DIFF./FLUX = .990775

THE INITIAL FLUX AT THE CATHODE IS .894684D-01

X = -.500000 C1C = .712203D-05 C3C = .183267 C4C = .534158

X = .500000 C1A = .329927 C3A = .676351D-02 C4A = .343454

THE INTEGRATION ROUTINE TOOK 123 + 1 STEPS

GUESSED CATHODE FLUX - CALC. ANODE FLUX IS .365793E-01 DIFF./FLUX = .408852

THE INITIAL FLUX AT THE CATHODE IS .894623D-01

X = -.500000 C1C = .712422D-05 C3C = .183284 C4C = .534158

X = .500000 C1A = .330706 C3A = .610240D-02 C4A = .342911

THE INTEGRATION ROUTINE TOOK 117 + 1 STEPS

=====

X

C1

C2

C3

C4

-.500000	.283003E-04	1.20660	1.31965	3.84592
-.299999	.648013E-04	.953987	1.31811	3.59028
-.999989E-01	.913236E-04	.689442	1.34248	3.37449
.100001	.212346E-03	.310105	1.40404	3.11840
.300001	.903280E-01	.756634E-03	1.45725	3.00559
.500000	2.38108	.453996E-05	.439372E-01	2.46896

FLUX FOR SUBCELL NUMBER 1 IS .894623D-01

CO2 REMOVAL RATE = .385582E-02 LB MOL/FT2.DAY
 = .169656 LB /FT2.DAY

TRANSFER INDEX = .537634 CC2 ANODE PRESSURE = 31.0086

CO2 REMOVAL EFFICIENCY = 19.55 %

ORIGINAL PAGE IS
OF POOR QUALITY

FULL SCALE CELL AT THE FOLLOWING CONDITIONS :

INLET AIR PCO2 = 10.00 MM HG
CURRENT DENSITY = 10.00 A /FT2
MATRIX THICKNESS= 25.00 MILS
AIR FLOW RATE = 10.00 FT3/MIN
AIR TEMPERATURE = 70.00 DEG. F
AIR DEW POINT = 60.00 DEG. F

OTHER CONDITIONS :

CELL VOLTAGE = 0.20 VOLT
HYDROGEN RATE = 0.07 FT3/MIN
ANODE PCO2IN = 0.0 MM HG

OUTLET AIR D.P. = 60.62 DEG. F

NO. OF SURCELL	TAIRIN	TAIROUT	TELEC	PH2OIN	PH2OOUT	CSCATH
1	70.00	73.09	74.78	13.29	13.57	3.74

UPPER FLUX LIMIT= .232960

LOWER FLUX LIMIT= .166400

THE INITIAL FLUX AT THE CATHODE IS .199680

X = -.500000

C1C = .913678D-03

C3C = .258806

C4C = .520307

X = .500000 C1A = .288555 C3A = .387471D-01 C4A = .366050

THE INTEGRATION ROUTINE TOOK 94 + 1 STEPS

GUESSED CATHODE FLUX - CALC. ANODE FLUX IS .699134 DIFF./FLUX = 3.50127

THE INITIAL FLUX AT THE CATHODE IS .183040

X = -.500000 C1C = .100282D-02 C3C = .258861 C4C = .520347

X = .500000 C1A = .324463 C3A = .636822D-04 C4A = .324591

THE INTEGRATION ROUTINE TOOK 155 + 1 STEPS

GUESSED CATHODE FLUX - CALC. ANODE FLUX IS -28.9639 DIFF./FLUX = 156.238

THE INITIAL FLUX AT THE CATHODE IS .191360

X = -.500000 C1C = .956312D-03 C3C = .258834 C4C = .520326

X = .500000 C1A = .329863 C3A = .189450D-03 C4A = .330242

THE INTEGRATION ROUTINE TOOK 132 + 1 STEPS

GUESSED CATHODE FLUX - CALC. ANODE FLUX IS -9.59076 DIFF./FLUX = 50.1189

THE INITIAL FLUX AT THE CATHODE IS .195520

X = -.500000 C1C = .934542D-03 C3C = .258821 C4C = .520316

X = .500000 C1A = .328437 C3A = .383880D-02 C4A = .336114

THE INTEGRATION ROUTINE TOOK 97 + 1 STEPS

GUESSED CATHODE FLUX - CALC. ANODE FLUX IS .218477 DIFF./FLUX = 1.11742

THE INITIAL FLUX AT THE CATHODE IS .193440

X = -.500000 C1C = .945310D-03 C3C = .258828 C4C = .520321

X = .500000 C1A = .331277 C3A = .396723D-03 C4A = .332070

THE INTEGRATION ROUTINE TOOK 110 + 1 STEPS

GUESSED CATHODE FLUX - CALC. ANODE FLUX IS -4.24515 DIFF./FLUX = 21.9456

THE INITIAL FLUX AT THE CATHODE IS .194480

X = -.500000 C1C = .939897D-03 C3C = .258824 C4C = .520319

X = .500000 C1A = .331563 C3A = .852408D-03 C4A = .333268

THE INTEGRATION ROUTINE TOOK 102 + 1 STEPS

GUESSED CATHODE FLUX - CALC. ANODE FLUX IS -1.59388 DIFF./FLUX = 8.19559

THE INITIAL FLUX AT THE CATHODE IS .195000

X = -.500000 C1C = .937213D-03 C3C = .258822 C4C = .520318

X = .500000 C1A = .330912 C3A = .166907D-02 C4A = .334250

THE INTEGRATION ROUTINE TOOK 99 + 1 STEPS

GUESSED CATHODE FLUX - CALC. ANODE FLUX IS -.465919 DIFF./FLUX = 2.33805

THE INITIAL FLUX AT THE CATHODE IS .195260

X = -.500000 C1C = .935876D-03 C3C = .258821 C4C = .520317

X = .500000 C1A = .329958 C3A = .254158D-02 C4A = .335041

THE INTEGRATION ROUTINE TOOK 97 + 1 STEPS

GUESSED CATHODE FLUX - CALC. ANODE FLUX IS -.466968E-01 DIFF./FLUX = .239152

THE INITIAL FLUX AT THE CATHODE IS .195390

X = -.500000 C1C = .935208D-03 C3C = .258821 C4C = .520317

X = .500000 C1A = .329264 C3A = .313947D-02 C4A = .335543

THE INTEGRATION ROUTINE TOOK 97 + 1 STEPS

GUESSED CATHODE FLUX - CALC. ANODE FLUX IS .102662 DIFF./FLUX = .525423

THE INITIAL FLUX AT THE CATHODE IS .195325

X = -.500000 C1C = .935541D-03 C3C = .253821 C4C = .520317

X = .500000 C1A = .329631 C3A = .282554D-02 C4A = .335282

THE INTEGRATION ROUTINE TOOK 97 + 1 STEPS

GUESSED CATHODE FLUX - CALC. ANODE FLUX IS .329991E-01 DIFF./FLUX = .164337

THE INITIAL FLUX AT THE CATHODE IS .195292

X = -.500000 C1C = .935708D-03 C3C = .258821 C4C = .520317

X = .500000 C1A = .329798 C3A = .268097D-02 C4A = .335159

THE INTEGRATION ROUTINE TOOK 97 + 1 STEPS

=====

X	C1	C2	C3	C4

-.500000	.371702E-02	.125181E-01	1.86351	3.74326
-.299999	.475508	.154255E-03	1.62076	3.71718
-.999989E-01	1.09363	.534455E-04	1.29152	3.67672

.100001	1.48795	.300804E-04	.988993	3.46597
.300001	1.82531	.157657E-04	.635874	3.89708
.500000	2.37454	.192994E-05	.193030E-01	2.41315

FLUX FOR SUBCELL NUMBER 1 IS .190292

CO2 REMOVAL RATE = .841710E-02 LB MOL/FT2.DAY
 = .370352 LB /FT2.DAY

TRANSFER INDEX = 2.34726 CO2 ANODE PRESSURE = 67.6904

CO2 REMOVAL EFFICIENCY = 85.36 %